

AD-A111 872 OHIO STATE UNIV COLUMBUS DEPT OF GEODETIC SCIENCE A--ETC F/G 8/5
GLOBAL GEOPOTENTIAL MODELLING FROM SATELLITE-TO-SATELLITE TRACK--ETC(U)
OCT 81 O L COLOMBO F19628-79-C-0027

UNCLASSIFIED

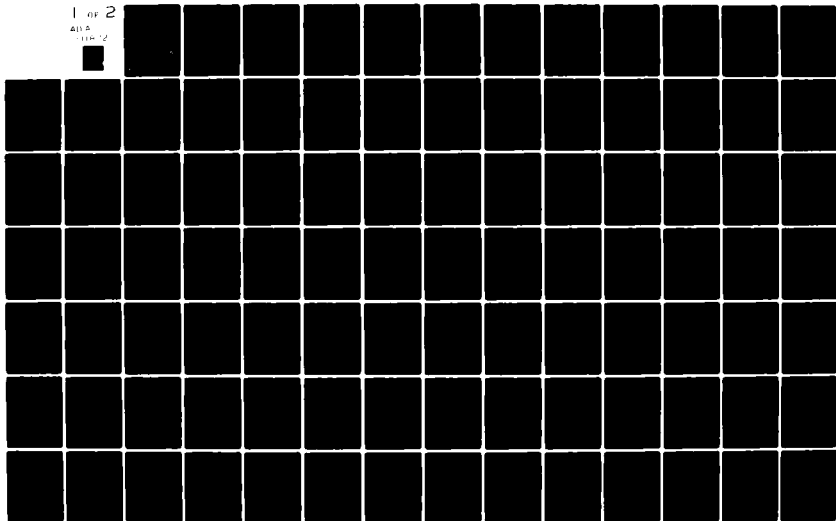
317

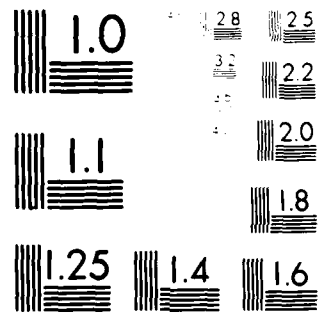
AFGL-TR-81-0319

NL

1 of 2

ALL INFORMATION CONTAINED
HEREIN IS UNCLASSIFIED





MICROCOPY RESOLUTION TEST CHART
NBS 1010-A-4

12

ADA111872

GLOBAL GEOPOTENTIAL MODELLING FROM SATELLITE-TO-SATELLITE TRACKING

Oscar L. Colombo

Department of Geodetic Science &
Surveying
The Ohio State University
1958 Neil Avenue
Columbus, Ohio 43210

October, 1981

Scientific Report No. 10

Approved for public release; distribution unlimited

AIR FORCE GEOPHYSICS LABORATORY
AIR FORCE SYSTEMS COMMAND
UNITED STATES AIR FORCE
HANSCOM AFB, MASSACHUSETTS 01731

DTIC
ELECTE
MAR 10 1982
H

DTIC FILE COPY

82 03 09 021

UNCLASSIFIED

SECURITY CLASSIFICATION OF THIS PAGE (When Data Entered)

REPORT DOCUMENTATION PAGE		READ INSTRUCTIONS BEFORE COMPLETING FORM
1. REPORT NUMBER AFGL-TR-81-0319	2. GOVT ACCESSION NO. AD-4111872	3. RECIPIENT'S CATALOG NUMBER
4. TITLE (and Subtitle) GLOBAL GEOPOTENTIAL MODELLING FROM SATELLITE-TO-SATELLITE TRACKING		5. TYPE OF REPORT & PERIOD COVERED Scientific Report No. 10
7. AUTHOR(s) Oscar L. Colombo		6. PERFORMING ORG. REPORT NUMBER Dept. of Geod. Sci. No. 317
		8. CONTRACT OR GRANT NUMBER(s) F19625-79-C-0027
9. PERFORMING ORGANIZATION NAME AND ADDRESS Department of Geodetic Science & Surveying The Ohio State University - 1958 Neil Avenue Columbus, Ohio 43210		10. PROGRAM ELEMENT, PROJECT, TASK AREA & WORK UNIT NUMBERS 61102F 2309G1AW
11. CONTROLLING OFFICE NAME AND ADDRESS Air Force Geophysics Laboratory Hanscom AFB, Massachusetts 01730 Contract Monitor: George Hadgigeorge /LWG		12. REPORT DATE October 1981
		13. NUMBER OF PAGES 137
14. MONITORING AGENCY NAME & ADDRESS (if different from Controlling Office)		15. SECURITY CLASS. (of this report) Unclassified
		15a. DECLASSIFICATION/DOWNGRADING SCHEDULE
16. DISTRIBUTION STATEMENT (of this Report) A - Approved for public release; distribution unlimited		
17. DISTRIBUTION STATEMENT (of the abstract entered in Block 20, if different from Report)		
18. SUPPLEMENTARY NOTES		
19. KEY WORDS (Continue on reverse side if necessary and identify by block number) geodesy, gravity, satellite-to-satellite tracking		
20. ABSTRACT (Continue on reverse side if necessary and identify by block number) ✓ The error analysis of the global modelling of the geopotential has been carried out up to degree and order 331 of the spherical harmonic expansion, for data from a low-low satellite-to-satellite tracking (SST) mission. The sphericity and the rotation of the Earth have been considered, as well as the discrete nature of the data, assumed to consist of time averages of the measured range-rate sampled at regular intervals. The expansion of the potential has been truncated at degree $n = 331$, because little information on higher degrees is likely to be present in the data. Two theories have been used: that of least		

DD FORM 1 JAN 73 1473

EDITION OF 1 NOV 65 IS OBSOLETE

UNCLASSIFIED

SECURITY CLASSIFICATION OF THIS PAGE (When Data Entered)

UNCLASSIFIED

SECURITY CLASSIFICATION OF THIS PAGE(When Data Entered)

squares adjustment, and that of least squares collocation; above degree $n = 200$ the accuracies predicted according to collocation are significantly better than those according to least squares. In this report there is also a discussion on how to process SST data to obtain very high resolution models of the gravitational field. Descriptions and listings of computer programs are included.

To reduce the computer time and storage needed to set up and to invert the normal matrix, a somewhat simplified orbital geometry and an approximate model of the data have been adopted; no orbit determination errors have been considered. Some arguments are given to justify these shortcuts, which may not affect seriously the validity of the results. An extension of the theory to non-polar orbits is given.

The main results according to collocation can be summed up as follows: if the two satellites move in much the same polar, circular orbit at a height of 160 km and at a distance of 300 km from each other; if the accuracy of the averaged range rate is $\sqrt{2} \times 10^{-6} \text{ m s}^{-1}$, the averaging interval is 4 s, and sampling takes place every 4 s; if residual data are used, with respect to a reference model of specified accuracy, complete to degree and order 20, then:

(1) the relative error in the estimated potential coefficients could be better than 1% up to degree $n = 130$, than 10% up to $n = 210$, and than 50% up to $n = 270$;

(2) the accuracy of point geoid undulation implied by the coefficients could be better than 0.05 mm rms in the band from 3000 km to 40030 km (total error in this band), and better than 10 cm rms in the band from 140 km to 3000 km (also total error).

UNCLASSIFIED

SECURITY CLASSIFICATION OF THIS PAGE(When Data Entered)

Foreword

This report was prepared by Dr. Oscar L. Colombo. Much of the research described in this report was carried out while Dr. Colombo was a Post Doctoral Research at The Ohio State University where the studies were supported under Air Force Contract No. F19628-79-C-0027, The Ohio State University Research Foundation Project 711664. The contract covering this research is administered by the Air Force Geophysics Laboratory, Hanscom Air Force Base, Massachusetts, with Mr. George Hadgigeorge, Contract Monitor. The actual writing of this report was carried out by Dr. Colombo at the Geodetic Institute of the University of Stuttgart in the Federal Republic of Germany.



Accession For	
NTIS GRA&I	<input checked="checked" type="checkbox"/>
DTIC TAB	<input type="checkbox"/>
Unannounced	<input type="checkbox"/>
Justification	
By	
Distribution/	
Availability Codes	
Avail and/or	
Dist	Special
A	

Acknowledgements

I wish to thank Professor Rapp, Project Supervisor, for providing the encouragement and the support that allowed me to begin and to carry out this research. Thanks also to Reiner Rummel, who is partly responsible for my interest in this problem, and who provided useful comments on parts of the manuscript; to Carl Wagner, for some interesting correspondence on SST; and to Susan Carroll, who did the typing.

This report was written during the first months of a visit to the Geodetic Institute of the University of Stuttgart, in the Federal Republic of Germany. This visit was sponsored by the Alexander von Humboldt Foundation. To the staff of this institution, and to Professor Erik Grafarend, whose liberality allowed me to finish this work, my most sincere appreciation.

Table of Contents

Foreword	iii
Acknowledgements	iv
1. Introduction	1
1.1 The Low-Low Configuration	5
1.2 The Band Limited Assumption	6
1.3 An Approximate Model for the Line of Sight Velocity	12
2. The Mathematical Model	17
2.1 Simplifying Assumptions	17
2.2 The Extended Legendre Function.	18
2.3 Time Series Expression of the Inertial Line of Sight Acceleration.	20
2.4 The Correction Term	22
2.5 The Observation Equation.	22
2.6 The Condition that N_r and N_d Must Be Relative Primes.	25
(a) Case where $m \neq q$	25
(b) Case where $m = q$	25
2.7 The Scalar Product of Two Columns of the A Matrix	26
2.8 Least Squares Adjustment.	28
2.9 The Structure of the Normal Matrix.	31
2.10 The Existence of G^{-1}	33
2.11 Least Squares Collocation.	35
2.12 Accuracy of the Computed Geoidal Heights	39
2.13 The Effect of Some Mission Parameters on Coefficient Accuracy	42
2.14 The Right Hand Sides of the Normals.	44
2.15 Oblique Orbits	46
3. Numerical Results.	50
3.1 Spectral Model and Error Formulas	50
3.2 Results According to Least Squares Adjustment	52
3.3 Results According to Least Squares Collocation.	54
3.4 Accuracies of Different Harmonics of the Same Degree.	63
4. Validity of the Results.	64
4.1 The Geometry of the Real Orbit.	64
4.2 Vertical Reduction to the Mean Sphere	66
4.3 The Effect of Errors in the Calculated Orbits	73
5. Data Processing.	74
5.1 An Iterative Approach	74
5.2 Other Methods	77
5.3 The Use of Local Solutions.	78
6. Conclusions.	78

References	81
Appendix A : Orbital Perturbations	84
Appendix B: Computer Programs	88
B.1 Main Program.	88
(a) Full Version	88
(b) Reduced Version.	92
B.2 Subroutine ONEREV	92
B.3 Subroutines LEGFDN, MODEL, and NVAR	93
B.4 Sample Output	94
Appendix C: Detailed Listings Degree by Degree.	123

1. Introduction

More than a decade ago, in 1968, Muller and Sjogren published their paper on lunar mass concentrations, or "mascons". In it they announced one of the most important conclusions about the internal structure of a member of the Solar System ever reached from the analysis of gravitation alone. With remarkable insight, they used the numerically differentiated range-rate tracking data of the lunar orbiters, deployed as part of the Apollo program, as "direct observations" of the acceleration of gravity along the line of sight between the tracking station on Earth and the spacecrafts circling the Moon. A simple plot of this information showed strong and roughly circular anomalies over the flatlands, or maria, suggesting the presence of large bodies of abnormal density buried in the lunar crust.

The idea that high resolution information on a gravitational field could be extracted by a simple analysis from differentiated range-rate data was seen, naturally enough, as having potential value for the study of our own planet. One more or less obvious adaptation of the idea was having two satellites: one in a very high orbit tracking the second one on a low orbit, much as the "high" station on Earth had tracked the "low" orbiters near the Moon. A different satellite-satellite tracking (SST) configuration, later to be known as the "low-low" approach (the first being the "high-low", of course), was proposed by Wolff in 1969: he thought that the relative velocity along the line of sight between two bodies following as close as possible the same near circular, polar orbit was, as a first approximation, the difference in anomalous potential between the two. As the Earth rotates, this pair would have eventually covered the whole planet with observations of gravity, all taken with the same "instrument", creating a global data set of extraordinary density and of uniform quality. From such data one should have been able to recover an almost as detailed, and far more complete, picture of the field than from terrestrial data alone. Though this idea suffered from some theoretical and practical problems, its appeal to the imagination was such that it inspired much research in spite of its shortcomings.

Among the first to help clarify the theory behind SST was Schwarz (1970), who proposed a rigorous mathematical formulation. Many studies followed to find out the best satellite arrangement, how the data could be processed, and what accuracy could be expected from the results. To all this one must add the work done on the development of suitable hardware, also along several lines.

In the mid-1970's, during the Apollo-Soyuz and the Geos-3 missions, "high-low" range-rate tracking data were gathered using the ATS-6 satellite, in geostationary orbit, as the high spacecraft, because of its steerable radar antenna. During the same period, the idea of a dedicated gravitational satellite mission began to develop. Both NASA and its European counterpart ESA drew up preliminary plans for a Gravity Satellite (GRAVSAT), and for a Space Laser Low Orbit Mission (SLALOM), respectively. Of the two, SLALOM is the most concretely defined at present (CSTG Bulletin No.2, 1980). It involves the simultaneous tracking by laser interferometry from the Space Laboratory, carried on the Space Shuttle, of two reflecting spheres to determine their relative velocities with respect to the shuttle and to each other. Recovery of gravity information is to be limited to a region

over the Eastern Mediterranean, and to a period of some seven days. This experiment is expected to be carried out during this decade. GRAVSAT, on the other hand, is a global concept that may take one of several possible configurations based on the SST principle or, alternatively, resort to an orbiting gradiometer. At present it appears likely that the SST idea will be tried first, in a GRAVSAT-A mission in the late 1980's, while the gradiometer, whose development into a practical instrument for this purpose is still at the "breadboard" stage, may be used in a GRAVSAT-B mission sometime in the 1990's. Several types of gradiometers have been considered. A promising design seems to be a supercooled instrument now under development at the University of Maryland, which may achieve a sensitivity of better than 0.001 E (Paik, 1981).

Of the various implementations of the "low-low" principle, the most likely to be adopted appears to be the DISCOS system of two drag-compensated satellites, capable of remaining in orbit for up to six months so close to the Earth that, without the periodical use of small rocket engines, their orbits would decay very quickly due to the atmospheric resistance. Two proof-masses, one inside each craft, will be kept in permanent free fall by the compensating mechanism, so only gravitational forces act upon them. Their relative line of sight velocity will be measured by an extremely accurate radar interferometric technique developed at the Applied Physics Laboratory of Johns Hopkins University (Pisacane and Yionoulis, 1980). Accuracies of better than 10^{-6} ms^{-1} are expected, provided that no serious problems due to ionospheric propagation are encountered.

Apart from the "high-low" and the "low-low" configurations, an intermediate "butterfly" arrangement, where two satellites follow different elliptical orbits, has been considered as well.

The SST data collected during the middle of the last decade were analysed in different ways. Among others, Kahn et al. (1978) tried to recover gravity anomalies using the "numerical" method of satellite geodesy, with the aid of the computer programme GEODYN; Hajela (1978) followed, instead, the original idea of treating the differentiated range-rates as gravity observations, and used least squares collocation as the processing technique. Marsh and Marsh (1978) attempted what was, in essence, an experiment like that of Muller and Sjogren with Earth data, to detect crustal and upper mantle structures. All these studies have been restricted to local areas, as no complete global set of SST has been obtained yet.

The work that has been done on the error analysis of the recovery of values of mean gravity anomalies, mean and point geoidal undulations, etc., can be divided, broadly, along two main lines: the "numerical" method of satellite geodesy, and the "direct" approach that goes back to Muller and Sjogren: using the differentiated range-rate values as observations. As an example of the first line, one can mention the work of Douglas et al. (1980), as one of the most recent. Of the second, the author is best familiar with the work of Hajela (1974), Rummel et al. (1976), Krynski (1978), Rapp and Hajela (1979), and Rummel (1980). All of these have considered local gravity field model improvements relying on the theory of least squares collocation. The ultimate accuracy of global recovery given a certain quality of data has been investigated, among others, by Breakwell (1979), who used a flat-earth approximation, while Jekeli and Rapp (1980) have employed a spherical, non-rotating Earth approximation.

While all the work mentioned above has been in progress, numerous meetings, involving government agencies and members of the scientific community that are potential users of GRAVSAT data, have taken place. Of several reports on these activities, there are two of particular importance that describe the objectives of a GRAVSAT mission and also define the required accuracies and other specifications for the results so they can be used meaningfully for geodetic and geophysical purposes. One is the report of a special panel of the Committee on Geodesy of the US National Academy of Sciences (1979); the other is by the GRAVSAT Users Working Group (1980). The main requirements defined so far are:

- a) For geological and geophysical applications, gravity information should be resolved at the Earth's surface through wavelengths of 100 km and to an accuracy of 2.5 to 10 mgals;
- b) Oceanographers need geoid heights accurate to some 10 cm in the band from 100 km to 3000 km.

The first specification is relevant to the study of the structure of the crust and the upper mantle. The second one is associated with the analysis of the instantaneous and average shape of the sea surface in studies that use such data as satellite altimetry. The difference between the sea surface and a horizontal surface can reveal many as yet unknown aspects of surface currents, tides, and transients of various kinds, particularly in regions of the oceans that are not sufficiently accessible by other means. Also of consequence to oceanography, as well as to many practical aspects of geodesy, such as satellite positioning techniques, is the obtention of a model for the gravity field that permits the calculation of very precise spacecraft orbits, so this is another important objective of GRAVSAT. Among the latest global studies those by Breakwell, and by Jekeli and Rapp, already mentioned, suggest that the DISCOS system could achieve both the quality and quantity of data needed to meet goals (a) and (b).

The present report describes the theory behind a global error analysis of a low-low mission of the DISCOS type, and gives the corresponding results. The latter are in broad agreement with some of the previous studies, notably Breakwell's and Jekeli and Rapp's. The approach taken has been the "direct" one of considering the differentiated range-rate signal as equal to the component of the gravitational line of sight acceleration, in an inertial frame, along the line of sight direction. This is only an approximation, but it simplifies greatly the mathematical treatment, and previous reports by Hajela (1978) and by Rummel (1980), already mentioned, indicate that it may be in good agreement with reality at short spatial wavelengths, both for the "high-low" and the "low-low" configurations, respectively. This model of the line of sight signal has been modified somewhat here by subtracting a term that depends only on radial distance to the geocenter to eliminate some unrealistic long-wave phenomena related to the large zero harmonic and to the other even zonals of the geopotential.

This work is concerned primarily with the optimal recovery of a geopotential model in the form of a spherical harmonic expansion of the potential of such a high degree and order (331) that its truncation error at satellite altitude (160 km) is nearly negligible, particularly in the presence of noise.⁽¹⁾ It differs from previous studies of this sort in that it considers a spherical, rotating Earth, and discrete data consisting of time-averages of the instantaneous range rate. Observation equations are obtained under the simplifying assumptions that the orbits are perfectly

circular, the satellites separation is constant, and that the orbits repeat themselves exactly every 179 days, i.e., the length of the whole mission. From these equations a normal matrix is formed that is then inverted taking advantage of its block-diagonal structure. Two adjustment techniques are considered and implemented: least squares adjustment, and least squares collocation. An argument based on an infinite series of successive approximations is used to show how the results obtained under such simplifying assumptions can be, in fact, close indicators of the maximum amount of information than can be extracted from a real, three-dimensional distribution of SST data. While orbital errors are not included in the analysis, it turns out that the effect of such errors on the estimated parameters is very small, although this particular result depends strongly on the model adopted for the line of sight signal.

The last section considers how the principles used in this study can be applied to the actual processing of SST data in order to obtain a very high resolution spherical harmonic model of the gravity field. Such models have important mathematical advantages, and there is no great problem in using them if this is done with adequate techniques (see Colombo (1981), for instance). Global data reduction is a very important problem, to which not enough attention has been paid so far.

The potential impact of SST and of satellite gradiometry on the future of geodesy and of geophysics appears great. It is a difficult and beautiful task, the work of many, through many years, to develop what begun as a simple and bright idea for studying the Moon into a tool for increasing our understanding of our own planet and, eventually, of the rest of the Solar System. If we are successful, this task could have a deeper and more lasting effect on pure and applied Earth sciences than any other ever attempted in geodesy before.

(1) In this "band-limited" situation, the optimal estimates of any other field-related quantities (undulations, gravity anomalies, etc.) can be obtained directly from the optimal estimates of the potential coefficients (see, for instance, Colombo (1981), paragraph 2.18). The same is true of the accuracies of those quantities.

1.1 The Low-low Configuration

Figure 1.1 shows two drag-compensated satellites S_1 and S_2 that have been placed almost in the same near-circular polar orbit so that, in inertial space, the plane of the common orbit contains the Earth's mean axis of rotation, which is aligned in the picture with the x_3 axis. The geocentric angle separating both satellites is $\psi = 2 \sin^{-1}(\frac{\rho}{2R})$ radians, where ρ is the length of the segment of line of sight between S_1 and S_2 . The positions of the spacecrafts in the system of geocentric inertial coordinates x_1, x_2, x_3 are represented by the vectors \underline{x}_1 and \underline{x}_2 , respectively. The line of sight vector $\underline{x}_{12} = \underline{x}_1 - \underline{x}_2$ is oriented, according to the picture, from South to North in the ascending passes. The sense of the orbit (prograde or retrograde) is not important. The mean orbital radius is R .

Both satellites turn round the Earth with approximately the same angular velocity $\omega = \sqrt{GM/R^3}$, while the Earth itself turns on its axis with mean angular velocity Ω . The points directly below each satellite describe groundtracks that envelope the whole surface of the planet as the mission progresses. Both satellites have the same instantaneous longitude, but their groundtracks are not identical: they are always ψ rad apart in the S-N direction and $\Omega\omega^{-1}\psi$ rad in the E-W direction. In what follows, the word "groundtrack", unless further explanation is given, should refer to that of the point midways between the satellites, along the line of sight, $P = \underline{x}_1 + \frac{1}{2} \underline{x}_{12}$.

The measuring device detects the relative velocity along the line of sight between two proof-masses, one inside each satellite, which are kept in permanent free-fall round the Earth by the drag-compensating mechanism. This mechanism compensates not only for drag, but for all other non-gravitational influences of consequence as well. The relative line of sight velocity is

$$\underline{v}_{12} = \dot{\underline{x}}_{12} \underline{e}_{12} \quad (1.1)$$

where

$$\dot{\underline{x}}_{12} = \dot{\underline{x}}_1 - \dot{\underline{x}}_2$$

is the relative inertial velocity, $\dot{\underline{x}}_1$ and $\dot{\underline{x}}_2$ being the absolute ones, while

$$\underline{e}_{12} = \rho^{-1} \underline{x}_{12} \quad (1.2)$$

is the unit vector along the line between S_1 and S_2 , and

$$\rho = ||\underline{x}_{12}|| = \sqrt{(x_{11}-x_{12})^2 + (x_{21}-x_{22})^2 + (x_{31}-x_{32})^2} \quad (1.3)$$

is the euclidean norm of \underline{x}_{12} , i.e., the distance between the two spacecrafts. The observed values of \underline{v}_{12} are averaged over Δa seconds and then transmitted to earth-side stations every Δt seconds, where $\Delta a < \Delta t$. These averages constitute the SST data to be studied here, and the expression for any one of them is

$$\bar{\underline{v}}_{12}(t) = \int_{t-\Delta a}^t \underline{v}_{12}(\tau) d\tau \quad (1.4)$$

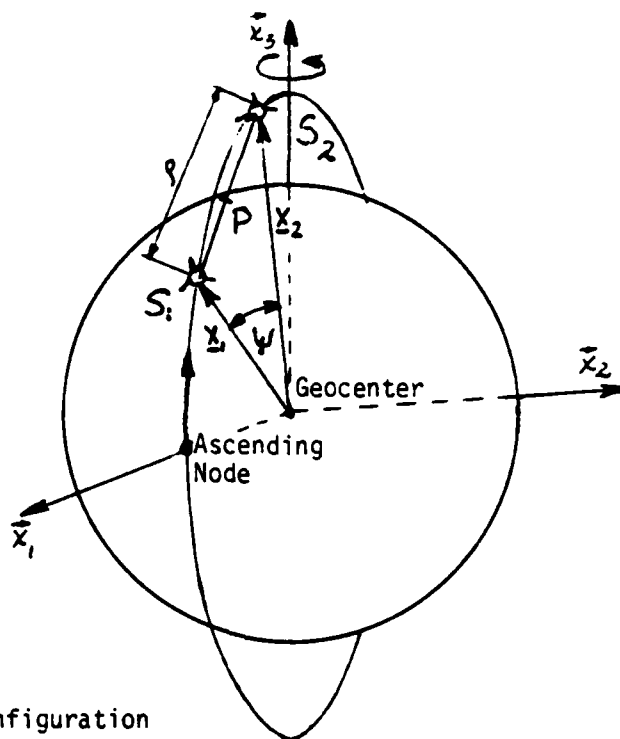


Figure 1.1:
The Low-Low Configuration

1.2 The Band-limited Assumption

The line of sight velocity v_{12} reflects small changes in the velocities of both satellites about their common average $v = R\omega$. These changes are brought about by the anomalous gravitational field, which is the difference between the true field and that of a homogeneous geocentric sphere of the same mass as the Earth and radius smaller than R .

The actual gravitational potential V can be represented in geocentric spherical coordinates (radial distance r , latitude ϕ , longitude λ) by a spherical harmonic expansion

$$V(r, \phi, \lambda) = \frac{GM}{r} \sum_{n=0}^{\infty} \sum_{m=0}^n \left(\frac{a}{r}\right)^n P_{nm}(\sin\phi) [\bar{C}_{nm} \cos m\lambda + \bar{S}_{nm} \sin m\lambda] \quad (1.5.a)$$

where $P_{nm}(\sin\phi)$ is the fully normalized associated Legendre function of the first kind, and \bar{C}_{nm} , \bar{S}_{nm} are fully normalized spherical harmonic coefficients. The following alternative notation will be used, wherever possible, in this work:

$$V(r, \phi, \lambda) = \frac{GM}{r} \sum_{n=0}^{\infty} \sum_{m=0}^n \sum_{\alpha=0}^1 \left(\frac{a}{r}\right)^n \bar{C}_{nm}^{\alpha} \bar{Y}_{nm}^{\alpha}(\phi, \lambda) \quad (1.5b)$$

with

$$\bar{C}_{nm}^{\alpha} \bar{Y}_{nm}^{\alpha}(\phi, \lambda) = P_{nm}(\sin\phi) \begin{cases} \bar{C}_{nm} \cos m\lambda & \alpha = 0 \\ \bar{S}_{nm} \sin m\lambda & \alpha = 1 \end{cases}$$

M is the mass of the Earth, G the universal constant of gravitation, "a" is the mean Earth radius, "n" indicates the degree, and "m" the order of each term in the expansion.

The three terms with $n=1$ are zero, because here the geocenter coincides with the origin on coordinates; the zero harmonic equals $\frac{GM}{r}$, so $C_{00}=1$. The anomalous potential is, therefore,

$$R(r, \phi, \lambda) = V(r, \phi, \lambda) - \frac{GM}{r} \quad (1.6)$$

The disturbing potential T , the modelling of which is the concern of this report, is the difference between the true potential V and some reference model potential U of the form

$$U(r, \phi, \lambda) = \frac{GM}{r} \sum_{n=0}^{NM} \sum_{m=0}^n \sum_{\alpha=0}^1 C_{nm}^{\alpha(M)} \bar{Y}_{nm}^{\alpha}(\phi, \lambda) \quad (1.7)$$

where NM is a relatively small integer (20 or 30). The objective of this study is finding out the accuracy with which a model of T of the same form as U , but truncated at a much higher order N , could be recovered from low-low SST data.

As explained later in this section, the time derivative of the line of sight velocity can be approximated by the component of the inertial acceleration aimed along the line of sight, minus a term independent from ϕ and λ . This acceleration is a linear combination of the three accelerations

$$a_r(r, \phi, \lambda) = \frac{\partial V}{\partial r} = -\frac{GM}{r^2} \sum_{n=0}^{\infty} \sum_{m=0}^n \sum_{\alpha=0}^1 \left(\frac{a}{r}\right)^n C_{nm}^{\alpha} \bar{Y}_{nm}^{\alpha}(\phi, \lambda) \quad (1.8,a)$$

$$a_{\phi}(r, \phi, \lambda) = \frac{1}{r} \frac{\partial V}{\partial \phi} = \frac{GM}{r^2} \sum_{n=0}^{\infty} \sum_{m=0}^n \sum_{\alpha=0}^1 \left(\frac{a}{r}\right)^n C_{nm}^{\alpha} \frac{\partial}{\partial \phi} \bar{Y}_{nm}^{\alpha} \quad (1.8,b)$$

$$a_{\lambda}(r, \phi, \lambda) = \frac{1}{r \cos \phi} \frac{\partial V}{\partial \lambda} = \frac{GM}{r^2 \cos \phi} \sum_{n=0}^{\infty} \sum_{m=0}^n \sum_{\alpha=0}^1 \left(\frac{a}{r}\right)^n C_{nm}^{\alpha} \frac{\partial}{\partial \lambda} \bar{Y}_{nm}^{\alpha} \quad (1.8,c)$$

where

$$\frac{\partial}{\partial \phi} \bar{Y}_{nm}^{\alpha} = \frac{d}{d\phi} P_{nm}(\sin \phi) \begin{Bmatrix} \cos \\ \sin \end{Bmatrix} m \lambda$$

and

$$\frac{\partial}{\partial \lambda} \bar{Y}_{nm}^{\alpha} = m P_{nm}(\sin \phi) \begin{Bmatrix} -\sin \\ \cos \end{Bmatrix} m \lambda$$

Because all these expansions converge outside the Earth's bounding sphere, the general terms of all of them should tend to zero with n tending to infinity, so the size of the harmonics should, in general, decrease as n increases. This decay must be accentuated by the factors $(\frac{a}{r})^n$, wherefore the field should become smoother with altitude, as the higher frequency terms vanish faster than the rest with increasing r . At satellite height $h=R-a$ this smoothing should mean that, above a certain degree N , all terms in the expansion can be neglected. Consequently, the field can be regarded as band-limited, with terms restricted to degrees in the band $0 \leq n \leq N$. As the error analysis method presented in section 2 requires computer time in proportion to N^4 , it is important to find a realistic value for N that is also as low as possible. The reasoning that follows attempts to provide a guide for such a choice using the decay in the spectrum of the line of sight inertial acceleration as a criterion.

To simplify matters, Earth rotation can be ignored, the orbit can be assumed to be perfectly circular, and the geocentric separation ψ to be constant. Under these conditions, all field dependent functions are periodical, the line of sight acceleration among them, and can be represented by Fourier series such as

$$a_{12}(t) = \sum_{k=0}^{\infty} a_k \cos k \omega t + b_k \sin k \omega t$$

As the Earth does not rotate in this case, one can choose an arbitrary system of geocentric coordinates $r'=r$, ϕ' , λ' where the "equator" coincides with the plane of the orbit, and then make the substitution

$$\lambda = [\omega t] \text{MODULE } 2\pi$$

so that the Fourier series becomes

$$a_{12}(\lambda) = \sum_{k=0}^{\infty} a_k \cos k \lambda + b_k \sin k \lambda$$

To find out the coefficients of this series, consider first the inertial line of sight acceleration in this system of coordinates. For the first satellite, let

$$a_1 = \begin{pmatrix} a_r(R, \phi' = 0, \lambda') \\ a_\phi(R, \phi' = 0, \lambda') \\ a_\lambda(R, \phi' = 0, \lambda') \end{pmatrix}^T \underline{e}_{12} \equiv \underline{a}_1^T \underline{e}_{12}$$

be the projection of its inertial acceleration along that line, and let

$$a_2 = \underline{a}_2^T \underline{e}_{12}$$

be the corresponding projection for the second satellite. Then the line of sight acceleration is

$$\begin{aligned} a_{12} &= a_1 - a_2 \\ &= \underline{e}_{12}^T (a_r(S_1) \underline{r}_0^{(S_1)} + a_{\phi'}(S_1) \underline{\phi}_0^{(S_1)} + a_{\lambda'}(S_1) \underline{\lambda}_0^{(S_1)}) \\ &\quad - \underline{e}_{12}^T (a_r(S_2) \underline{r}_0^{(S_2)} + a_{\phi'}(S_2) \underline{\phi}_0^{(S_2)} + a_{\lambda'}(S_2) \underline{\lambda}_0^{(S_2)}) \end{aligned} \quad (1.9)$$

where $\underline{r}(P)$, $\underline{\phi}(P)$, and $\underline{\lambda}(P)$ are the unit vectors pointing upwards, "S-N", and "W-E" at the general point $P(r, \phi', \lambda')$. Because the circular orbit now lies on the equatorial plane of the rotated system of coordinates, we have

$$\underline{e}_{12}^T \underline{\phi}_0^{(S_1)} = \underline{e}_{12}^T \underline{\phi}_0^{(S_2)} = 0 \quad (1.10, a)$$

From Figure 1.2 it is easy to see that

$$\underline{e}_{12}^T \underline{r}_0^{(S_1)} = -\underline{e}_{12}^T \underline{r}_0^{(S_2)} = -\sin \frac{\psi}{2} \quad (1.10, b)$$

and

$$\underline{e}_{12}^T \underline{\lambda}_0^{(S_1)} = \underline{e}_{12}^T \underline{\lambda}_0^{(S_2)} = \cos \frac{\psi}{2} \quad (1.10, c)$$

Calling the longitudes of S_1 and S_2 λ' and $\lambda' + \psi$, respectively,

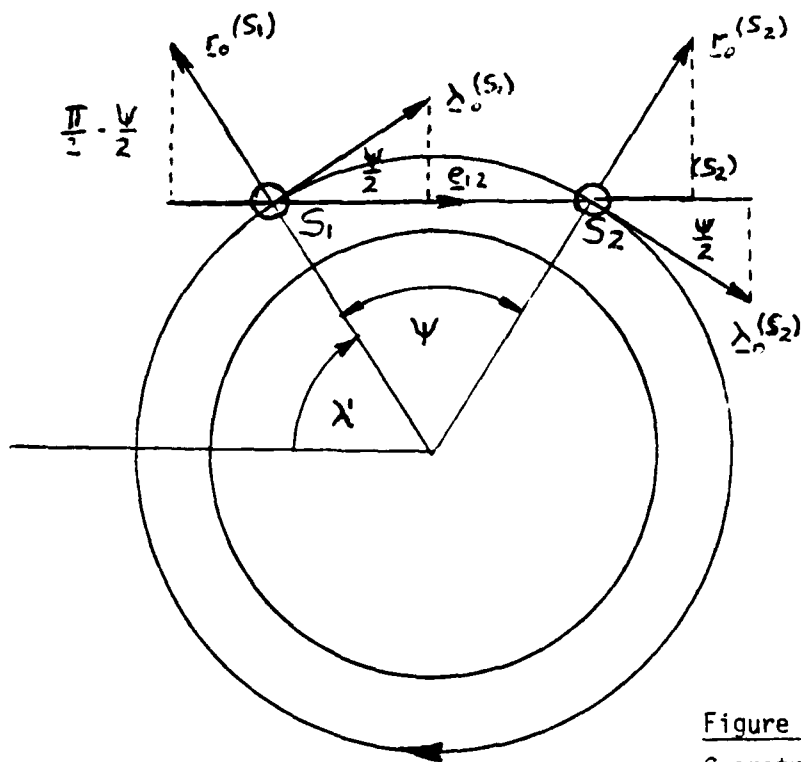


Figure 1.2:

Geometry of the Satellite Pair

replacing (1.8, a-c) and (1.10, a-c) in (1.9), rearranging terms (which is valid, because all the expansions converge uniformly outside the bounding sphere), and making use of simple trigonometric identities,

$$\begin{aligned}
 a_{12}(R, \phi'=0, \lambda') &= \frac{GM}{R^2} \sum_{m=0}^{\infty} \sum_{n=m}^{\infty} P_{nm}(0) \left(\frac{a}{r}\right)^n [(n+1)\bar{C}_{nm} \sin \frac{\psi}{2} + m\bar{S}_{nm} \cos \frac{\psi}{2}] \cos n\lambda' \\
 &+ [(n+1)\bar{S}_{nm} \sin \frac{\psi}{2} - m\bar{C}_{nm} \cos \frac{\psi}{2}] \sin n\lambda' - [-(n+1)\bar{C}_{nm} \sin \frac{\psi}{2} + m\bar{S}_{nm} \cos \frac{\psi}{2}] \\
 &- [-(n+1)\bar{S}_{nm} \sin \frac{\psi}{2} - m\bar{C}_{nm} \cos \frac{\psi}{2}] \sin m(\lambda' + \psi) \cdot \cos m(\lambda' + \psi) \quad (1.11)
 \end{aligned}$$

Therefore, the coefficients of the Fourier series for a_{12} are

$$\begin{aligned}
 a_m &= \frac{GM}{R^2} \sum_{n=m}^{\infty} P_{nm}(0) \left(\frac{a}{r}\right)^n \{ \bar{C}_{nm} [(n+1) \sin \frac{\psi}{2} (1 + \cos m\psi) + \\
 &+ m \cos \frac{\psi}{2} \sin m\psi] + \bar{S}_{nm} [m \cos \frac{\psi}{2} (1 - \cos m\psi) + (n+1) \sin \frac{\psi}{2} \sin m\psi] \} \quad (1.12, a)
 \end{aligned}$$

and

$$\begin{aligned}
 b_m &= \frac{GM}{R^2} \sum_{n=m}^{\infty} P_{nm}(0) \left(\frac{a}{r}\right)^n \{ \bar{C}_{nm} [-(n+1) \sin \frac{\psi}{2} - m \cos \frac{\psi}{2} (1 - \cos m\psi)] + \\
 &+ \bar{S}_{nm} [(n+1) \sin \frac{\psi}{2} (1 + \cos m\psi) + m \cos \frac{\psi}{2} \sin m\psi] \} \quad (1.12, b)
 \end{aligned}$$

where "m" has replaced the original subscript "k" for obvious reasons. The time integral $\int a_{12}(t) dt$ has a term of the form $a_0 t$ so it cannot be identical to v_{12} because the latter is periodical under the current assumptions. This problem can be solved by removing the constant term from the Fourier series of a_{12} , so the time derivative of v_{12} would be (approximately)

$$\begin{aligned}\hat{a}_{12} &= a_{12} - a_0 \\ &\approx \dot{v}_{12}\end{aligned}\quad (1.13)$$

and

$$\begin{aligned}v_{12} &= \int_0^\lambda \hat{a}_{12}(R, 0, \lambda') \frac{d\lambda'}{\omega} = \int_0^{\frac{t-\lambda}{\omega}} \hat{a}_{12}(\omega t') dt' \\ &= \sum_{m=1}^{\infty} a_m \frac{\sin \omega t}{m \omega} - b_m \frac{\cos m \omega t}{m \omega} + \sum_{m=1}^{\infty} \frac{b_m}{m \omega}\end{aligned}$$

If (1.13) can be accepted as a valid approximation, then

$$\begin{aligned}\frac{1}{T_S} \int_0^{T_S} \hat{a}_{12}^2 dt &= \frac{1}{2} \sum_{m=1}^{\infty} a_m^2 + b_m^2 \quad (\text{where } T_S = \frac{2\pi}{\omega}) \\ &= \sum_{m=1}^{\infty} P_m\end{aligned}\quad (1.14)$$

where $P_m = \frac{1}{2}(a_m^2 + b_m^2)$ is the power at the m th frequency. Consider now the averaging operator $M\{\}$, which will be encountered again in Section 2 in connection with the use of least squares collocation as an alternative to the usual least squares adjustment for obtaining a field model. This operator represents an average over all rotations; here it can be seen as averaging over all possible circular orbits round a non-rotating Earth. As shown, for instance, in (Colombo, 1981, Section 2),

$$M\{\bar{C}_{nm}^2\} = M\{\bar{S}_{nm}^2\} = \frac{\sigma_n^2}{2n+1} \quad (1.15,a)$$

$$M\{\bar{C}_{nm} \bar{S}_{kq}\} = 0 \quad \text{for all integer } n, m, k, \text{ and } q \quad (1.15,b)$$

$$M\{\bar{C}_{nm} \bar{C}_{kq}\} = M\{\bar{S}_{nm} \bar{S}_{kq}\} = 0 \quad \text{for } n \neq k, m \neq q \quad (1.15,c)$$

$$\text{where } \sigma_n^2 = \sum_{m=0}^n \bar{C}_{nm}^2 + \bar{S}_{nm}^2 \quad (1.16)$$

is usually called the "nth degree variance" of the potential coefficients. The average orbital power per wavelength is, then,

$$\hat{P}_m = M\{P_m\} = \frac{1}{2} M\{a_m^2 + b_m^2\} \quad (1.17,a)$$

for \hat{a}_{12} , and

$$S_m = \frac{1}{\omega^2 m^2} \hat{P}_m \quad (1.17,b)$$

for v_{12} . Squaring (1.12, a-b) and modifying the resulting expansion according to (1.15,a-c), (1.17,b) finally becomes

$$S_m = P_{rm} (1 + \cos m\psi) + P_{tm} (1 - \cos m\psi) + 2P_{rtm} \sin m\psi \quad (1.18)$$

where

$$P_{rm} = \frac{G^2 M^2}{2R^4 \omega^2 m^2} \sum_{n=m}^{\infty} \frac{\sigma_n^2}{2n+1} \left(\frac{a}{R}\right)^{2n} (n+1)^2 (1 - \cos \psi) \bar{p}_{nm}^2(0) \quad (1.19,a)$$

is the contribution from the radial acceleration,

$$P_{tm} = \frac{G^2 M^2}{2R^4 \omega^2 m^2} \sum_{n=m}^{\infty} \frac{\sigma_n^2}{2n+1} \left(\frac{a}{R}\right)^{2n} m^2 (1 + \cos \psi) \bar{p}_{nm}^2(0) \quad (1.19,b)$$

the corresponding contribution from the along-track acceleration, and

$$P_{rtm} = \frac{G^2 M^2}{2R^4 \omega^2 m^2} \sum_{n=m}^{\infty} \frac{\sigma_n^2}{2n+1} \left(\frac{a}{R}\right)^{2n} m(n+1) \sin \psi \bar{p}_{nm}^2(0) \quad (1.19,c)$$

is the average crossspectral power of the two.

At a height $R-a = 160$ km, the angular frequency of the satellites is $\omega = \sqrt{\frac{GM}{R^3}} = 1.196 \times 10^{-3}$ rad. s⁻¹. If the separation between the satellites is $\rho = 300$ km, so $\psi = 0.04594$ rad., and if the σ_n are those used in the error analysis of Section 3, empirically derived from terrestrial and satellite data, then the S_m are as listed in the table below:

Table 1.1

Spectral R.M.S. $(S_m)^{\frac{1}{2}}$ of the Line of Sight Velocity,
and $(\hat{p}_m)^{\frac{1}{2}}$ (acceleration)

spatial frequency m (cycles per rev.)	$(S_m)^{\frac{1}{2}}$ (cm s ⁻¹)	$(\hat{p}_m)^{\frac{1}{2}}$ (mgal)
0	0.	---
1	.335	.410
2	48.854	119.813
3	.348	1.279
4	.205	1.005
5	.170	1.044
10	.678 x 10 ⁻¹	.833
20	.268 "	.656
30	.192 "	.706
40	.130 "	.637
50	.932 x 10 ⁻²	.572
100	.855 x 10 ⁻³	.105
200	.394 x 10 ⁻⁴	.967 x 10 ⁻²
300	.107 x 10 ⁻⁵	.394 x 10 ⁻³
400	.207 x 10 ⁻⁷	.101 x 10 ⁻⁴
700	.817 x 10 ⁻¹¹	.701 x 10 ⁻⁸
1000	.544 x 10 ⁻¹⁴	.660 x 10 ⁻¹¹

Total rms of signal above

m = 0	48.86 cm s ⁻¹	120.32 mgal
20	0.06 cm s ⁻¹	4.44 mgal

To obtain the values listed above, the series in (1.19,a-c) were truncated at $n=1100$, though much the same results were obtained with $n=500$ (up to $m=300$), which suggests a strongly band-limited nature for \hat{a}_{12} and v_{12} . The prepon-

derance of the term with $m=2$ is due to the large second zonal and is related to the Earth oblateness. The signal in the data consists of time averages of v_{12} , so its spectrum should be smoother than the entries in the table suggest. For the purpose of this discussion, such a refinement is not necessary, and the effect of time-averaging will not be considered until Section 2.

With $\Delta t=4$ seconds, some $\frac{2\pi}{\Delta t \omega} \approx 1427$ samples of v_{12} are taken during each revolution of the satellites. Accordingly, the "Nyquist frequency" of the data is $N_y=713$. It is clear from the table that the power above this frequency is negligible, so that aliasing problems related to the sampling rate are likely to be insignificant. The question of choosing N , the highest degree in a band-limited model of the potential, so that this model can be regarded as realistic, is not an easy one, except for the fact that N does not have to be larger than 713. For this study the value of $N=331$ has been chosen purely on the basis that this number appeared to be, on preliminary estimates, the largest N compatible with the computing resources available to the author. The results in Section 3 show recovery errors of more than 80% of the actual values for the coefficients of harmonic $n=330$ and, for a number of reasons discussed in Section 4, these estimates are rather optimistic at the upper end of the spectrum. So, perhaps, $N=331$ is truly close to the upper limit of resolution for global estimation procedures of the kind considered here (least squares and collocation).

1.3 An Approximate Model for the Line of Sight Velocity

To estimate the accuracy with which the spherical harmonic coefficients of the geopotential can be recovered from SST data, one needs a model that relates the information in these data to those coefficients. A rigorous approach involves the solution of many variational differential equations for the two satellites, which could be done, in an average sense, by the "analytical" method so well described in Kaula's "Satellite Geodesy" (1966), and in an instantaneous sense, by the "numerical" approach, an example of which is the theory behind the famous "GEODYN" computer programme (Martin et al., 1970). Regrettably, except for some major break-through in computer science, the exact application of either technique to the global study of SST data from low-orbiting satellites does not seem feasible. The problem is the sheer size of the spherical harmonic model needed to represent this data realistically, with $N > 300$, as suggested in the previous paragraph, and some 4×10^6 observations over a six month mission. The largest models obtained to date (for instance GEM 9, by Lerch et al., 1977) by either technique from satellite tracking data alone have not exceeded $N=30$, and have already involved very lengthy operations. This does not mean that these methods have no role in the analysis of SST data: the "numerical", at any rate, has been used already for the recovery of gravity anomalies from

Apollo-Soyuz data (Kahn, 1979), and for the error analysis of a GRAVSAT mission (Douglas et al., 1980), but all this has been done on a local basis, and the purpose of this report is to look at the problem globally.

If a rigorous approach is not practicable, then one must seek some reasonable approximation that makes the task easier. In this work the author has followed the example of previous studies (Hajela, 1978; Rumme! 1980), assuming that the time-derivative of the line of sight velocity can be approximated to a sufficient extent by the line of sight component of the inertial acceleration. As explained in the previous paragraph, the inertial acceleration due to gravitation has an average component along that line that is not zero, due to the powerful zero harmonic GMr^{-2} and, to a much lesser extent, to the even zonals (consider (1.12,a) with $m=0$). A non-zero mean acceleration would bring the two satellites (in this case) together, contradicting the assumption that they can follow (with the right initial conditions) the same orbit with the same mean angular velocity. The effect of the zero harmonic alone, for a height of 160 km and $\rho=300$ km, is

$$a_0 = 2 \sin\left(\frac{\psi}{2}\right) \frac{GM}{R^2} \approx 43 \text{ gal.}$$

and the interpretation of this is plain enough: in the field of a central point mass two objects initially at rest would fall along the lines joining their initial positions to the attracting mass and, because their motions converge at this point, they would be moving closer to each other as well. Clearly, this is not the case when the two bodies turn in the same circular orbit, where the relative velocity and its derivative are always zero.

The approximation, it can be argued, can be much better for higher frequency effects, i.e., the departures of both velocity and acceleration from their values for a central mass field caused by the mass anomalies. The question is too complex to be settled by a simple argument, so the conclusions arrived at by previous authors and by this one, too, for that matter, are of necessity no more than educated guesses of a provisional nature. In the discussion that follows, I start by deriving rigorously the relationship between velocity and acceleration, and then introduce "order of magnitude" estimates for some of the factors involved.

To get directly to the results of interest, one should consider the residual line of sight velocity

$$\delta v_{12} = v_{12} - \dot{\sqrt{(c)}}_{12} \quad (1.20)$$

where $\dot{\sqrt{(c)}}_{12}$ is the velocity $(\dot{x}_1 - \dot{x}_2)^T \dot{e}_{12}$ computed by integrating the equations of motion numerically with the reference potential model U : this can be called the reference velocity. The residual velocity is what is likely to constitute the data in a real life situation, and has been taken for such in the error analysis of Section 3. Removing the reference velocity (at least in the ideal case where the model truly represents the field up to degree and order NM) has the advantage of taking away the very large effect of the second zonal whose presence is undesirable from a numerical point of view. As the computed orbit is likely to reflect very closely the effect of the attraction of the Sun, the Moon, and of the major planets, as well as the indirect effect of the tidal deformation of the Earth, the residual data are likely to be freer from these unwanted gravitational signals than the original data, resulting in less interference with the desired

information. Non-gravitational effects are removed, presumably, by the drag-compensating mechanism.

The time-derivative of the residual line of sight velocity is

$$\begin{aligned}\delta \dot{v}_{12} &= \frac{d}{dt} (\dot{x}_{12}^T \underline{e}_{12} - \dot{x}_{12}^{(c)T} \underline{e}_{12}^{(c)}) = \ddot{x}_{12}^T \underline{e}_{12} - \ddot{x}_{12}^{(c)T} \underline{e}_{12}^{(c)} + \dot{x}_{12}^T \dot{\underline{e}}_{12} - \dot{x}_{12}^{(c)T} \dot{\underline{e}}_{12}^{(c)} \\ &= \ddot{x}_{12}^T \underline{e}_{12} - \ddot{x}_{12}^{(c)T} \underline{e}_{12}^{(c)} + \dot{x}_{12}^T (\dot{x}_{12} - \dot{x}_{12} \underline{e}_{12} \underline{e}_{12}^T) \rho^{-1} - \dot{x}_{12}^{(c)T} (\dot{x}_{12}^{(c)} - \dot{x}_{12}^{(c)} \underline{e}_{12}^{(c)} \underline{e}_{12}^{(c)T}) \rho^{-1(c)} \\ &\approx [\ddot{x}_{12} - \ddot{x}_{12}^{(c)}]^T \underline{e}_{12} + \rho^{-1} [\dot{x}_{12}^T \dot{x}_{12} - \dot{x}_{12}^{(c)T} \dot{x}_{12}^{(c)} + (\dot{x}_{12}^{(c)T} \underline{e}_{12}^{(c)})^2 - (\dot{x}_{12}^T \underline{e}_{12})^2]\end{aligned}\quad (1.21)$$

assuming that the computed orbit differs from the true orbit by only a few meters, as it is believed to be the case when using contemporary tracking data and field models, so $\underline{e}_{12}^{(c)} \approx \underline{e}_{12}$ and $\rho^{(c)} \approx \rho$. The first term in (1.21) is the residual inertial line of sight acceleration, so the second term corresponds to the discrepancy between δv_{12} and $\delta a_{12} = a_{12} - a_{12}^{(c)}$. This second term can be written

$$\epsilon = \rho^{-1} [(\dot{x}_{12}^T \underline{e}_n)^2 - (\dot{x}_{12}^{(c)T} \underline{e}_n)^2] \quad (1.22)$$

where \underline{e}_n is the unit vector pointing outward along the normal to the line of sight. Therefore

$$\begin{aligned}\delta \dot{v}_{12} &= \delta a_{12} + \epsilon \\ &= \delta a_{12} + \rho^{-1} \delta (\dot{x}_{12}^T \underline{e}_n)^2\end{aligned}\quad (1.23)$$

So far the rigorous analysis. How large can ϵ be? Taking the mean value of ϵ over all rotations

$$M\{\epsilon\} = -M\{\delta (\dot{x}_{12}^T \underline{e}_n)^2\} = \rho^{-1} \left(\sum_{m=1}^{\infty} S_m^n - \sum_{m=1}^{\infty} S_m^{n(c)} \right) \quad (1.24)$$

where S_m^n and $S_m^{n(c)}$ are the average power at m cycles per revolution in $\dot{x}_{12}^T \underline{e}_n$ and $\dot{x}_{12}^{(c)T} \underline{e}_n$, respectively. These are, probably, of the same order of magnitude as $\dot{x}_{12}^T \underline{e}_{12}$ and $\dot{x}_{12}^{(c)T} \underline{e}_{12}$. As the model is restricted to spacial frequencies of NM cycles per revolution or less, it should be $S_m^{n(c)} = 0$ if $m > NM$. Replacing S_m^n with the S_m in (1.24), for $m > NM$ the summation should add up to

$$M_{\{\epsilon\}}^{m > NM} \approx \rho^{-1} \sum_{m=NM+1}^{\infty} S_m \quad (1.25)$$

where $M_{\epsilon}^{m \geq NM}$ symbolizes the contribution to ϵ from frequencies above NM . Comparing the mean value for the m th component of ϵ to the root mean square value for the corresponding component of δa_{12} , or $\dot{P}_m^{\frac{1}{2}}$,

$$\frac{M\{\epsilon_m\}}{\hat{p}_m^{\frac{1}{2}}} = \rho^{-1} \frac{S_m}{P_m^{\frac{1}{2}}} = \rho^{-1} \frac{\hat{p}_m^{\frac{1}{2}}}{m^2 \omega^2} \approx 3 \frac{\hat{p}_m^{\frac{1}{2}}}{m^2} \quad (1.26)$$

if $\rho=300\text{km}$ and $\omega \approx 1.2 \times 10^{-3}$. In spite of the presence of $\hat{p}_m^{\frac{1}{2}}$, this result is, in fact, dimensionless. From Table 1.1 follows that for $NM=20$, for instance, the right hand side of the expression above is $5. \times 10^{-3}$, Rummel (1981) has found, by a similar reasoning, that the ratio of $M\{\delta \dot{x}_{12}\}$ to the total rms of δa_{12} (with $NM=20$) may be less than 1.5×10^{-7} , which may be in agreement with expression (1.26): the relative error decreases with frequency because of the m^{-2} factor and of the fast decay of $\hat{p}_m^{\frac{1}{2}}$ with m , so the total ratio should be less than the partial ratio at $m=20$. Clearly, there are several assumptions involved in these results which have no obvious justification, except that they are not too unreasonable. As the question of "reasonable" or "unreasonable" is a tricky one, this author would conclude that, at this point, the omens look favorable for the model of the line of sight signal proposed here, but detailed studies should be done to verify this question further. It is not just a matter of deciding how to conduct an error analysis of a SST mission, but also whether it may be possible to find an algorithm for reducing the data from such a mission which, along the lines explained in section 5, could be capable of resolving potential coefficients to a much higher degree and order than it is possible at present with existing techniques. One way of conducting a more conclusive study of this matter may be to compute simulated orbits using a field with a broad spectrum, such as that of the point mass model used by Wagner and Colombo (1979), making this model rotate like the Earth, and to compute also the orbits corresponding to a "model potential" consisting of the first NM harmonics of the point mass field. From both sets of orbits one can obtain all the information needed to calculate the two terms in (1.23) and to compare them with each other in various ways, thus throwing a much brighter light on this whole subject. The field of the point mass model referred to above has, roughly, the same power spectrum as that of the Earth, but it is very easy to compute because it consists only of 200 mascons.

Not only the issue of the accuracy of the model proposed here for the line of sight signal can be clarified by numerical studies, but perhaps better models may emerge that share with the present one all the practical advantages and that are also truer to the real situation.

The model chosen for \dot{v}_{12} in this work is not a_{12} but, as explained in the previous paragraph, $\hat{a}_{12} = a_{12} - a_0$, where a_0 is a term independent of ϕ and λ , about which more will be said in section 2, and equal to the contribution to a_{12} of the zero harmonic and of the zero frequency terms in the Fourier expansions of the even zonals. It could be argued that the difference between this and the model used by previous workers (who like Rummel, have chosen $\dot{v}_{12} = a_{12}$) is trivial, because a_0 must be almost entirely removed when the reference velocity is subtracted from the data. This is true only if the orbit along which the reference velocity is computed coincides with the true orbit. In general, this is not the case, as orbital errors are present in the reference orbit. Because of these errors, the "removal" of the zero harmonic and even zonal effects accomplished by subtracting the reference velocity is not as thorough as if such effects had never been included in the definition of the time-derivative of v_{12} , as proposed here. If left in, the very large pseudo-effect of the zero harmonic would give the impression that orbital errors

have an influence on the estimated potential coefficients that is more important than with the present model. Therefore, the choice between the two models is not at all trivial. This is another aspect that could be clarified by careful numerical simulations.

2. The Mathematical Model

This section presents the observation and normal equations for the adjustment of spherical harmonic coefficients of the Earth's gravitation potential from low-low tracking data. These equations are derived here under some simplifying assumptions. The admissibility of such simplifications is discussed elsewhere, particularly in sections 1 and 4.

2.1 Simplifying Assumptions

Computations involving spherical harmonic expansions can be speeded up greatly if there are regularities in the distribution of the data. While such regularities may not occur in reality, actual and ideal distributions may be close enough to each other to ensure that the results obtained for the ideal situation are also applicable to the real one. The assumptions in question are:

- 1) both satellites describe coplanar, circular, polar orbits with the same geocentric radius R and with the same mean angular velocity ω ;
- 2) the plane of the orbits is fixed in inertial space, and fluctuations in the geocentric angle ψ between the two satellites are disregarded;
- 3) the Earth's angular velocity vector is fixed in inertial space, its magnitude is constant and equal to Ω , and its direction coincides with that of the figure axis;
- 4) the mission lasts an integer number of days N_D ; ω and Ω are commensurable, so the groundtracks of the satellites repeat themselves (for the first time) after N_D days; the total number of revolutions of the mid-point between satellites, N_r , is prime with respect to N_D ;
- 5) there is perfect compensation for ionospheric propagation, for radar pointing errors, and for all non-gravitational forces such as drag and solar pressure; the attractions of the Sun, Moon and major planets have been accounted for exactly when computing the satellite reference orbits and velocities (the data consists of residual velocities, i.e., differences between measured and reference values);
- 6) data are sampled at constant intervals of Δt seconds without interruptions during the whole mission; there is an exact number N_p of sampling intervals in the total time $T = N_D \times 24 \times 3600$ s, and $N_p = \frac{T}{\Delta t}$ is an even number;
- 7) the sampled values consist of the residual line of sight velocities averaged over Δa seconds, where $\Delta a \leq \Delta t$;
- 8) all data errors are uncorrelated, have zero mean, and the same standard deviation;
- 9) the line of sight inertial acceleration differs from the time derivative of the line of sight velocity only by a function of r (constant for a circular orbit);
- 10) at satellite altitude, the detectable gravitational signal is confined to harmonic terms of degree no larger than $N = 331$; the highest frequency in such terms is less than half of the sampling frequency $\frac{1}{\Delta t}$ c/s;

11) The only source of uncertainty is the presence of errors in the measured line of sight velocities.

Assumptions (5), (6), (7), and (8) by and large state what a perfectly successful mission should produce in terms of data; assumptions (9) and (10) have been explained already in section 1; assumption (11) is basically sound if assumption (9) is admissible, because as mentioned in paragraph (1.3) and further argued in section 4, (9) implies that the coupling between orbit determination and field modelling is weak, so orbital errors, provided they do not exceed a few meters, have little effect on the recovered potential coefficients. Assumptions (1) through (4) define a simplified geometry, the validity of which is treated in detail in section 4.

2.2 The Extended Legendre Function

The equation

$$L_{nm}(\phi) = \frac{(-1)^m (2n!)}{2^n n! (n-m)!} \cos^m \phi \left[\sin^{n-m} \phi - \frac{(n-m)(n-m-1)}{2(2n-1)} \sin^{n-m-2} \phi \right. \\ \left. + \frac{(n-m) \dots (n-m-3)}{2 \cdot 4 (2n-1)(2n-3)} \sin^{n-m-4} \phi \dots \right] \quad (2.1)$$

defines the function L_{nm} of ϕ that has the following properties:

- (a) $L_{nm}(\phi) = P_{nm}(\sin \phi)$ and $\frac{d^h}{d\phi^h} L_{nm}(\phi) = \frac{d^h}{d\phi^h} P_{nm}(\sin \phi)$ if $-\frac{\pi}{2} \leq \phi \leq \frac{\pi}{2}$
- (b) $L_{nm}(\phi) = L_{nm}(-\phi)$ if $n-m$ is even (2.2,a)
- $L_{nm}(\phi) = -L_{nm}(-\phi)$ if $n-m$ is odd (2.2,b)
- $L_{nm}(\phi) = L_{nm}(\pi-\phi)$ if m is even (2.2,c)
- $L_{nm}(\phi) = -L_{nm}(\pi-\phi)$ if m is odd (2.2,d)

in the interval $0 \leq \phi \leq 2\pi$.

From (a) and (b) one can infer that

- (1) $L_{nm}(\phi)$ is even if $n-m$ is even, odd if $n-m$ is odd;
- (2) $L_{nm}(\phi)$ has a finite Fourier expansion where the highest term is the n th harmonic and only sines or cosines are present, depending on the parity of $(n-m)$:

$$L_{nm}(\phi) = \sum_{p=0}^n h_p^{nm} \cos p\phi \quad \text{if } n-m \text{ is even} \quad (2.3,a)$$

$$L_{nm}(\phi) = \sum_{p=0}^n h_p^{nm} \sin p\phi \quad \text{if } n-m \text{ is odd;} \quad (2.3,b)$$

- (3) $L_{nm}(\phi)$ has half wave symmetry ($L_{nm}(\phi) = L_{nm}(\pi-\phi)$) if m is even, and half wave antisymmetry ($L_{nm}(\phi) = -L_{nm}(\pi-\phi)$) if m is odd. Sums of sines or of cosines which have such symmetries can contain only even or odd harmonics, so the Fourier expansion of L_{nm} must have only even terms if n is even, and only odd terms if n is odd. As a consequence, the Fourier coefficients

h_p^{nm} with p of opposite parity from n are all zero;
 (4) $L_{nm}(\phi)$ is continuous and infinitely differentiable in $0 \leq \phi < 2\pi$ and takes, together with all its derivatives, the same values as P_{nm} and all its derivatives in the interval $-\frac{\pi}{2} \leq \phi \leq \frac{\pi}{2}$.

The function L_{nm} is the analytical continuation of P_{nm} in the interval $0 \leq \phi \leq 2\pi$, and can be called for this reason the extended Legendre function of the first kind, degree n and order m in $0 \leq \phi \leq 2\pi$. Multiplying L_{nm} by the same normalizing factor as P_{nm} one obtains the fully normalized extended Legendre function

$$\bar{L}_{nm}(\phi) = \begin{cases} \sqrt{2n+1} L_{nm}(\phi) & \text{if } m = 0 \\ \sqrt{2(2n+1)} \frac{(n-m)!}{(n+m)!} L_{nm}(\phi) & \text{otherwise} \end{cases} \quad (2.4)$$

Consider now the spherical harmonic of degree n and order m

$$\bar{Y}_{nm}^{\alpha}(\phi, \lambda) = \bar{P}_{nm}(\sin \phi) \begin{Bmatrix} \cos \\ \sin \end{Bmatrix}_m \lambda \quad (2.5)$$

The maximum circle containing both poles and the point $(\phi=0, \lambda)$ on the equator consists of two meridians, of longitudes λ and $\lambda+\pi$, respectively. Along this circle, points can be ordered according to a parameter ϕ' in the interval $0 \leq \phi' \leq 2\pi$, which increases continuously from $(\phi'=0, \lambda)$ towards the N pole and beyond. The geocentric latitude ϕ , on the other hand, first increases towards the pole like ϕ' , but on crossing the pole begins to decrease again as it approaches the equator at $(\phi=0, \lambda+\pi)$, and it is negative in the southern hemisphere. The harmonic \bar{Y}_{nm}^{α} is a continuous function of ϕ' along the meridional circle, the same as its derivatives, and it follows from (2.5) and (2.2,c-d) that

$$\begin{aligned} \bar{Y}_{nm}^{\alpha}(\phi, \lambda+\pi) &= \bar{P}_{nm}(\sin \phi) \begin{Bmatrix} \cos \\ \sin \end{Bmatrix}_m(\lambda+\pi) \\ &= (-1)^m \bar{P}_{nm}(\sin \phi) \begin{Bmatrix} \cos \\ \sin \end{Bmatrix}_m \lambda \\ &= \bar{L}_{nm}(\pi-\phi) \begin{Bmatrix} \cos \\ \sin \end{Bmatrix}_m \lambda \\ &= \bar{L}_{nm}(\phi') \begin{Bmatrix} \cos \\ \sin \end{Bmatrix}_m \lambda = \bar{Y}_{nm}(\phi', \lambda) \end{aligned}$$

This relationship shows that by using \bar{L}_{nm} and ϕ' instead of \bar{P}_{nm} and ϕ one can formulate \bar{Y}_{nm}^{α} avoiding the complications that would arise otherwise because of the discontinuity in the value of the longitude at the poles. This is not a real discontinuity in the function \bar{Y}_{nm}^{α} , but merely a consequence of the way in which longitudes are defined.

Replacing $\bar{L}_{nm}(\phi')$ with its Fourier expansion (2.3,a-b) the harmonic becomes

$$\bar{Y}_{nm}^{\alpha}(\phi', \lambda) = \sum_{p=0}^n \bar{h}_p^{nm} \cos p \phi' \begin{Bmatrix} \cos \\ \sin \end{Bmatrix}_m \lambda \quad \text{if } n-m \text{ is even} \quad (2.7)$$

$$\sum_{p=0}^n \bar{h}_p^{nm} \sin p \phi' \begin{Bmatrix} \cos \\ \sin \end{Bmatrix}_m \lambda \quad \text{if } n-m \text{ is odd}$$

where

$$h_p^{nm} = \begin{cases} \sqrt{2n+1} & h_p^{nm} \quad \text{if } m = 0 \\ \sqrt{2(2n+1)} \frac{(n-m)!}{(n+m)!} & h_p^{nm} \quad \text{otherwise} \end{cases}$$

and there are only even Fourier terms if n is even, and odd terms if n is odd.

2.3 Time Series Expression of the Inertial Line of Sight Acceleration

Reasoning as in paragraph (1.2), but considering the line of sight oriented along a meridian (polar orbit) instead of along the equator, one gets the following expression for the line of sight relative inertial acceleration

$$\begin{aligned} a_{12} &= a_1 - a_2 \\ &= \underline{e}_{12}^T (\underline{r}_0^{(S_1)} a_r(S_1) + \underline{\phi}_0^{(S_1)} a_\phi(S_1) - \underline{r}_0^{(S_2)} a_r(S_2) + \underline{\phi}_0^{(S_2)} a_\phi(S_2)) \\ &= -(a_r(S_1) + a_r(S_2)) \sin \frac{\psi}{2} + (a_\phi(S_1) - a_\phi(S_2)) \cos \frac{\psi}{2} \end{aligned} \quad (2.8)$$

where terms containing the "across track" acceleration a_λ have been dropped because $\underline{\lambda}_0$ is always normal to the orbital plane and to the line of sight. Writing the radial and "along track" components a_r and a_ϕ according to (1.8,a-b), replacing P_{nm} with L_{nm} , and choosing the mid-point coordinates $\phi' = \frac{\phi_1 + \phi_2}{2}$, $\lambda = \frac{\lambda_1 + \lambda_2}{2}$ as independent variables,

$$\begin{aligned} a_{12}(R, \phi', \lambda) &= \frac{GM}{R^2} \sum_{n=0}^N \sum_{m=0}^n \{ (n+1) [L_{nm}(\phi' - \frac{\psi}{2}) + L_{nm}(\phi' + \frac{\psi}{2})] \sin \frac{\psi}{2} \\ &\quad + \frac{d}{d\phi} [L_{nm}(\phi' - \frac{\psi}{2}) - L_{nm}(\phi' + \frac{\psi}{2})] \cos \frac{\psi}{2} \} \left(\frac{a}{R} \right)^n C_{nm}^{\alpha} \cos m \lambda \\ &\quad + S_{nm} \sin m \lambda \} \end{aligned} \quad (2.9)$$

where N is the smallest degree such that $C_{nm}^{\alpha} = 0$, $n > N$, according to the band-limited assumption.

$$\text{Since } \bar{L}_{nm}(\phi' + \beta) = \sum_{p=0}^n \bar{h}_p^{nm} \begin{Bmatrix} \cos \\ \sin \end{Bmatrix} p(\phi' + \beta)$$

($\cos p(\phi' + \beta)$ if $n-m$ is even, $\sin p(\phi' + \beta)$ if $n-m$ is odd), it follows from elementary trigonometric relationships that

$$L_{nm}(\phi' + \beta) = \sum_{p=0}^n \bar{h}_p^{nm} \begin{Bmatrix} \cos p\phi' \cos p\beta - \sin p\phi' \sin p\beta \\ \sin p\phi' \cos p\beta + \cos p\phi' \sin p\beta \end{Bmatrix}$$

so

$$L_{nm}(\phi' - \frac{\psi}{2}) + L_{nm}(\phi' + \frac{\psi}{2}) = 2 \sum_{p=0}^n \bar{h}_p^{nm} \cos p \frac{\psi}{2} \begin{Bmatrix} \cos \\ \sin \end{Bmatrix} p\phi'$$

while

$$[C_{nm}(\phi' - \frac{\psi}{2}) - C_{nm}(\phi' + \frac{\psi}{2})] = 2 \sum_{p=0}^n \bar{h}_p^{nm} \sin p \frac{\psi}{2} \begin{Bmatrix} \sin \\ -\cos \end{Bmatrix} p \phi'$$

and therefore

$$\frac{d}{d\phi'} [C_{nm}(\phi' - \frac{\psi}{2}) - C_{nm}(\phi' + \frac{\psi}{2})] = 2 \sum_{p=0}^n \bar{h}_p^{nm} p \sin p \frac{\psi}{2} \begin{Bmatrix} \cos \\ \sin \end{Bmatrix} p \phi' \quad (2.10, b)$$

From expressions (2.9) and (2.10, a-b) follows that

$$a_{12}(R, \phi', \lambda) = \frac{GM}{R^2} \sum_{n=0}^N \sum_{m=0}^n [\sum_{p=0}^n 2\bar{h}_p^{nm} (n+1) \cos p \frac{\psi}{2} \begin{Bmatrix} \cos \\ \sin \end{Bmatrix} p \phi' + \sum_{p=0}^n 2\bar{h}_p^{nm} p \sin p \frac{\psi}{2} \begin{Bmatrix} \cos \\ \sin \end{Bmatrix} p \phi'] (\frac{a}{R})^n [\bar{C}_{nm} \cos m\lambda + \bar{S}_{nm} \sin m\lambda] \quad (2.11)$$

is the relationship between the value of the line of sight relative inertial acceleration for the two satellites and the spherical harmonic coefficients of the gravitational potential, the \bar{C}_{nm} . Carrying out various multiplications indicated in (2.11), and making use of the trigonometric equations

$$2\cos p\phi' \cos m\lambda = \cos(p\phi' + m\lambda) + \cos(p\phi' - m\lambda)$$

$$2\cos p\phi' \sin m\lambda = \sin(p\phi' + m\lambda) - \sin(p\phi' - m\lambda)$$

$$2\sin p\phi' \cos m\lambda = \sin(p\phi' + m\lambda) + \sin(p\phi' - m\lambda)$$

$$2\sin p\phi' \sin m\lambda = -\cos(p\phi' + m\lambda) + \cos(p\phi' - m\lambda)$$

leads to the expression

$$a_{12}(R, \phi', \lambda) = \frac{GM}{R^2} \sum_{n=0}^N \sum_{m=0}^n [\bar{C}_{nm} (\frac{a}{R})^n \sum_{p=0}^n a_p^{nm} \{ \cos(p\phi' + m\lambda) + \cos(p\phi' - m\lambda) \} + \bar{S}_{nm} (\frac{a}{R})^n \sum_{p=0}^n a_p^{nm} \{ \sin(p\phi' + m\lambda) - \sin(p\phi' - m\lambda) \}] \quad (2.12)$$

where

$$a_p^{nm} = \bar{h}_p^{nm} [(n+1) \cos p \frac{\psi}{2} \sin \frac{\psi}{2} + p \sin p \frac{\psi}{2} \cos \frac{\psi}{2}] \quad (2.13)$$

so

$$a_p^{nm} = 0 \quad \text{if } n \text{ and } p \text{ have different parities (par. 2.2, remark (3)).}$$

Introducing time as the independent variable through the formulas

$$\phi' = [\omega t]_{\text{mod } 2\pi} \quad (2.14, a)$$

and

$$\lambda = -[\Omega t]_{\text{mod } 2\pi} \quad (2.14, b)$$

and introducing the scaled harmonic coefficients

$$\tilde{C}_{nm} = \bar{C}_{nm} (\frac{a}{R})^n \frac{GM}{R^2} \quad (2.15, a)$$

$$\tilde{S}_{nm} = \bar{S}_{nm} (\frac{a}{R})^n \frac{GM}{R^2} \quad (2.15, b)$$

expression (2.13) becomes

$$a_{12}(t) = \sum_{n=0}^N \sum_{m=0}^n \tilde{C}_{nm} \sum_{p=0}^n a_p^{nm} \begin{Bmatrix} \cos(p\omega + m\Omega)t + \cos(p\omega - m\Omega)t \\ \sin(p\omega + m\Omega)t + \sin(p\omega - m\Omega)t \end{Bmatrix} \\ + \tilde{S}_{nm} \sum_{p=0}^n a_p^{nm} \begin{Bmatrix} -\sin(p\omega + m\Omega)t + \sin(p\omega - m\Omega)t \\ \cos(p\omega + m\Omega)t - \cos(p\omega - m\Omega)t \end{Bmatrix} \quad (2.16)$$

This last formula shows a_{12} as a time series representable by a finite Fourier series where the angular frequencies present have all possible values $p\omega \pm m\Omega$, $0 \leq p, m \leq N$, and the Fourier coefficients are sums of terms of the type $\tilde{C}_{nm} a_p^{nm}$ and $\tilde{S}_{nm} a_p^{nm}$, respectively. The time origin chosen should not influence the outcome of this analysis. The choice implied by (2.14,a-b) corresponds to $t = 0$ when the mid-point between the satellites is directly over the equatorial point (0,0).

2.4 The Correction Term

As explained in paragraph (1.2), the model for the time derivative of the relative line of sight velocity used in this study is not the relative inertial line of sight acceleration a_{12} , but this acceleration minus a time-invariant term a_0 (expression (1.13)), or modified acceleration \hat{a}_{12} . According to (2.16), this time-invariant part can only be due to terms where $p\omega \pm m\Omega = 0$. As indicated later in paragraph (2.6), one of the assumptions made in this study imply that $p\omega \pm m\Omega \neq 0$ if $0 < m \leq N$ so this leaves only the case $p=0, m=0$, corresponding to the even zonals, $n=0$ in particular. Therefore, the corrected acceleration is

$$\hat{a}_{12}(t) = a_{12}(t) - a_0$$

where

$$a_0 = \sum_{n=0}^N a_0^{n0} \tilde{C}_{n0} = \sum_{n=0}^N a_0^{n0} \tilde{C}_{n0} \left(\frac{a}{R}\right)^n \frac{GM}{R^2} \quad (2.17)$$

is a term that depends only on R , as expected.

2.5 The Observation Equation

One of the assumptions made in paragraph (2.1) was that the orbits are periodic with a period T equal to the length of the whole mission. Consequently, the various angular frequencies ($p\omega \pm m\Omega$) present in the right hand side of (2.16) are harmonics of fundamental frequency $\omega_0 = \frac{2\pi}{T}$. The modified line of sight relative inertial acceleration \hat{a}_{12} is regarded here as the true time derivative of the relative line of sight velocity, in accordance with expression (1.13). Therefore

$$v_{12}(t) = \int_0^t \hat{a}_{12}(t) dt + v_{12}(0) \quad (2.18)$$

Because of the assumption of orbital periodicity, replacing the integrand in (2.18) with the difference between the right hand side of (2.16) and a_0 according to (2.17), and integrating this difference term by term, one gets the following expression, where no zero frequency term is present:

$$v_{12}(t) = \sum_{n=2}^N \sum_{m=0}^n \tilde{C}_{nm} \sum_{p=z}^n a_p^{nm} \left\{ \frac{\sin(p\omega + m\Omega)t}{p\omega + m\Omega} + \frac{\sin(p\omega - m\Omega)t}{p\omega - m\Omega} \right. \\ \left. - \frac{\cos(p\omega + m\Omega)t}{p\omega + m\Omega} - \frac{\cos(p\omega - m\Omega)t}{p\omega - m\Omega} \right\} \\ + \tilde{S}_{nm} \sum_{p=z}^n a_p^{nm} \left\{ \frac{\cos(p\omega + m\Omega)t}{p\omega + m\Omega} - \frac{\cos(p\omega - m\Omega)t}{p\omega - m\Omega} \right. \\ \left. - \frac{\sin(p\omega + m\Omega)t}{p\omega + m\Omega} + \frac{\sin(p\omega - m\Omega)t}{p\omega - m\Omega} \right\} \quad (2.19)$$

where $z = \begin{cases} 0 & \text{if } m \neq 0 \\ 1 & \text{if } m = 0 \end{cases}$ and where \tilde{C}_{10} , \tilde{C}_{11} , \tilde{S}_{11} have been dropped as unknowns, because the origin of coordinates coincides with the geocenter. (2.20)

The actual observations consist of time averages \bar{v}_{12} of the measured relative line of sight velocity. This averages are taken over identical intervals of length Δa seconds, spaced Δt seconds apart. The signal in the observations is, then, the line of sight velocity averaged over Δa :

$$\bar{v}_{12}(t) = \frac{1}{\Delta a} \int_{t-\Delta a}^t v_{12}(\tau) d\tau \\ = \frac{1}{\Delta a} \sum_{n=2}^N \sum_{m=0}^n \tilde{C}_{nm} \sum_{p=z}^n a_p^{nm} \left\{ \frac{S((p\omega + m\Omega)t, \Delta a)}{(p\omega + m\Omega)^2} + \frac{S((p\omega - m\Omega)t, \Delta a)}{(p\omega - m\Omega)^2} \right. \\ \left. - \frac{C((p\omega + m\Omega)t, \Delta a)}{(p\omega + m\Omega)^2} - \frac{C((p\omega - m\Omega)t, \Delta a)}{(p\omega - m\Omega)^2} \right\} \\ + \tilde{S}_{nm} \sum_{p=z}^n a_p^{nm} \left\{ \frac{C((p\omega + m\Omega)t, \Delta a)}{(p\omega + m\Omega)^2} - \frac{C((p\omega - m\Omega)t, \Delta a)}{(p\omega - m\Omega)^2} \right. \\ \left. - \frac{S((p\omega + m\Omega)t, \Delta a)}{(p\omega + m\Omega)^2} + \frac{S((p\omega - m\Omega)t, \Delta a)}{(p\omega - m\Omega)^2} \right\} \quad (2.21)$$

where

$$C((p\omega \pm m\Omega)t, \Delta a) = \cos(p\omega \pm m\Omega)t \sin(p\omega \pm m\Omega) \Delta a \\ + \sin(p\omega \pm m\Omega)t (1 - \cos(p\omega \pm m\Omega) \Delta a) \quad (2.22,a)$$

and

$$S((p\omega \pm m\Omega)t, \Delta a) = \sin(p\omega \pm m\Omega)t \sin(p\omega \pm m\Omega) \Delta a \\ - \cos(p\omega \pm m\Omega)t (1 - \cos(p\omega \pm m\Omega) \Delta a) \quad (2.22,b)$$

The observed value at t_i consists of \bar{v}_{12} plus the measurement noise average over $t_i - \Delta a \leq t \leq t_i$, or n_i :

$$\bar{v}_{12}(t_i) + n_i = v_{12}(t_i)_{\text{obs}} \quad (2.23)$$

Rearranging the order of summation with respect to n and m in (2.19) and replacing the result in (2.23) one arrives to the observation equation as it will be used in the error analysis

$$\frac{1}{\Delta a} \sum_{m=0}^N \sum_{n=\max(m,2)}^N \tilde{C}_{nm} \sum_{p=z}^n a_p^{nm} \left\{ \frac{S((p\omega + m\Omega)t_i, \Delta a)}{(p\omega + m\Omega)^2} + \frac{S((p\omega - m\Omega)t_i, \Delta a)}{(p\omega - m\Omega)^2} \right. \\ \left. - \frac{C((p\omega + m\Omega)t_i, \Delta a)}{(p\omega + m\Omega)^2} - \frac{C((p\omega - m\Omega)t_i, \Delta a)}{(p\omega - m\Omega)^2} \right\} \\ -23-$$

$$+ \tilde{s}_{nm} \sum_{p=2}^n a_p^{nm} \left\{ \frac{C((p\omega + m\Omega)t_j, \Delta a)}{(p\omega + m\Omega)^2} - \frac{C((p\omega - m\Omega)t_j, \Delta a)}{(p\omega - m\Omega)^2} \right\} = \tilde{v}_{(obs)}^{(t_j)} + r_i \quad (2.24)$$

where $\max(m, 2)$ indicates the largest of m and 2 , and where r_i is the residual or difference between the measurement and the value calculated by replacing the \tilde{C}_{nm}^α with numbers in the left hand side. When these numbers are the true values of the unknown \tilde{C}_{nm}^α and the model is perfect (as it is supposed to be in the case here), then

$$r_i = -n_i$$

(all this is in keeping with established practice in geodetic literature). Consider the following vector notation

$$\underline{\tilde{v}}_{12}(obs) = [\tilde{v}_{12}^{(0)}(obs) \quad v_{12}^{(\Delta t)}(obs) \quad \dots \quad v_{12}^{(i\Delta t)}(obs) \quad \dots \quad v_{12}^{(T-\Delta t)}(obs)]^T \quad (2.25,a)$$

$$\underline{r} = [r_0 \quad r_1 \quad \dots \quad r_i \quad \dots \quad r_{N_p-1}]^T \quad (2.25,b)$$

$$\underline{c}_m = [\tilde{C}_{mm} \quad \tilde{C}_{(m+1)m} \quad \dots \quad \tilde{C}_{Nm}]^T \quad (2.25,c)$$

$$\underline{s}_m = [\tilde{s}_{mm} \quad \tilde{s}_{(m+1)m} \quad \dots \quad \tilde{s}_{Nm}]^T \quad (2.25,d)$$

$$\underline{c} = [\underline{c}_0^T \quad \underline{c}_1^T \quad \underline{s}_1^T \quad \underline{c}_2^T \quad \underline{s}_2^T \quad \dots \quad \underline{c}_m^T \quad \underline{s}_m^T \quad \dots \quad \underline{c}_N^T \quad \underline{s}_N^T]^T \quad (2.25,e)$$

where $\underline{\tilde{v}}_{12}(obs)$ and \underline{r} are both N_p - vectors and \underline{c} is a N_c - vector, N_p being the total number of observations (some 3.9×10^6 measurements over six months if $\Delta t = 4$) and $N_c = (N+1)^2 - 3$, the number of coefficients in the band (1) $2 \leq n \leq N$. The set of all observation equations, or system of observation equations, in matrix notation, is

$$\underline{A}\underline{c} = \underline{\tilde{v}}_{12}(obs) + \underline{r} \quad (2.26)$$

where A is the $N_p \times N_c$ matrix of the observation equations. The unknowns, according to (2.24), are the scaled potential coefficients \tilde{C}_{nm}^α , instead of the actual coefficients C_{nm}^α , which are the ones desired. Once the \tilde{C}_{nm} are known, however, the C_{nm}^α can be obtained by a trivial operation based on (2.15,a-b). The same is true of the standard deviations, which are the quantities relevant to this error analysis.

The observation equation (2.24) presents the relationship between data and unknowns in time. The corresponding relationship in space can be obtained directly from (2.24) by replacing ϕ' and λ for t in accordance to (2.14,a-b). The temporal representation, however, makes the overall treatment of what is to follow simpler, and is adopted here for this reason.

(1) Coefficients with $n > NM$ are actual field coefficients; with $n \leq NM$ (NM being the highest degree in the reference field model mentioned in paragraph (1.2)) the \tilde{C}_{nm}^α correspond to residual coefficients: the differences between the actual coefficients and the coefficients of the model, if the data consists of residual velocities, as assumed in section 3.

2.6 The Condition that N_r and N_D be Relative Primes

If Earth rotation and satellites revolution are congruent over the length of the mission, the total number of revolutions N_r and the total number of days N_D are both positive integers. According to condition (4) in paragraph 2.1 they are also relative primes, i.e., without common factors other than the unity. As shown here this property rules out certain relationships between the frequencies $p\omega \pm m\Omega$ in (2.24), the absence of which simplifies the mathematical treatment of the error analysis, as it will be explained in paragraph 2.7. Taking m in the interval $-N \leq m \leq N$, $p\omega \pm m\Omega$ can be written more simply as $p\omega + m\Omega$. The relationships of interest have the form

$$p\omega + m\Omega = j\omega + q\Omega \quad (2.27)$$

where either $p \neq j$, $m \neq q$, or both. The question as to whether such relationships are possible can be answered in two parts:

(a) Case where $m \neq q$:

If (2.27) is possible, then

$$\frac{m - q}{j - p} = \frac{\omega}{\Omega} = \frac{\omega \omega_0^{-1}}{\Omega \omega_0^{-1}} = \frac{N_r}{N_D} \quad (2.28)$$

where ω_0 is the fundamental angular frequency of the mission: $\omega_0 = \frac{2\pi}{T}$. As both N_r and N_D are positive it follows that $\frac{|m-q|}{|j-p|} = \frac{N_r}{N_D}$ so

$$|m - q| N_D = |j - p| N_r$$

As $|m - q| N_D$ and $|j - p| N_r$ are both positive integers and N_r and N_D have no common factors, it must be $|m - q| = N_r K$ for some $K \geq 1$, so

$$|m - q| \geq N_r \quad (2.29,a)$$

As $-N \leq m \leq N$ and $-N \leq q \leq N$, it follows that, under the band-limited assumption,

$$|m - q| \leq 2N \quad (2.29,b)$$

As a consequence of (2.29,a-b)

$$N_r \leq 2N \quad (2.29,c)$$

if (2.28) is true. In the present case, the number of revolutions over six months with the satellites at a height of 160 km exceeds 2900, while the maximum degree n of the harmonics in the band considered here is, according to paragraph (1.2), $N = 331$. This means that $2N < N_r$, contradicting (2.29,c) and thus, (2.28). Therefore, for the given satellite height and field bandwidth, (2.27) is impossible if $m \neq q$.

(b) $m = q$:

In this case (2.28) is never true, because the first member is always zero except in the trivial case $p = j$, where it is indeterminate. Therefore

(2.27) is also impossible when $m = q$ and, thus, whenever either $p \neq j$ or $m \neq q$ apply.

An immediate consequence of the impossibility of (2.27) under the assumptions of paragraph 2.1 is that

$$p\omega \pm m\Omega = 0 \quad (2.30)$$

is also impossible, except in the trivial case $p = 0, m = 0$, which has been excluded by the way in which the modified line of sight acceleration is defined (see expressions (1.13) and (2.17)). Since the rate of precession of the node of a polar orbit is nil, condition (2.30) corresponds to what is known in satellite geodesy as a resonant orbit. So the assumption that N_r and N_D are relative primes excludes resonances. This means that the orbit is not allowed to repeat itself after a number of revolutions that is a submultiple of N_r , so no sub-cycles occur within the grand cycle whose period is the length of the whole mission, i.e., T seconds or N_D days. Because of this, the sampling of the gravity field over the face of the Earth is the most even that is possible, as with resonances many arcs would be superimposed, so the "footprint" of the mid-point between the satellites would cover the ground rather coarsely. Without resonances, the arcs are all different and, thus, better spread out.

In reality, resonance is most unlikely to occur exactly: the actual situation is much too complicated. How realistic is, even so, the assumption that N_r and N_D are relative primes? While perfect congruence (both numbers integers) is also quite unlikely, the situation need not be too different from that implied by the assumption. Choosing $N_D = 179$ (a prime number) and $N_r = 2933$ (another prime), both are then relative primes. For the satellites to orbit, at 160 km, 2933 times around the Earth in precisely 179 days, a change in ω of only -4 parts per thousand from its actual value is needed or, equivalently, an increase in Ω of 4 p.p. thousand.

2.7 The Scalar Product of Two Columns of the A Matrix

If the N_p - vectors $\underline{a}_{nm}^\alpha$ and \underline{a}_{kq}^β are the columns in the matrix of observation equations A of (2.26) corresponding to the scaled coefficients \tilde{C}_{nm}^α and \tilde{C}_{kq}^β , respectively, then their scalar product

$$p_{nmkq}^{\alpha\beta} = (\underline{a}_{nm}^\alpha)^T \underline{a}_{kq}^\beta = \sum_{i=0}^{N_p-1} a_{nm}^{\alpha}(t_i) a_{kq}^{\beta}(t_i) \quad (2.31)$$

should depend, according to (2.24), on what the mission parameters $\Delta a, \Delta t$, and ψ are, and also on the values of sums of products of cosines and sines of the various arguments $(p\omega \pm m\Omega)t_i$, where the discrete values t_i cover the whole length of the mission. The products of the columns of A have to be obtained as part of the formation of the normal matrix of the adjustment, the inverse of which provides the a posteriori accuracies that are the main objective of the error analysis. Sums of products of sines and cosines sampled at regular intervals are strongly influenced by the relationship between the sampling frequency (inverse of the sampling interval Δt) and the highest frequency in the arguments of the trigonometric functions involved. In particular, it is important to know whether the highest frequency is below the Nyquist frequency (one half the sampling frequency) or not, in order to choose the most convenient treatment for those sums of trigonometric

products. In the case at hand $\Delta t = 4$ s, so the Nyquist frequency is

$$N_y = \frac{1}{2\Delta t} \text{ cycles/s} \\ = 0.125 \text{ c/s}$$

while the highest frequency, corresponding to the term $(N\omega + N\Omega)t$ is, for $N = 331$.

$$f_{\max} = \frac{331}{2\pi}(\omega + \Omega) = 0.066 \text{ c/s}$$

Therefore,

$$f_{\max} < N_y \quad (2.32)$$

or the highest frequency is less than the Nyquist frequency. Under this condition, the following formulas apply:

$$\sum_{i=0}^{N_p-1} \cos(p\omega \pm m\Omega)t_i \cos(j\omega \pm q\Omega)t_i = \sum_{i=0}^{N_p-1} \sin(p\omega \pm m\Omega)t_i \sin(j\omega \pm q\Omega)t_i \\ = \begin{cases} \frac{N_p}{2} & \text{if } (p\omega \pm \Omega) = (j\omega \pm q\Omega) \\ 0 & \text{otherwise} \end{cases} \quad (2.33,a)$$

$p = j = m = q = 0$ being excluded, and N_p being even;

$$\sum_{i=0}^{N_p-1} \cos(p\omega \pm m\Omega)t_i \sin(j\omega \pm q\Omega)t_i = 0 \text{ always} \quad (2.33,b)$$

From these formulas, and from expressions (2.22,a-b), one gets

$$\sum_{i=0}^{N_p-1} C((p\omega \pm m\Omega)t_i, \Delta a) C((j\omega \pm q\Omega)t_i, \Delta a) \\ = \sum_{i=0}^{N_p-1} S((p\omega \pm m\Omega)t_i, \Delta a) S((j\omega \pm q\Omega)t_i, \Delta a) = \begin{cases} N_p(1 - \cos(p\omega \pm m\Omega)\Delta a) & \text{if } p\omega \pm m\Omega = j\omega \pm q\Omega \\ 0 & \text{otherwise} \end{cases} \quad (2.34,a)$$

$p = j = m = q = 0$ being excluded, and N_p being even;

$$\sum_{i=0}^{N_p-1} C((p\omega \pm m\Omega)t_i, \Delta a) S((j\omega \pm q\Omega)t_i, \Delta a) = 0 \text{ always} \quad (2.34,b)$$

As a result of expressions (2.34,a-b) above, of the fact that $a_p^{nm} = 0$ if p has different parity from n , and of the fact that $p\omega \pm m\Omega \neq j\omega \pm q\Omega$ if at least $p \neq j$, as explained in the previous paragraph, replacing $a_{nm}^\alpha(t_i)$ and $a_{kq}^\beta(t_i)$ in (2.31) by their respective expressions according to (2.24), i.e.,

$$a_{nm}^{\alpha}(t_i) = \frac{1}{\Delta a} \sum_{p=z}^n a_p^{nm} \{ \}^{\alpha}$$

where $\{ \}^{\alpha}$ is the first or the second bracket in (2.24), depending on α , and similarly for $a_{kq}^{\beta}(t_i)$, one gets

$$p_{nmkq} = \begin{cases} 0 & \text{if } \alpha \neq \beta, m \neq q, n \begin{cases} \text{even} \\ \text{odd} \end{cases} \text{ and } k \begin{cases} \text{odd} \\ \text{even} \end{cases} \\ \frac{N_p}{\Delta a} \sum_{p=z}^{\min(n,k)} a_p^{nm} a_p^{km} \left[\frac{1 - \cos(p\omega + m\Omega) \Delta a}{(p\omega + m\Omega)^4} + \frac{1 - \cos(p\omega - m\Omega) \Delta a}{(p\omega - m\Omega)^4} \right] & \text{otherwise} \end{cases}$$

(2.35)

min(n,k) being the smallest of n and k.

as the expression for the scalar product, which shows that under the assumptions the product is zero in the majority of cases. This results in many elements in the normal matrix being zero as well, which is a major advantage when setting up this matrix, as only the relatively few non-zero elements have to be computed. Moreover, as shown in paragraph (2.9), a suitable ordering of the unknowns groups this non-zero elements in a block-diagonal structure, so inverting the very large normal matrix reduces itself to inverting the much smaller diagonal blocks, a crucial fact as far as the feasibility of obtaining the a posteriori covariance matrix is concerned. Finally, expression (2.35) shows that the non-zero elements can be computed from the values of the a_p^{nm} , which are the Fourier coefficients of the L_{nm} multiplied by scale factors (expression (2.13)). Because the a_p^{nm} are zero when p and n have different parities, because L_{nm} are expansions of sines only or of cosines only, and because n cannot be larger than $N = 331$, the total number of terms in the summation of (2.35) is much less than that of the terms in the summation of (2.31), resulting in considerable economies when computing the non-zero elements of the normal matrix.

The Fourier coefficients can be obtained by computing $\bar{L}_{nm}(\phi')$ at regular intervals $\Delta\phi' = \frac{2\pi}{2n}$ (the highest frequency in $L_{nm}(\phi')$ is that of $\cos n\phi'$ or $\sin n\phi'$) and then carrying out a numerical Fourier analysis, or discrete Fourier transform, of these values. This is done in the program of appendix B by means of a mixed-radix Fast Fourier Transform algorithm chosen on grounds of efficiency. Finding the required value of \bar{L}_{nm} in the interval $0 \leq \phi' < 2\pi$ is simplified by the use of expressions (2.2,a-c) and of the relationship $\bar{L}_{nm}(\phi') = \bar{P}_{nm}(\phi')$ if $0 \leq \phi' \leq \frac{\pi}{2}$, which reduces most of the effort to that of computing the values of \bar{P}_{nm} at regular intervals in $0 \leq \phi' \leq \frac{\pi}{2}$.

2.8 Least Squares Adjustment

Consider the quadratic form

$$Q = \underline{r}^T P \underline{r} \quad (2.36)$$

where P is a symmetric $N_p \times N_p$ matrix and where \underline{r} is the vector of residuals

$$\underline{r} = \underline{A}\underline{c} - \bar{\underline{v}}_{12}(\text{obs}) \quad (2.37)$$

according to (2.24), (2.25,b) and (2.26). The form (2.36) is a function of \underline{c} , the vector of potential coefficients, through (2.37). The vector $\hat{\underline{c}}$ that minimizes the quadratic form must satisfy the condition

$$\left(\frac{\partial Q}{\partial \underline{c}}\right)^T = (A^T P A) \hat{\underline{c}} - A^T P \bar{\underline{v}}_{12}(\text{obs}) = \underline{0} \quad (2.38)$$

(where $\underline{0}$ is a null N_c - vector) so

$$\hat{\underline{c}} = (A^T P A)^{-1} A^T P \bar{\underline{v}}_{12}(\text{obs}) \quad (2.39)$$

and the form has a minimum at $\hat{\underline{c}}$ provided P is a positive matrix. Expression (2.39) above can be written

$$\hat{\underline{c}} = F_p \bar{\underline{v}}_{12}(\text{obs}) \quad (2.40)$$

where F_p is the optimal estimator matrix corresponding to the weights matrix P . In general $\hat{\underline{c}} \neq \underline{c}$, because, even if the signal in the data ($\bar{\underline{v}}_{12}$) and the unknown parameters (\underline{c}) are related exactly to each other by the matrix equations $\bar{\underline{v}}_{12} = A \underline{c}$, the data $\bar{\underline{v}}_{12}(\text{obs})$ contains noise \underline{n} in addition to the signal. The noise \underline{n} propagates into the estimate

$$\hat{\underline{c}} = F_p \bar{\underline{v}}_{12}(\text{obs}) = F_p (\bar{\underline{v}}_{12} + \underline{n}) = F_p \bar{\underline{v}}_{12} + F_p \underline{n} \quad (2.41)$$

resulting in a difference between $\hat{\underline{c}}$ and \underline{c} , or error,

$$\hat{\underline{c}} - F_p \bar{\underline{v}}_{12} = F_p \underline{n} = -\underline{e}_n \quad (2.42)$$

The variance-covariance matrix of these errors in $\hat{\underline{c}}$, or a posteriori random errors, is

$$E_n = E \{ \underline{e} \underline{e}^T \} \quad (2.43)$$

where $E \{ \}$ is the usual mathematical expectation operator of statistics. The diagonal elements of the error matrix are the a posteriori variances of the estimated coefficients, or formal accuracies of the adjustment. If

$$P^{-1} = D = E \{ \underline{n} \underline{n}^T \} \quad (2.44)$$

where D is the $N_p \times N_p$ symmetrical and positive matrix corresponding to the data errors and known as the a priori variance-covariance matrix, then

$$\begin{aligned} E_n &= E \{ F_D \underline{n} (F_D \underline{n})^T \} = E \{ F_D \underline{n} \underline{n}^T F_D^T \} \\ &= F_D E \{ \underline{n} \underline{n}^T \} F_D^T = F_D D F_D^T \\ &= (A^T D^{-1} A)^{-1} A^T D^{-1} D D^{-1} A (A^T D^{-1} A)^{-1} \\ &= (A^T D^{-1} A)^{-1} = G^{-1} \end{aligned} \quad (2.45)$$

where $F_D = (A^T D^{-1} A)^{-1} A^T D^{-1}$

Matrix

$$G = A^T D^{-1} A \quad (2.46)$$

is known as the normal matrix, because (2.38) can be written

$$G \hat{c} = b \quad (2.47,a)$$

with

$$b = A^T D^{-1} \bar{v}_{12}(\text{obs}) \quad (2.47,b)$$

and (2.47,a) is the system of the normal equations. Therefore, when $P = D^{-1}$, the a posteriori variance-covariance matrix is identical to the inverse of the normal matrix. In particular, when all data errors are uncorrelated ($E \{n_i n_j\} = 0$) and all have the same standard deviation σ , then

$$D = \sigma^2 I$$

where I is the unit $N_p \times N_p$ matrix, so

$$G = A^T \sigma^2 I A = \sigma^2 A^T A \quad (2.48)$$

and the elements of the normal matrix have the form

$$g_{nmkq}^{\alpha\beta} = \sigma^{-2} (a_{nm}^{\alpha})^T a_{kq}^{\beta} = \sigma^{-2} p_{nmkq}^{\alpha\beta} \quad (2.49)$$

where, in the case under study, $p_{nmkq}^{\alpha\beta}$ can be calculated from (2.35). Among the important properties of the least squares estimate \hat{c} is that of being a minimum variance estimate when $P = D^{-1}$, which means that the diagonal elements of G^{-1} (and, then, their sum or trace $\text{tr} \{E_n\}$) are minimized. If the probability distribution of the error is gaussian, then the estimate \hat{c} is best in the sense that the a posteriori variances are the smallest for all estimates, linear or nonlinear. Moreover, the most likely value of \hat{c} coincides with \underline{c} , so \hat{c} is also the maximum likelihood estimate. When the model $\bar{v}_{12} = A \underline{c}$ is perfect, as assumed here, and $E \{n\} = 0$, then

$$E \{\hat{c}\} = (A^T D^{-1} A)^{-1} A^T D^{-1} (E \{\bar{v}_{12}\} + E \{n\}) = (A^T D^{-1} A)^{-1} A^T D^{-1} A \underline{c} = \underline{c} \quad (2.50)$$

For this reason, the estimate \hat{c} is called unbiased. Expression (2.50) further indicates that, in the absence of noise, the estimates are identical to the true values of the unknowns.

The rather impressive list of properties of the least squares estimator (2.39) with $P = D^{-1}$, together with the relative simplicity of the theory and rather straightforward nature of the calculations involved, have made this type of estimator the most widely used in geodesy as well as in many other branches of technology and of natural science. In reality, models are never exact, statistics never truly gaussian (this would include cases where the error is extremely large, but such occurrences are usually edited-out during pre-processing), or even truly known, so the practical implications of the theoretical properties of the estimator are somewhat obscure. What is clear is that (2.39) with $P = D^{-1}$ is a "sensible" way

of processing data, as it gives larger weights to the better measurements (those with smaller variances), and less weight to the worst (larger variances), at least when D is diagonal. If, as in the present case, all measurements are assumed to be equally good (same σ), then they are all weighted equally. From the point of view of the error analysis which is the purpose of this study, the determination of the formal accuracies requires creating and inverting the normal matrix G .

2.9 The Structure of the Normal Matrix

One of the assumptions made in paragraph (2.1) was that the errors in the data, the elements n_i of \underline{n} , were random, uncorrelated, and had all the same standard deviation σ . Consequently, the elements of the normal matrix G can be calculated from (2.49) and (2.35) which, combined, give

$$g_{nmkq}^{\alpha\beta} = \begin{cases} 0 & \text{if } m \neq q, \alpha \neq \beta, n \begin{cases} \text{even} \\ \text{odd} \end{cases} \text{ and } k \begin{cases} \text{odd} \\ \text{even} \end{cases} \\ \sigma^{-2} \frac{N_D}{\Delta a^2} \sum_{p=z}^{\min(n,k)} a_p^{nm} a_p^{km} \left[\frac{(1 - \cos(p\omega + m\Omega)\Delta a)}{(p\omega + m\Omega)^4} + \frac{(1 - \cos(p\omega - m\Omega)\Delta a)}{(p\omega - m\Omega)^4} \right] & \text{otherwise} \end{cases} \quad (2.51)$$

As already pointed out (par. (2.7)), there are many elements in G that are zero and it is possible to arrange the unknown $\underline{C}_{nm}^{\alpha}$ so that G exhibits a very convenient structure. Consider the ordering given in expressions (2.25,c-e) to the elements of \underline{c} , where

$$\begin{aligned} \underline{c} &= [\underline{c}_0^T \underline{c}_1^T \underline{s}_1^T \underline{c}_2^T \underline{s}_2^T \dots \underline{c}_m^T \underline{s}_m^T \dots \underline{c}_N^T \underline{s}_N^T]^T \\ \underline{c}_m &= [\underline{c}_{nm} \underline{c}_{(n+1)m} \underline{c}_{(n+2)m} \dots \underline{c}_{Nm}]^T \\ \underline{s}_m &= [\underline{s}_{nm} \underline{s}_{(n+1)m} \dots \underline{s}_{Nm}]^T \end{aligned}$$

and now separate each \underline{c}_m and \underline{s}_m in two halves $\underline{c}_m^{Y=0}$, $\underline{c}_m^{Y=1}$, and $\underline{s}_m^{Y=0}$, $\underline{s}_m^{Y=1}$, so $\underline{c}_m^{Y=0}$, $\underline{s}_m^{Y=0}$ contain only $\underline{C}_{nm}^{\alpha}$ where n is even, $\underline{c}_m^{Y=1}$, $\underline{s}_m^{Y=1}$ only $\underline{C}_{nm}^{\alpha}$ where n is odd. With the unknowns arranged in this way, the \underline{c}_m , \underline{s}_m contain coefficients of the same order m , the \underline{C}_{nm} "cosine" coefficients and the \underline{S}_{nm} "sine" coefficients, and each of these are split further according to parity. If all this is done, then G can be partitioned, as shown in figure 2.1, into blocks G_{mq} . Those along the main diagonal, or G_{mm} , correspond to unknowns of equal order m , and are further partitioned each into four blocks, according to α and β , and each of these four blocks into another four, according to the parities of n and k . All G_{mq} , except for those along the main diagonal, are zero matrices according to (2.51). In the diagonal G_{mm} only the sub-blocks where $\alpha = \beta$ and n and k have the same parity (dashed in the picture) can contain nonzero elements. This sub-blocks are diagonal sub-blocks, so the whole normal matrix is zero except for those diagonal sub-blocks: G is block diagonal.

More concretely, G contains $4 \times (N+1) - 4$ diagonal blocks that are not null matrices. According to (2.51), the elements of "cosine" blocks ($\alpha = \beta = 0$) are identical to those of "sine" blocks ($\alpha = \beta = 1$) in corresponding positions. This means that only the $2 \times (N+1) - 1$ "odd n " and "even n "

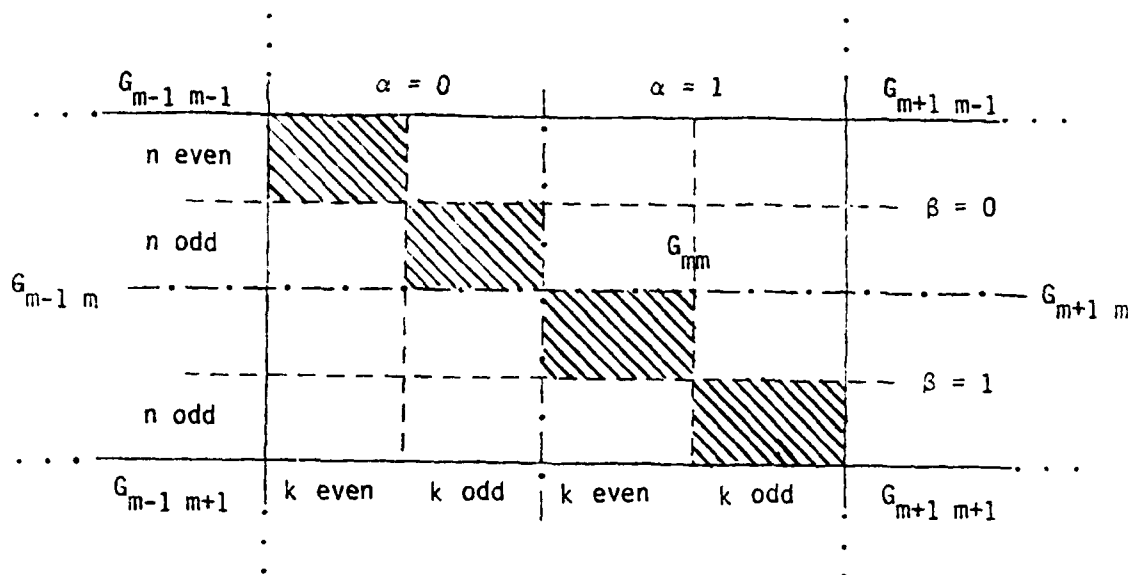


Figure 2.1: structure of the normal matrix

blocks have to be formed when setting up G , and only they have to be inverted when inverting G . The smallest blocks to be inverted have only one element and correspond to $m = N$; the two largest blocks have $\frac{1}{2}(N+1)^2$ elements each and correspond to $m = 0$ (zonals) with n even and odd, respectively. Altogether, the $2 \times (N+1) - 1$ blocks contain in the order of $\frac{1}{4}(N+1)^3$ different elements, as the blocks are also symmetrical. In the case of a general symmetrical matrix the total number of different elements to be computed is, approximately, $\frac{1}{2}(\text{dimension})^2$, or $\frac{1}{2}(N+1)^4$ in the case at hand. The reduction in calculations when setting up G is, therefore, of the order of $\frac{1}{2}(N+1)$. Furthermore, expression (2.13) shows that the a_p^{nm} can be computed from the scaled Fourier coefficients h_p^{nm} of the L_{nm} . As many h_p^{nm} are zero, as pointed out in paragraph (2.7), the number of operations using (2.51) rather than the general expression (2.49) is reduced by at least an order of magnitude. All these savings in computing make the setting up of such an enormous matrix (332^2 elements) quite feasible, although certainly not trivial when one adds to it the effort needed to obtain the values of L_{nm} from which the h_p^{nm} are then computed by Fourier analysis to give the a_p^{nm} according to (2.13). This whole operation required 50 c.p.u. minutes in the AMDHAL 470v/VI-II computer at O.S.U., using double precision and FORTRAN H extended in the highest optimizing mode. Another advantage of (2.51) is that it permits the setting up of the normal matrix without first having to form the observation equations matrix A , which is truly gigantic ($3.9 \times 10^6 \times 11 \times 10^4$ elements).

The inversion of a general matrix of the size of G , since the number of operations required to invert a $d \times d$ matrix is of the order of d^3 , would be impossibly laborious, requiring something like $(N+1)^6$ operations, or thereabouts. As only the small non-zero diagonal blocks have to be inverted, and only half of those are different, the actual number of operations is of the order of $\frac{1}{6}(N+1)^4$, or some $96(N+1)^2 = 1.06 \times 10^7$ times less than for a general matrix. Using the same computer, compiler, etc. mentioned

above, the inversion of G required some 15 min of central processor unit time. This is still a very large number of calculations. However, because the inversion involves the processing of independent blocks, each relatively small, the rounding errors due to finite register length (64 bits each double word) are confined so they can not affect the results in any appreciable way. Another property of a block-diagonal matrix is that, as the blocks are created and inverted independently, the whole procedure is ideally suited for parallel processing.

The programs used to form and invert G are documented and listed in appendix B.

2.10 The Existence of G^{-1}

Differential measurement, such as the relative line of sight velocity between the satellites, tend to be associated with observation and normal matrices that are rank-deficient, so it is reasonable to wonder whether the inverse of G , so important to an error analysis, does in fact exist at all. As shown here, this is not an entirely idle question, because there are cases where G is singular, though fortunately not with the mission parameters chosen in this study.

Two trivial examples of singular configurations are $\psi = 0$, when the whole matrix A vanishes, and G with it, and $\psi = \pi$, when all the columns of A corresponding to odd harmonic degrees are zero. If A is singular, G is singular too, so G^{-1} does not exist if

$$Az = 0$$

for some

$$z \neq 0$$

Calling Z_{nm}^α to the element of z corresponding to C_{nm}^α in c , then, according to (2.13), (2.22,a-b), and (2.24), the elements y_i of the vector $y = Az$ have the form

$$y_i = \sum_{\beta=0}^1 \sum_{m=0}^N \sum_{p=z}^N f_{pm}^\beta \begin{Bmatrix} \cos \\ \sin \end{Bmatrix} (p\omega \pm m\Omega)t_i \quad (2.52,a)$$

where

$$f_{pm}^\beta = \sum_{\alpha=0}^1 \sum_{j=m}^N a_p^{jm} f(\Delta a) Z_{jm}^\alpha \quad (2.52,b)$$

with

$$f(\Delta a) = \frac{1}{(p\omega \pm m\Omega)} \begin{Bmatrix} \sin(p\omega \pm m\Omega)\Delta a \\ 1 - \cos(p\omega \pm m\Omega)\Delta a \end{Bmatrix};$$

$$a_p^{jm} = h_p^{nm} \left[(j+1) \cos p \frac{\psi}{2} \sin \frac{\psi}{2} + p \sin p \frac{\psi}{2} \cos \frac{\psi}{2} \right] \text{ (expression (2.13))}$$

Expression (2.52.a) is a Fourier expansion with coefficients f_{pm}^β , and it can be zero only if all such coefficients vanish, as long as the sampling rate is higher than the highest frequency in the expansion, as it is the case here according to paragraph (2.7). In general, some elements

of \underline{z} can be zero, so assume that Z_{nm}^{α} is the element of highest degree and order that is not zero. In such case, $(n\omega + m\Omega)$ is the highest angular frequency in y_i . The only terms of this frequency are $f_{nm}' \sin(n\omega + m\Omega)$ and $f_{nm}'' \cos(n\omega + m\Omega)$ which cannot cancel each other out. For both to be zero for all t_i must be $f_{nm}' = f_{nm}'' = 0$. The other relevant factors involved in (2.52,b) are: Z_{nm}^{α} , which is assumed to be not zero; n_{nm}^R which is the Fourier coefficient of $\left[\frac{\psi}{2}\right]$ of highest frequency and cannot, for this reason, be zero; $\sin(n\omega + m\Omega)\Delta a$ and $1 - \cos(n\omega + m\Omega)\Delta a$ with $\Delta a > 0$, which cannot be simultaneously zero because for this to occur must be $(n\omega + m\Omega)\Delta t \geq (n\omega + m\Omega)\Delta a = k2\pi$, as $\Delta a \leq \Delta t$, but this is precluded by the sampling ratio Δt^{-1} being more than twice the highest frequency $(n\omega + m\Omega)/2\pi$ and, therefore, $(n\omega + m\Omega)\Delta a < (n\omega + m\Omega)\Delta t < 2\pi$. The only way in which the terms of frequency $(n\omega + m\Omega)$ can vanish for all t_i , for a given ψ , is that

$$(n+1) \cos n \frac{\psi}{2} \sin \frac{\psi}{2} + n \sin n \frac{\psi}{2} \cos \frac{\psi}{2} = 0 \quad (2.53)$$

for some n in $2 \leq n \leq N$, as $n = 0$ and $n = 1$ have been excluded from the model (paragraphs 2.4 and 2.5). This is a necessary condition for G^{-1} not to exist. Conversely,

$$(n+1) \cos n \frac{\psi}{2} \sin \frac{\psi}{2} + n \sin n \frac{\psi}{2} \cos \frac{\psi}{2} \neq 0 \quad (2.54)$$

for all n in $2 \leq n \leq N$ is a sufficient condition for G^{-1} to exist, or G not to be singular. Fortunately (2.54) is met by all n in $2 \leq n \leq 331$ with the chosen inter-satellite distance of 300 km (ψ approx. 0.046 rad). According to (2.53), the critical values of ψ at which (2.53) is met for some n in the band must be isolated points in $0 \leq \psi \leq 2$. If ψ coincided with some ϕ , and this were truly a point of singularity (remember that (2.53) gives only a necessary condition), then one could choose $\psi = \phi + \delta\psi$, with $\delta\psi$ arbitrarily small, and G^{-1} would still exist. From a practical point of view, G should become increasingly ill-conditioned as $\delta\psi \rightarrow 0$ and singularity is approached, so eventually it would be impossible to calculate G^{-1} numerically even when, theoretically, the inverse does exist. For that reason the stability of the numerical inversion of G should be checked by obtaining the differences

$$\Delta \underline{z} = \underline{z} - G_c^{-1} G \underline{z} \quad (2.55)$$

where G_c^{-1} is the computed inverse and \underline{z} an arbitrary N_c vector whose components are chosen from a sequence of random numbers. The stability can be judged from the number of significant figures that \underline{z} and $G_c^{-1} G \underline{z}$ have in common.

For small ψ , as it is the case with intersatellite separations, the first term in (2.53) can be much smaller than the second term, so the necessary condition for singularity can be written, after some obvious simplification

$$\sin n \frac{\psi}{2} = 0 \quad (2.56)$$

which is met for those critical values ϕ where $n\phi = 0, 2\pi, 4\pi, \dots, k2\pi, \dots$. Looking at the derivation of (2.13), on which (2.53) is based, one can see that the term ignored corresponds to the effect of the radial

component of the inertial acceleration on the line of sight velocity. In a flat Earth this component would be always perpendicular to the line of sight and have no effect at all, so (2.56) could be applicable to a flat Earth geometry. Breakwell (1979) has used a flat Earth approach, his results showing peaks in the noise to signal ratio, or percentage error, at those spatial wavelengths γ satisfying the condition $\psi = k\gamma$ with k integer. The spatial wavelength on the sphere for a harmonic of degree n is $\frac{2\pi}{n}$; replacing γ with $\frac{2\pi}{n}$ in "Breakwell's condition" $\psi = k\gamma$, one gets (2.56). A singularity in the operator involved, the G matrix for instance, would result in the relative error being infinite at some wavelength, indicating complete loss of information at the corresponding frequencies due to the differential nature of the measurements. While such singularities were not found in the spherical Earth analysis reported here because of the parameters chosen, there were nevertheless, some very gentle and broad ripples in the relative error as a function of the harmonic degree n , with maxima at those degrees where $n\psi$ was closest to $k2\pi$, as the reader can see by looking carefully at the results listed in appendix C.

2.11 Least Squares Collocation

In general, a linear estimator of \underline{c} from $\bar{v}_{12}(\text{obs})$ has the form

$$\hat{\underline{c}} = F \bar{v}_{12}(\text{obs}) = F(\bar{v}_{12} + \underline{n}) \quad (2.57)$$

where F is the $N_c \times N_p$ estimator matrix. In the case of least squares adjustment, as the reader may remember, this matrix was called F_p (expression (2.41)). As the least squares estimator of paragraph 2.8 is unbiased when the model $\bar{v}_{12} = A\underline{c}$ is perfect, the error in $\hat{\underline{c}}$ is due purely to the data errors:

$$\underline{e}_n = \underline{c} - \hat{\underline{c}} = -F\underline{n} \quad (\text{see (2.42)})$$

The purpose of least squares adjustment is to minimize the covariances of the elements of \underline{e}_n or, equivalently, the trace of the error matrix

$$E_n = E \{ \underline{e}_n \underline{e}_n^T \} = E \{ F \underline{e}_n \underline{e}_n^T F^T \} = F E \{ \underline{e}_n \underline{e}_n^T \} F^T = F D F^T \quad (2.58)$$

Not all linear estimators are unbiased. In general

$$\underline{e}_b = \underline{c} - F \bar{v}_{12} \neq 0 \quad (2.59)$$

where \underline{e}_b is the N_c - vector of bias errors in $\hat{\underline{c}}$. The gravity field (\underline{c} , \bar{v}_{12}) is "deterministic" (albeit unknown), while the noise \underline{n} is "stochastic", and the errors in $\hat{\underline{c}}$ that one and the other give rise to are also "deterministic" and "stochastic", respectively. What this difference boils down to is that the noise can be interpreted mathematically as a random process while the field and the bias cannot. To obtain estimators that minimize the total error (bias plus the effect of the noise) a method known as least squares collocation has been developed (Moritz, 1967, Krarup 1969) that treats both parts of the error in a way that is formally very similar, by using the operator $E\{\}$ for the noise, and the operator

$M\{\}$ (average over all rotations) for the bias. $E\{\}$ is a stochastic operator, while $M\{\}$ is a geometrical operator. If ε_b is the bias in the estimate \hat{c}_{nm} and ε_n the effect of the noise, then the error measure or "covariance" to be minimized is

$$\sigma_e^2 = M\{\varepsilon_b^2\} + E\{\varepsilon_n^2\}$$

This is a hybrid error measure (geometric plus stochastic), but has the advantage of being quadratic while ε_b and ε_n are linear functions of \hat{v}_{12} and \hat{n} , which simplifies the mathematical treatment. The rotations involved in the application of $M\{\}$ are those of the system of coordinates and, "attached" to it, as it were, of the pattern in which the data are sampled (i.e., the orbits). After each rotation both measurement sites and coordinates are different, and so are the values measured and the estimates, together with the bias. $M\{\}$ averages the error over all such "possible outcomes" (one outcome = one rotation). If the statistics of the noise \hat{n} are gaussian, so are those of ε_n . If $\varepsilon_b = 0$, one can determine the likelihood of \hat{c}_{nm} being within so many "sigmas" of the true value, if one knows only the covariance and the mean value of the data errors. With the "geometrical" statistics based on $M\{\}$ one would need, in general, not only $M\{\varepsilon_b^2\}$, but the higher moments $M\{\varepsilon_b^3\}$, $M\{\varepsilon_b^4\}$, . . . as well, as there is no great reason at present to believe that the gravity field is sufficiently "gaussian" to ignore them. Such moments can be "propagated" (in the sense in which covariances are "propagated") from the corresponding moments of the geopotential. The second moment is the covariance function (the Legendre transform of the spectrum σ_n^2) which depends only on the geocentric angle between two points on the same sphere. Higher moments are functions of many such angles. Determining the second moment or covariance from empirical data is not easy; obtaining the higher moments must be even harder, so probably working with these moments to obtain intervals of confidence is not practicable, at least at present. In practice, the choice of any approximation technique, such as collocation, should depend on how well it works for the sort of problem to be solved with it. In the case of geopotential coefficients determination, this author has conducted several numerical tests (Colombo, 1981) and found out that the square of the actual errors in \hat{c} can be very close to their hybrid a posteriori covariances when estimating \hat{c} with collocation. The data considered, however, were point and mean gravity anomalies, not SST data. For a discussion of the theory and applications of collocation in geodesy, the reader could see Moritz (1980).

To treat biases and propagated errors in a way that is formally the same, one could define a "variance-covariance" matrix for the biases

$$E_b = M\{\underline{\varepsilon}_b \underline{\varepsilon}_b^T\} \quad (2.60)$$

As already mentioned in paragraph 1.2, expressions (1.15,a-c),

$$M\{\hat{c}_{nm}^\alpha\} = 0; \quad M\{(\hat{c}_{nm}^\alpha)^2\} = \frac{\sigma_n^2}{2n+1}; \quad M\{\hat{c}_{nm}^\alpha \hat{c}_{kq}^\beta\} = 0 \quad \text{if } \alpha \neq \beta, n \neq k, \text{ or}$$

$m \neq q$, so the matrix

$$C = M\{\underline{\hat{c}} \underline{\hat{c}}^T\} \quad (2.61)$$

is diagonal. Each diagonal element in C equals

$$C_{nmkq}^{\alpha\beta} = \begin{cases} \delta\sigma_n^2 (2n+1)^{-1} & \text{if } n \leq M \\ \sigma^2 (2n+1)^{-1} & \text{if } n > M \end{cases}$$

where the $\delta\sigma_n^2$ correspond to the discrepancies $\hat{C}_{nm}^{\alpha} - \bar{C}_{nm}^{\alpha}$ between the actual coefficients and those of the reference model (paragraph 1.2). Replacing (2.59) in (2.60) and multiplying out one gets

$$\begin{aligned} E_b &= M \{ (\underline{C} - F \bar{V}_{12}) (\underline{C} - F \bar{V}_{12})^T \} = M \{ \underline{C} \underline{C}^T \} - 2M \{ \underline{C} \bar{V}_{12}^T F^T \} + M \{ F \bar{V}_{12} \bar{V}_{12}^T F^T \} \\ &= C - 2CA^T F^T + FACA^T F^T \end{aligned} \quad (2.62)$$

because $\bar{V}_{12} = A_c$. The error measure to be minimized is the trace of the combined error matrix

$$E_T = E_b + E_n = C - 2CA^T F^T + FACA^T F^T + FDF^T = C - 2CA^T F^T + F(ACA^T + D) F^T \quad (2.63)$$

according to (2.58) and (2.62), or $\text{tr} \{E_T\}$. The optimal estimator matrix minimizes $\text{tr} \{E_T\}$, so it must satisfy the matrix equation

$$\frac{\partial}{\partial F} \text{tr} \{E_T\} = F(ACA^T + D) - CA^T = 0 \quad (\text{null matrix}) \quad (2.64)$$

This equation is known as the "normal" equation. The solution is

$$F = CA^T (ACA^T + D)^{-1} \quad (2.65)$$

Using the matrix identity

$$CA^T (ACA^T + D)^{-1} = (A^T D^{-1} A + C^{-1}) A^T D^{-1} \quad (2.66)$$

(see, for instance, Uotila (1967), equation (29)) the optimal estimator is, finally, according to (2.46), (2.57), (2.65), and (2.66),

$$\begin{aligned} \hat{\underline{C}} &= (A^T D^{-1} A + C^{-1})^{-1} A^T D^{-1} \bar{V}_{12}(\text{obs}) \\ &= (G + C^{-1}) A^T D^{-1} \bar{V}_{12}(\text{obs}) \end{aligned} \quad (2.67)$$

which, except for the term C^{-1} , is the same as expression (2.39) (with $P = D^{-1}$) for leastsquares adjustment. If all the degree variances σ_n^2 of the potential are non zero for $2 \leq n \leq N$, C^{-1} exists, $G + C^{-1}$ is positive definite (sufficient condition for F in (2.65) to minimize $\text{tr} \{E_T\}$), and $(G + C^{-1})^{-1}$ exists as well, regardless of whether G is positive definite or singular. This is the case in the present study, so the problem discussed in paragraph 2.10 is not relevant, at least in theory, to least squares collocation. Ill-conditioning in $G + C^{-1}$, as distinct from singularity, is another matter. Fortunately, the stability of the inversion of $G + C^{-1}$ was as good as for G alone. As C^{-1} is diagonal, $G + C^{-1}$ retains the block-diagonal structure of G .

Expression (2.63) can be transformed as follows, when F satisfies (2.64):

$$\begin{aligned}
E_T &= C - FAC = C - (A^T D^{-1} A + C^{-1})^{-1} A^T D^{-1} AC \\
&= [I - (A^T D^{-1} A + C^{-1})^{-1} A^T D^{-1} A] C \\
&= (A^T D^{-1} A + C^{-1})^{-1} [A^T D^{-1} A C^{-1} - A^T D^{-1} A] C \\
&= (A^T D^{-1} A + C^{-1})^{-1} I \\
&= (G + C^{-1})^{-1}
\end{aligned} \tag{2.68}$$

so $(G + C^{-1})^{-1}$ is the "hybrid" variance-covariance matrix of the estimates, corresponding to G^{-1} in least squares, from which it differs only in the term C^{-1} . Expressions such as (2.67) and (2.68) have been used already in satellite geodesy for modelling the geopotential (Lerch et al., 1977).

In general, the bias matrix

$$\begin{aligned}
E_b &= (A^T D^{-1} A + C^{-1})^{-1} - E_n = (G + C^{-1})^{-1} - (G + C^{-1})^{-1} G (G + C^{-1})^{-1} \\
&= (G + C^{-1})^{-1} C^{-1} (G + C^{-1})^{-1}
\end{aligned} \tag{2.69}$$

is not zero, so the optimal estimator of collocation can be a biased estimator. Before the introduction of collocation in geodesy, the deliberate use of biased estimators in this discipline was unusual. In other fields, statistics for instance, biased estimators have had considerable application, for example in so-called "ridge regression" (see Bibby and Toutenberg, 1977) which is formally very similar to least squares collocation. The intentional use of biased estimators is quite common in communications, control engineering and in data processing generally, where the Wiener and Kalman filters have many uses. Both types of filter are, in fact, biased estimators whose mathematical formalism resembles that of collocation. But biased estimators are extensively used in everyday life too: every radio and audio system contains filters that "estimate" the desired component in the input signal (voice, music) by rejecting those frequencies at which unwanted signals, or noise, are most prevalent, and reinforcing those where the desired ones dominate. While the output is made intelligible, the signal itself has been distorted because those frequencies where it overlaps the noise have been smoothed out while the others have been boosted. If no noise were present, the true signal would not be identical to the "estimate" or audible output, the difference being a bias. The example is quite germane, as the amplifiers and filters in question are usually linear, like the estimators of collocation.

Estimating the covariance function or the power spectrum of the gravitational potential from existing data, always incomplete and imperfect, is a problem that entails some deep and difficult theoretical questions (Moritz, 1980). From a practical point of view, one could estimate the degree variances needed for C in (2.67) and (2.68) from the SST data itself by using expressions (1.18) and (1.19,a-c) to set up observation equations relating the average spectral power S_n (observable, in principle) to the unknown σ_n^2 ($0 < n < N$), and then adjusting the latter in the manner proposed by Wagner and Colombo (1979) for high-low SST data. The short-arc spectral technique discussed there for circular orbits was later extended by Wagner (1980) to elliptical orbits as well.

In the last analysis, how well the σ_n^2 must be known depends on how sensitive the estimates and the posteriori "hybrid covariances" are to errors in the adopted values of the degree variances. In section 3 there is a comparison of results obtained using two different models for the power spectrum, showing low sensitivity even when the discrepancy between the spectra is considerable, so this may not be a serious problem.

Throughout the discussion one has considered the estimation of the actual potential coefficients \tilde{C}_{nm}^α instead of the scaled \tilde{C}_{nm}^α . The only real change needed is in expression (2.61), where the scaled elements of the diagonal of C are

$$\tilde{C}_{nmnm}^{\alpha\alpha} = \frac{(GM)^2 a^2 n}{R^2 n^4} \times \begin{cases} \delta \sigma_n^2 (2n+1)^{-1} & n \leq M \\ \sigma_n^2 (2n+1)^{-1} & n > M \end{cases} \quad (2.70)$$

After inverting the thus modified $(G + C^{-1})$ matrix, the actual a posteriori degree variances

$$\tilde{\sigma}_n^2 \varepsilon_n = \sum_{\alpha=0}^1 \sum_{m=0}^n M\{(\varepsilon \tilde{C}_{nm}^\alpha)^2\} + E\{(\varepsilon \tilde{C}_{nm}^\alpha)^2\}, \text{ where } \varepsilon \tilde{C}_{nm}^\alpha = \tilde{C}_{nm}^\alpha - \tilde{C}_{nm}^\alpha,$$

can be obtained from the scaled a posteriori variances

$$\sigma_n = \sum_{\alpha=0}^1 \sum_{m=0}^n M\{(\varepsilon \tilde{C}_{nm}^\alpha)^2\} + E\{(\varepsilon \tilde{C}_{nm}^\alpha)^2\}$$

with the relationship

$$\sigma_n^2 \varepsilon_n = \frac{R^{2n+4}}{(GM)^2 a^2 n} \tilde{\sigma}_n^2 \varepsilon_n \quad (2.71)$$

2.12 Accuracy of the Computed Geoidal Heights

One of the main geophysical applications of GRAVSAT should be to provide an accurate description of the geoid at sea, as reference surface for oceanographic studies of currents, eddies, etc. The geoid height, or difference in ellipsoidal height between the geoid and the reference ellipsoid, is

$$N(r, \phi, \lambda) = r \sum_{\alpha=0}^1 \sum_{n=2}^{\infty} \sum_{m=0}^n \tilde{C}_{nm}^\alpha \tilde{V}_{nm}^\alpha(\phi, \lambda) \left(\frac{a}{r}\right)^n \quad (2.72)$$

assuming that all masses are contained inside the ellipsoid. When this is not the case, and the \tilde{C}_{nm}^α correspond to the expansion of the geopotential outside the bounding sphere (i.e. those that can be sensed by SST data for $2 \leq n \leq N$), expression (2.72) can be said to correspond to the free air geoid. As the geoid experiences periodical and secular variations, what is discussed here should be regarded as an average geoid for a given period of time (say, during the GRAVSAT mission), but this average can be corrected for the main fluctuations, such as tidal effects, to obtain the instantaneous geoid.

Using the estimated potential coefficients one can compute the first $(N+1)^2 - 3$ terms in (2.72) (the band-limited assumption does not apply at sea level)

$$\hat{N}(r, \phi, \lambda) = r \sum_{\alpha=0}^1 \sum_{n=2}^N \sum_{m=0}^n \hat{C}_{nm}^{\alpha} Y_{nm}^{\alpha}(\phi, \lambda) \left(\frac{a}{r}\right)^n \quad (2.73)$$

and the difference between (2.72) and (2.73) is the error in geoid height

$$\delta N(r, \phi, \lambda) = r \sum_{\alpha=0}^1 \sum_{n=2}^N \sum_{m=0}^n \varepsilon_{nm}^{\alpha} \bar{Y}_{nm}^{\alpha} \left(\frac{a}{r}\right)^n + r \sum_{\alpha=0}^1 \sum_{n=N+1}^{\infty} \sum_{m=0}^n \bar{C}_{nm}^{\alpha} Y_{nm}^{\alpha} \left(\frac{a}{r}\right)^n \quad (2.74)$$

The square of this error is

$$\delta N(r, \phi, \lambda)^2 = r^2 \sum_{\alpha=0}^1 \sum_{\beta=0}^1 \sum_{n=2}^{\infty} \sum_{k=2}^{\infty} \sum_{m=0}^n \sum_{q=0}^n \bar{D}_{nm}^{\alpha} \bar{D}_{kq}^{\beta} \bar{Y}_{nm}^{\alpha} \bar{Y}_{kq}^{\beta} \left(\frac{a}{r}\right)^{2n},$$

$$\text{where } \bar{D}_{nm}^{\alpha} = \begin{cases} \varepsilon_{nm}^{\alpha} & n \leq N \\ \bar{C}_{nm}^{\alpha} & n > N \end{cases}$$

If the \hat{C}_{nm}^{α} are obtained by least squares adjustment, the variance of the errors would be

$$E\{\delta N(r, \phi, \lambda)^2\} = \sigma^2 \delta N(r, \phi, \lambda)$$

Keeping r constant and averaging $\sigma^2 \delta N(r, \phi, \lambda)$ over the unit sphere (i.e., with respect to ϕ and λ alone)

$$\begin{aligned} \sigma^2 \delta N(r) &= \frac{1}{4\pi} \int_0^{\pi} \int_0^{2\pi} \sigma^2 \delta N(r, \phi, \lambda) \cos \phi \, d\phi \, d\lambda = \\ &= \frac{r^2}{4\pi} \sum_{\alpha, \beta, n, k, m, q} \left(\frac{a}{r}\right)^{2n} E\{\bar{D}_{nm}^{\alpha} \bar{D}_{kq}^{\beta}\} \int_0^{\pi} \int_0^{2\pi} \bar{Y}_{nm}^{\alpha} \bar{Y}_{kq}^{\beta} \cos \phi \, d\phi \, d\lambda = \\ &= r^2 \sum_{\alpha, n, m} \sigma^2 \varepsilon_{nm}^{\alpha} \left(\frac{a}{r}\right)^{2n} = r^2 \left(\sum_{n=2}^N \sigma^2 \varepsilon_n \left(\frac{a}{r}\right)^{2n} + \sum_{n=N+1}^{\infty} \sigma^2_n \left(\frac{a}{r}\right)^{2n} \right) \quad (2.75) \end{aligned}$$

because of the orthogonality properties of spherical harmonics. In an entirely similar way one can arrive to exactly the same expression for the mean square error when the \hat{C}_{nm}^{α} are estimated by collocation, except that $\sigma^2 \varepsilon_n$ is now a hybrid degree variance in the sense explained in the previous paragraph. As the error depends on r , and r is not constant on the ellipsoid, one could settle for an "average" error by choosing $r = a$, where a is the mean Earth radius, so

$$\sigma_{\delta N}^2 = a^2 \left(\sum_{n=2}^N \sigma_{\varepsilon_n}^2 + \sum_{n=N+1}^{\infty} \sigma_n^2 \right) \quad (2.76)$$

which is the expression used in section 3. Notice that the correlations between the errors $\varepsilon_{nm}^{\alpha}$, which exist when they have the same order n because $(G + C^{-1})^{-1}$ has the same block-diagonal structure as $(G + C^{-1})$,

are eliminated from (2.75) and (2.76) by the orthogonality of the $\varphi_{nm}^{\alpha}(\phi, \lambda)$.

To obtain the accuracy of the geoid height computed with the SST derived model, one has to know the a posteriori accuracies of the coefficients, represented by the $\sigma^2 \varepsilon_{nmnm}^{\alpha}$, and also the actual degree variances of the field for $n > N$. The first we know, to some extent, as formal accuracies derived from the diagonal elements of $(G + C^{-1})^{-1}$; the second are largely unknown, as they correspond to the part of the potential not analyzed yet. Therefore, one must adopt some approximate model for this spectral "tail" between N and ∞ , based largely on indirect evidence, which means that the estimated contribution of this "tail" to ∂N , or truncation error, must depend on rather weak assumptions. A further problem, of more theoretical nature, is that (2.72) is valid only when the potential can be expanded in spherical harmonics. When there are masses above the geoid, as it is the case in reality, the expansion is known to converge only outside the smallest sphere bounding all those masses, or external bounding sphere, and not necessarily at the Earth's surface itself, where it is actually needed. This question is partially answered by a theorem first proposed by Walsh (1927), reported later by Keldych and Lavrentieff (1939), and independently stated by Krarup (1969), according to which there are always spherical harmonic expansions like the one in (2.72) that approximate uniformly the potential, to within any arbitrary accuracy, on and above the Earth's surface. A consequence of this theorem is that the C_{nm}^{α} for $n \leq N$, with N finite, in the convergent expansion outside the external bounding sphere (which can be detected by SST) must differ from those in some of the internal approximating expansions also by an arbitrarily small amount. In this sense, the coefficients detected from SST data can be considered to be valid also at the Earth's surface.

The approximating expansions in Walsh's theorem converge uniformly to the functions they approximate above the topography. Their analytical continuations inside the Earth, where they also take definite values, have no physical meaning and are, thus, free from the natural constraints that determine the character of the functions represented (potential, geoid height, the estimation error ∂N according to (2.74)) above the topography or bathymetry (near the sea surface, for example). The free air geoid, say, coincides in the limit with the true geoid where this surface runs above the solid Earth, so it is rather smooth and gentle in such a region, but it can be argued that it may be much rougher in places elsewhere, under the terrain. The mean square value of ∂N in (2.76) corresponds to an average over the sphere of radius $r = a$. This can be interpreted as a spherical approximation to the reference ellipsoid after all masses outside it have been removed by an atmospheric and topographic correction. This is the interpretation made in Section 3, and it involves a spherical approximation error not accounted for in (2.76). One can also regard the average as being done on an actual sphere that dips in and out of the topography and, more importantly, of the equatorial bulge, so a correction for the masses above this sphere is too large to be reliably computed. In this case the average includes the squares of true errors ∂N above the Earth's surface, and of the analytical continuation of ∂N below. As the continuation can have a very different character from that of ∂N in free space, one may wonder just how meaningful is this average, how well does it represent the real errors, particularly where one is most concerned: near the sea surface, for instance. Finally,

the presence of sharp features such as ridges, trenches, cordilleras, etc., results usually in strong variations of the geoid which may cause oscillations in the truncated series of the estimated $N(r, \phi, \lambda)$ of the type called "Gibson's phenomenon" in Fourier series, oscillations that may affect the practical use of the global model in areas that are among the most interesting from a geophysical point of view. While all these problems may have simple solutions, none are known to this author yet, so there may be some need for improvement in our present understanding of these rather basic questions, and for a grain of salt when taking some of the results distilled from existing theories. With such reservations in mind, one can regard the undulation estimate of (2.73) as optimal in the sense that if the SST data were used to estimate N directly, instead of finding the \tilde{C}_{nm} first, the result would be exactly the same. This is so because the field at satellite height has been assumed to be band limited, and in such case any linear combination of the \tilde{C}_{nm} , such as $N(r, \phi, \lambda)$ is according to (2.73), can be optimally estimated by replacing the \tilde{C}_{nm} with their optimal estimates \tilde{C}_{nm}^{α} in the linear combination (see Colombo (1981), paragraph 2.18). The truncated part ($n > N$) is regarded here as an additional, unknown signal on which there is no information in the satellite data, while the terms with $n \leq N$ constitute the estimated variable.

2.13 The Effect of Some Mission Parameters on Coefficient Accuracy

The diagonal elements of the inverse of the normal matrix, $\sigma^2 \epsilon_{nmnm}^{\alpha\alpha}$ in the sort of notation used for the elements of G in paragraph 2.9, depend on the values of certain mission parameters, such as data accuracy, sampling interval, mission duration, etc., according to simple formulas. Such formulas enable one to recalculate the accuracy of the adjusted coefficients for different values of those parameters without having to repeat the lengthy computations required by the formation and inversion of the normal matrix. This paragraph contains the derivation of some of these convenient formulas, both for least squares adjustment and for least squares collocation.

(a) Least Squares Adjustment:

When $D = \sigma^2 I$, where I is the $N_p \times N_p$ unit matrix, the normal matrix is

$$G = A^T D^{-1} A = \sigma^{-2} A^T I^{-1} A = \sigma^{-2} A^T A$$

and the variance-covariance matrix is

$$G^{-1} = \sigma^2 (A^T A)^{-1}$$

so the diagonal elements of G^{-1} are related to σ by

$$\sigma^2 \epsilon_{nmnm}^{\alpha\alpha}(\sigma) = \left(\frac{\sigma}{\sigma_0}\right)^2 \sigma^2 \epsilon_{nmnm}^{\alpha\alpha}(\sigma_0) \quad (2.77,a)$$

The elements of G depend on the sampling interval Δt through the number of samples $N_p = \frac{t}{\Delta t}$ (expression (2.51)). Consequently, the elements of G are inversely proportional to Δt , and those of G^{-1} are directly proportional to it, so

$$\sigma^2 \epsilon_{nmnm}^{\alpha\alpha}(\Delta t) = \left(\frac{\Delta t}{\Delta t_0}\right) \sigma^2 \epsilon_{nmnm}^{\alpha\alpha}(\Delta t_0) \quad (2.77,b)$$

As the elements of G are directly proportional to T , the length of the mission, those of G^{-1} should be inversely proportional to T , provided that $T = k T_0$, where k is an integer and T_0 the value originally used when setting up G (i.e., 179 days in the case studied in Section 3). As the orbit has a grand period T_0 , extending this period k times results in the orbit being repeated also k times, and a measurement at any given location being taken k well, so the adjustment contains repeated but uncorrelated measurements. Consequently

$$\sigma^2 \epsilon_{nmnm}^{\alpha\alpha}(T) = \left(\frac{T_0}{T}\right) \sigma^2 \epsilon_{nmnm}^{\alpha\alpha}(T_0) \quad (2.77,c)$$

provided T/T_0 is integer.

For small changes in height above or below h (the height used to calculate G originally) the changes in satellite angular velocity ω and, consequently, in the shape of the groundtrack of the mid-point, and in the distribution of the measurements along it are small, too, and can be ignored. If ψ is kept constant by changing the separation ρ between satellites so $\sin \frac{\psi}{2} = \frac{\rho}{2R} = \frac{\rho}{2(a+h)}$ is unchanged, then A and G will vary so little as to be considered independent from h . The de-scaled diagonal elements of G^{-1} are then related to h as follows

$$\sigma^2 \epsilon_{nmnm}^{\alpha\alpha}(h) = \left(\frac{a+h}{a+h_0}\right)^{2n} \sigma^2 \epsilon_{nmnm}^{\alpha\alpha}(h_0) \quad (2.77,d)$$

where a is the mean Earth radius. Expressions (2.77,a-d) can be written together

$$\sigma^2 \epsilon_{nmnm}^{\alpha\alpha}(\sigma, \Delta t, T, h) = \frac{\sigma^2 \Delta t T_0 (a+h)^{2n}}{\sigma_0^2 \Delta t_0 (a+h_0)^{2n}} \sigma^2 \epsilon_{nmnm}^{\alpha\alpha}(\sigma_0, \Delta t_0, T_0, h_0) \quad (2.78)$$

The degree variance of the error is $\sigma^2 \epsilon_n = \sum_{\alpha=0}^1 \sum_{m=0}^n \sigma^2 \epsilon_{nmnm}^{\alpha\alpha}$

$$\text{so} \quad \sigma^2 \epsilon_n(\sigma, \Delta t, T, h) = \frac{\sigma^2 \Delta t T_0 (a+h)^{2n}}{\sigma_0^2 \Delta t_0 (a+h_0)^{2n}} \sigma^2 \epsilon_n(\sigma_0, \Delta t_0, T_0, h_0) \quad (2.79)$$

in accordance with (2.78), provided T/T_0 is integer, $|h-h_0|$ is small compared to $R = a+h$, and ψ is kept constant.

(b) Least Squares Collocation:

Rummel et al. (1979) have shown how a singular value decomposition of the normal matrix greatly simplifies the recalculation of the a posteriori variances with different levels of data noise. This idea can be adapted to the global case under consideration. It follows from the previous discussion that

$$G'(\sigma, \Delta t, T) = \frac{\sigma_0^2 \Delta t_0 T}{\sigma^2 \Delta t T_0} G'(\sigma_0, \Delta t_0, T_0) \quad (2.80)$$

where $G'(\sigma_0, \Delta t_0, T_0)$ is the normal matrix G of least squares adjustment pre- and post-multiplied by C^2 and calculated with the parameter values

$\sigma_0, \Delta t_0, T_0$. If Λ_0 is the diagonal matrix whose diagonal elements λ_i are the eigenvalues of $G'(\sigma_0, \Delta t_0, T_0)$, if all the λ_i are different and nonzero, and if M_0 is the matrix whose columns \underline{m}_i are the corresponding normalized eigenvectors of $G'(\sigma_0, \Delta t_0, T_0)$, so $\underline{m}_i^T \underline{m}_j = 1$, then

$$G'(\sigma, \Delta t, T) = \frac{\sigma_0^2 \Delta t_0 T}{\sigma^2 \Delta t T_0} M_0 \Lambda_0 M_0^T \quad (2.81)$$

It follows that

$$\begin{aligned} C^{\frac{1}{2}} (G(\sigma, \Delta t, T) + C^{-1}) C^{\frac{1}{2}} &= G'(\sigma, \Delta t, T) + I \\ &= \frac{\sigma_0^2 \Delta t_0 T}{\sigma^2 \Delta t T_0} M_0 \Lambda_0 M_0^T + I \end{aligned}$$

The eigenvalues of $G'(\sigma, \Delta t, T) + I$ are $\frac{\sigma_0^2 \Delta t_0 T}{\sigma^2 \Delta t T_0} \lambda_i + 1$, while the eigenvectors are those of $G'(\sigma, \Delta t, T)$. The eigenvectors of a real symmetric matrix with distinct eigenvalues are orthogonal and equal in number to the dimension of the matrix, so M_0 is a square orthogonal matrix (the columns are orthogonal unit vectors, if one assumes that all the λ_i are different). Consequently, $M_0^{-1} = M_0^T$, so

$$(G'(\sigma, \Delta t, T) + I)^{-1} = M_0 \left(\frac{\sigma_0^2 \Delta t_0 T}{\sigma^2 \Delta t T_0} \Lambda_0 + I \right)^{-1} M_0^T \quad (2.82)$$

Therefore, the de-scaled diagonal elements of the inverse of the normal matrix,

$$C^{-\frac{1}{2}} (G'(\sigma, \Delta t, T) + I)^{-1} C^{-\frac{1}{2}} = C^{-\frac{1}{2}} M_0 \left(\frac{\sigma_0^2 \Delta t_0 T}{\sigma^2 \Delta t T_0} \Lambda_0 + I \right)^{-1} M_0^T C^{-\frac{1}{2}} \quad (2.83)$$

are

$$\sigma^2 \epsilon_{nmnm}^{\alpha\alpha} = \frac{2n+1}{\sigma^2 h} \underline{m}_i^T \left(\frac{\sigma_0^2 \Delta t_0 T}{\sigma^2 \Delta t T_0} \Lambda_0 + I \right)^{-1} \underline{m}_i \frac{R^{2n+4}}{(GMa\eta)^2} \quad (2.84)$$

where $\sigma^2 \epsilon_{nmnm}^{\alpha\alpha}$ has the same position in the diagonal of $(G + C^{-1})^{-1}$ as λ_i in the diagonal of Λ_0 . The presence of C^{-1} in the expression of the normal matrix seems to preclude a simple relationship between the a posteriori variance and, h like that of (2.77,c), because C depends on $R = a+h$, so $G' = C^{\frac{1}{2}} G C^{\frac{1}{2}}$ and Λ_0 are also functions of h (expressions (2.70) and (2.81)).

While not as straightforward as (2.78), (2.84) is relatively easy to apply, compared to a full recalculation of the normal and its inverse. To apply this expression one needs to have the eigenvalues and eigenvectors of the normal, instead of its inverse. Obtaining either requires much the same amount of computing.

2.14 The Right Hand Sides of the Normals

What follows, though not applicable to the error analysis that is the main subject of this report, is relevant to the question of data processing discussed in Section 5.

The normal equations of least squares adjustment and of least squares collocation have the same independent terms which, in vector form, can be represented by the N_c - vector \underline{b}

$$\underline{b} = A^T D^{-1} \bar{v}_{12}(\text{obs}) \quad (\text{expressions (2.47,b) and (2.67)})$$

An individual component of \underline{b} , corresponding in position to \tilde{c}_{nm}^α in \underline{c} , can be written

$$b_{nm}^\alpha = (\underline{a}_{nm}^\alpha)^T D^{-1} \bar{v}_{12}(\text{obs}) = \frac{1}{\sigma^2} \sum_{i=0}^{N_p} a_{nm}^\alpha(t_i) \bar{v}_{12}(t_i) \quad (2.85)$$

where $\underline{a}_{nm}^\alpha$ is the column vector in A corresponding to the unknown \tilde{c}_{nm}^α (paragraph 2.7). According to (2.24), the elements of $\underline{a}_{nm}^\alpha$ are

$$a_{nm}^0(t_i) = \frac{1}{\Delta a} \sum_{p=z}^n a_p^{nm} \left\{ \begin{array}{l} \frac{S((p\omega + m\Omega)t_i, \Delta a)}{(p\omega + m\Omega)^2} + \frac{S((p\omega - m\Omega)t_i, \Delta a)}{(p\omega - m\Omega)^2} \\ - \frac{C((p\omega + m\Omega)t_i, \Delta a)}{(p\omega + m\Omega)^2} - \frac{C((p\omega - m\Omega)t_i, \Delta a)}{(p\omega - m\Omega)^2} \end{array} \right\} \quad (2.86,a)$$

$$a_{nm}^1(t_i) = \frac{1}{\Delta a} \sum_{p=z}^n a_p^{nm} \left\{ \begin{array}{l} \frac{C((p\omega + m\Omega)t_i, \Delta a)}{(p\omega + m\Omega)^2} - \frac{S((p\omega - m\Omega)t_i, \Delta a)}{(p\omega - m\Omega)^2} \\ \frac{S((p\omega + m\Omega)t_i, \Delta a)}{(p\omega + m\Omega)^2} - \frac{C((p\omega - m\Omega)t_i, \Delta a)}{(p\omega - m\Omega)^2} \end{array} \right\} \quad (2.86,b)$$

The $C((p\omega + m\Omega)t_i, \Delta a)$ and $S((p\omega - m\Omega)t_i, \Delta a)$ are orthogonal functions of t_i , according to (2.34,a-b), so the data $\bar{v}_{12}(t_i)$ can be expanded into a sum of these functions:

$$\bar{v}_{12}(t_i) = \sum_{p=0}^{N_y} \sum_{m=-N_r}^{N_r} \bar{v}_{pm}^0 C((p\omega + m\Omega)t_i, \Delta a) + \bar{v}_{pm}^1 S((p\omega + m\Omega)t_i, \Delta a) \quad (2.87)$$

where $N_y = \frac{\pi}{\omega \Delta t}$ is the Nyquist frequency as defined in paragraph 1.2, while $N_r = \frac{1}{2} \omega \Omega^{-1} N_d$. The $\bar{v}_{pm}^0, \bar{v}_{pm}^1$ coefficients can be obtained from the ordinary Fourier coefficients in $\bar{v}_{12}(t_i) = \sum_{p=0}^{N_y} \sum_{m=-N_r}^{N_r} A_{pm} \cos(p\omega + m\Omega)t_i + B_{pm} \sin(p\omega + m\Omega)t_i$ with the relationships

$$\bar{v}_{pm}^0 = A_{pm} \sin(p\omega + m\Omega)\Delta a + B_{pm} (1 - \cos(p\omega + m\Omega)\Delta a) \quad (2.88,a)$$

$$\bar{v}_{pm}^1 = A_{pm} (1 - \cos(p\omega + m\Omega)\Delta a) + B_{pm} \sin(p\omega + m\Omega)\Delta a \quad (2.88,b)$$

According to (2.34,a-b), (2.85), and (2.86,a-b), the elements of \underline{b} are

$$b_{nm}^0 = \frac{N_r}{\sigma^2 \Delta a} \sum_{p=z}^n a_p^{nm} \left\{ \begin{array}{l} \frac{\bar{v}_{pm}^1}{\omega^2 +} + \frac{\bar{v}_{p-m}^1}{\omega^2 -} \\ - \frac{\bar{v}_{pm}^0}{\omega^2 +} - \frac{\bar{v}_{p-m}^0}{\omega^2 -} \end{array} \right\} \quad (2.89,a)$$

$$\text{and} \quad b_{nm}^1 = \frac{N_p}{\sigma^2 \Delta a} \sum_{p=z}^n a_p^{nm} \left\{ \begin{array}{l} \frac{\bar{v}_{pm}^0}{\omega^2 +} - \frac{\bar{v}_{p-m}^0}{\omega^2 -} \\ \frac{\bar{v}_{pm}^1}{\omega^2 +} - \frac{\bar{v}_{p-m}^1}{\omega^2 -} \end{array} \right\} \quad (2.89,b)$$

where $z = \begin{cases} 0 & \text{if } m \neq 0 \\ 1 & \text{if } m = 0 \end{cases}$

(as in (2.20))

where, as before, the upper parts of the curly brackets correspond to $(n-m)$ even, the lower to $(n-m)$ odd, $\omega^2 \pm = \frac{(p\omega \pm m\Omega)^2}{(1 - \cos(p\omega \pm m\Omega)\Delta a)}$, and p and n have the same parity.

The Fourier coefficients C_{pm} , S_{pm} can be obtained by means of the Fast Fourier Transform in any of the special forms designed to handle data sets too large to store in the central memory of a computer.

2.15 Oblique Orbits

The error analysis reported in this work is concerned only with polar orbits, which provide the fullest data coverage because they include the polar regions. In the case of oblique orbits, the inclination of the orbital plane with respect to the equator is neither 0° nor 90° . With oblique orbits, even if the other assumptions in paragraph 2.1 are maintained, expression (2.9) for the line of sight inertial acceleration, which is the starting point for deriving the observation equations, has to be modified. Calling, as in Figure 2.2, F to the geocentric angle between the ascending node and a point P along the orbit, and L to the longitude of that node, the band-limited gravitational field potential can be written as follows

$$V(r, F, L) = \frac{GM}{r} \sum_{n=0}^N \sum_{m=0}^n \left(\frac{a}{r}\right)^n \sum_{q=0}^n \bar{F}_{nmq}(1) \left[\left\{ \begin{matrix} \bar{C}_{nm} \\ \bar{S}_{nm} \end{matrix} \right\} \cos((n-2q)F + mL) + \left\{ \begin{matrix} \bar{S}_{nm} \\ \bar{C}_{nm} \end{matrix} \right\} \sin((n-2q)F + mL) \right] \quad (2.90)$$

where the upper part of each bracket corresponds to $(n-m)$ even and the lower part to $(n-m)$ odd; 1 is the inclination angle between the equator and the orbital plane; F and L are functions of time

$$F = [\omega t]_{\text{mod } 2\pi} \quad (2.91,a)$$

and

$$L = -[(\Omega - \beta(1))t]_{\text{mod } 2\pi} \quad (2.91,b)$$

$$= -[\Omega' t]_{\text{mod } 2\pi}$$

where

$$\beta(1) \approx -1.35 \times 10^{-6} \cos 1 \text{ rad s}^{-1} \quad (2.91,c)$$

is the rate of precession of the node, which is zero for polar orbits ($1 = \frac{\pi}{2}$); $\bar{F}_{nmq}(1)$ is the normalized inclination function

$$\bar{F}_{nmq}(1) = \left\{ \begin{matrix} \sqrt{2n+1} & (m=0) \\ \sqrt{\frac{2(2n+1)(n-m)!}{(n+m)!}} & \end{matrix} \right\} \sum_{t=0}^{\min(q,k)} \frac{(2n-2t)! (\sin 1)^{n-m-2t}}{t! (n-t)! (n-m-2t)! 2^{2(n-t)}} \quad (2.92)$$

$$\times \sum_{s=0}^m \binom{m}{s} (\cos 1)^s \sum_c \binom{n-m-2t+s}{c} \binom{m-s}{q-t-c} (-1)^{c-k}$$

where k is the integer part of $\frac{n-m}{2}$ and c is summed over all values that make the binomial coefficients nonzero. For the derivation of (2.90) and (2.92), see, for instance, Kaula (1966), Chapter 3 (the notation is somewhat different).

The line of sight between the satellites lies always in the instantaneous orbital plane. The inertial acceleration can be decomposed into three orthogonal components: the radial, the normal to the radial in the instantaneous orbital plane, and the perpendicular to this plane. Of these, only the first two accelerations have nonzero projections on the direction of the line of sight. The radial acceleration is

$$\frac{\partial V}{\partial r} = -\frac{GM}{r^2} \sum_{n=0}^N \sum_{m=0}^n \left(\frac{a}{r}\right)^n (n+1) \sum_{q=0}^n F_{nmq}(1) [\{\tilde{C}_{nm}\} \cos((n-2q)F + mL) + \{\tilde{S}_{nm}\} \sin((n-2q)F + mL)] \quad (2.93,a)$$

and the normal to the radial acceleration (in the instantaneous orbital plane) is

$$\frac{1}{r} \frac{\partial V}{\partial F} = \frac{GM}{r^2} \sum_{n=0}^N \sum_{m=0}^n \left(\frac{a}{r}\right)^n \sum_{q=0}^n F_{nmq}(1) (n-2q) [\{-\tilde{C}_{nm}\} \sin((n-2q)F + mL) + \{\tilde{S}_{nm}\} \cos((n-2q)F + mL)] \quad (2.93,b)$$

The coordinate L is common to both satellites, as their orbits are coplanar. Adopting $F = \frac{B+E}{2}$, the midpoint nodal distance, as the other independent variable ($r = R$ is fixed), the modified inertial line of sight acceleration (inertial accel. minus constant term due to even zonals) is

$$\hat{a}_{12}(R, F, L) = -\left(\frac{\partial V}{\partial r}(R, F - \frac{\psi}{2}, L) + \frac{\partial V}{\partial r}(R, F + \frac{\psi}{2}, L)\right) \sin \frac{\psi}{2} + \frac{1}{R} \left(\frac{\partial V}{\partial F}(R, F - \frac{\psi}{2}, L) - \frac{\partial V}{\partial F}(R, F + \frac{\psi}{2}, L)\right) \cos \frac{\psi}{2} - a_0 \quad (2.94)$$

Replacing F and L with t as the independent variable in (2.93,a-b), substituting the \tilde{C}_{nm} with the scaled \tilde{C}_{nm}^a , introducing $p = n-2q$ as subscript, instead of q , eliminating all terms of frequency zero, and replacing the result in (2.94), one can finally arrive to an expression for the observation equation resembling (2.24), after a rather laborious process quite similar to that in paragraph 2.2:

$$\begin{aligned} \frac{1}{\Delta a} \sum_{m=0}^N \sum_{\substack{n=m \\ \max(m,z)}}^N \tilde{C}_{nm} \sum_{p=z}^n \alpha_{nm}^{\frac{n-p}{2}}(1) \left\{ \begin{array}{l} S((p\omega + m\Omega')t_i, \Delta a) \\ -C((p\omega + m\Omega')t_i, \Delta a) \end{array} \right\} (p\omega + m\Omega')^{-2} \\ + \alpha_{nm}^{\frac{n+p}{2}}(1) \left\{ \begin{array}{l} S((p\omega - m\Omega')t_i, \Delta a) \\ C((p\omega - m\Omega')t_i, \Delta a) \end{array} \right\} (p\omega - m\Omega')^{-2} + \\ + \sum_{p=z}^n \tilde{S}_{nm} \alpha_{nm}^{\frac{n-p}{2}}(1) \left\{ \begin{array}{l} C((p\omega + m\Omega')t_i, \Delta a) \\ S((p\omega + m\Omega')t_i, \Delta a) \end{array} \right\} (p\omega + m\Omega')^{-2} \end{aligned}$$

$$+ \alpha_{nm}^{(n \pm p)}(i) \left\{ \frac{-C((p\omega - m\Omega')t_i, \Delta a)}{S((p\omega - m\Omega')t_i, \Delta a)} \right\} (p\omega - m\Omega')^{-2} = \bar{v}_1 \left\{ \begin{matrix} t_i \\ \text{obs} \end{matrix} \right\} + r_i \quad (2.95)$$

where

$$\alpha_{nm}^{(n \pm p)}(i) = 2\bar{F}_{nm}^{(n \pm p)}(i) [(n+1) \csc \frac{\psi}{2} \sin \frac{\psi}{2} + p \sin \frac{\psi}{2} \cos \frac{\psi}{2}] \quad (2.96)$$

While their coefficients are now different in each pair, corresponding pairs of frequencies $p\omega \pm m\Omega$ and $p\omega \pm m\Omega'$, in the same order, appear in (2.24) as they do in (2.95). As a result of this, the same columns in A are orthogonal to each other regardless of the angle i and, therefore, the same elements in $G = \sigma^{-2} A^T A$ are zero as before, so the normal matrices of least squares adjustment and least squares collocation have the block-diagonal structure shown in Figure 2.1, paragraph 2.9, for oblique as well as for polar orbits. This is true provided that ω and Ω' are congruent, so the total number of satellite revolutions N_r and the total number of apparent turns of the Earth in a node-fixed system of coordinates, during the whole mission, N_D , are relative primes.

For polar orbits, the inclination functions have the property

$$\bar{F}_{nm}^{(n-p)}\left(\frac{\pi}{2}\right) = (-1)^{n-m} \bar{F}_{nm}^{(n+p)}\left(\frac{\pi}{2}\right) \quad (2.97)$$

($p \neq 0$, p and n with the same parity). Comparing (2.13) and (2.96) one gets, therefore,

$$\bar{h}_p^{nm} = 2\bar{F}_{nm}^{(n-p)}\left(\frac{\pi}{2}\right) \quad (2.98)$$

Consequently, the Fourier coefficients \bar{h}_p^{nm} of the \bar{L}_{nm} used in the case of polar orbits can be calculated using the formulas

$$\begin{aligned} \bar{h}_p^{nm} = & \left\{ \begin{matrix} \sqrt{2n+1} & (m=0) \\ \sqrt{2(2n+1)(n-m)!} & (n-m) \end{matrix} \right\} \sum_{t=0}^{\min(k, \frac{n-p}{2})} \frac{(2n-2t)!}{t! (n-t)! (n-m-2t)! 2^{2(n-t)}} \\ & \times \sum_c \binom{n-m-2t}{c} \left(\left(\frac{n-p}{2} \right)^m - t - c \right) (-1)^{c-k} \quad (2.99) \end{aligned}$$

derived from (2.92) with $i = \frac{\pi}{2}$. This formula is an alternative to the use of the Fast Fourier Transform as explained in paragraph 2.7.

The similitudes between (2.24) and (2.95) indicate that the computer programs needed to carry out the error analysis of a mission where the orbital plane is inclined with respect to the equator are very similar to those for polar orbits explained and listed in Appendix B. Reasoning once more as in paragraph 2.9, one arrives to an expression for the general element of the G matrix

$$g_{nmkq}^{\alpha\beta} = \begin{cases} 0 & \text{if } n \neq \beta, m \neq q, n \begin{cases} \text{even} \\ \text{odd} \end{cases} \text{ and } k \begin{cases} \text{odd} \\ \text{even} \end{cases}, \\ \frac{N_p}{\sigma^2 \Delta a} \sum_{p=z}^{\min(n,k)} \alpha_{\left(\frac{n-p}{2}\right)}^{nm(1)} \alpha_{\left(\frac{n-k}{2}\right)}^{km(1)} \frac{(-\cos(p\omega + m\Omega')\Delta a)}{(p\omega + m\Omega')^4} \\ + \alpha_{\left(\frac{n+p}{2}\right)}^{nm(1)} \alpha_{\left(\frac{n+k}{2}\right)}^{km(1)} \frac{(1-\cos(p\omega - m\Omega')\Delta a)}{(p\omega - m\Omega')^4} \end{cases} \quad (2.100)$$

that is comparable to (2.51), showing at once the similitudes and the differences between the polar orbit and the oblique.

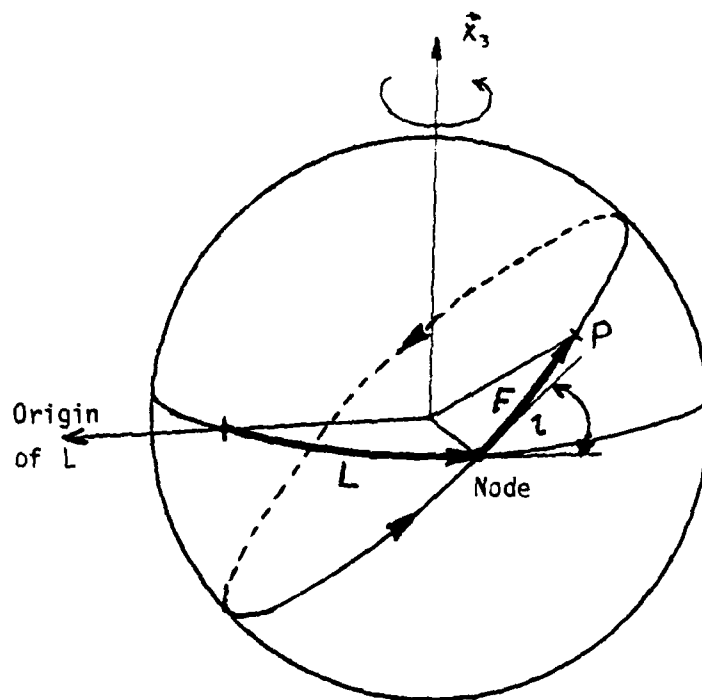


Figure 2.2: Geometry of the Oblique Orbit

3. Numerical Results

This section presents the results of the error analysis whose theory has been given in sections 1 and 2. The calculations have been done in accordance to least squares adjustment and to least squares collocation, and both sets of results are shown for comparison.

3.1 Spectral Model and Error Formulas

The degree variance of the error is, according to paragraph 2.13,

$$\sigma_n^2 \epsilon_n = \sum_{m=0}^n \sum_{\alpha=0}^1 \sigma^2 \epsilon_{nm\alpha}^{\alpha} \quad (3.1)$$

where $\sigma_{nm\alpha}^2$ is the variance of the estimated coefficient \bar{C}_{nm}^{α} . The relative error per degree is

$$\rho_n = \frac{\sigma \epsilon_n}{\sigma_n} \quad (3.2)$$

where

$$\sigma_n^2 = \sum_{m=0}^n \sum_{\alpha=0}^1 (\bar{C}_{nm}^{\alpha})^2 \quad (3.3)$$

is the degree variance of the n harmonic of the potential. The set of all σ_n^2 for $0 \leq n < \infty$ is the power spectrum of the potential. This relative error, multiplied by 100, is listed as percentage error per degree in the various tables shown in this section. To calculate (3.2) it is necessary to know the power spectrum, the σ_n^2 . The spectrum, like the potential itself, is not entirely known, but there are estimates of the σ_n^2 obtained from the analysis of terrestrial and satellite data. For low degree harmonics the σ_n^2 can be calculated using (3.3) with the values for the \bar{C}_{nm}^{α} taken from one of the existing spherical harmonic models of the potential. For higher terms, the "tail" beyond the highest degree whose \bar{C}_{nm}^{α} are known, one can choose among the several formulas for σ_n^2 as a function of n that are available, each based on a different type of approximation, or on different data. For this study the degree variances up to degree $n = 100$ were taken from a spherical harmonics model complete to $n = 180$, obtained by Rapp and associates at OSU from the analysis of a global set of mean $1^\circ \times 1^\circ$ gravity anomalies using quadrature formulas. The anomalies themselves were obtained from gravimetry and altimetry by means of least squares collocation. As a further step the anomalies were adjusted in a combination solution that included the coefficients of GEM-9 as data. For a report on this adjusted data set, see Rapp (1978) and also Rapp (1979a). GEM-9 is described in (Lerch et al., 1977). If one ignores orbit errors, then expression (1.23) is reduced to an identity between the time derivative of the residual line of sight velocity and the residual line of sight inertial acceleration. The residual inertial acceleration corresponds to the difference between the true field and the field model used to compute the orbit. If $\bar{C}_{nm}^{\alpha}(\text{Model})$ is a coefficient of the model, and NM the maximum degree in that model, then the geopotential coefficients corresponding to the residual accelerations are $\Delta \bar{C}_{nm}^{\alpha} = \bar{C}_{nm}^{\alpha} - \bar{C}_{nm}^{\alpha}(\text{Model})$ for $n \leq NM$, and \bar{C}_{nm}^{α} for $NM < n < \infty$. The degree variances of the power spectrum are, therefore, $\sigma_n^2 = \sum_{m,\alpha} (\bar{C}_{nm}^{\alpha} - \bar{C}_{nm}^{\alpha}(\text{Model}))^2$ for $n \leq NM$, and $\sigma_n^2 = \sum_{m,\alpha} (\bar{C}_{nm}^{\alpha})^2$ for $NM < n$. The σ_n^2 are the degree

variances corresponding to the errors in the reference field. As these errors are not known exactly, one must use some "likely numbers" instead, such as the formal error variances of the coefficients obtained during the adjustment of the reference model. This criterion has been adopted here, the error variances being those of the first NM degrees in Rapp's model, with NM = 20. For $n > NM$, the σ_n^2 as implied by Rapp's coefficients have been used up to degree 100. For $n > 100$ the σ_n^2 have been calculated with the two-term formula

$$\sigma^2 = \frac{a^2}{G^2 M^2} (n-1)^{-1} [A_1(n+A)^{-1} S_1^{n+2} + A_2(n+B)^{-1} (n-2)^{-1} S_2^{n+2}] \quad (3.4)$$

where $a = 6371$ km, $\frac{GM}{a} = 982026.41$ mgal, $A = 1$, $B = 2$, $A_1 = 3.4050$, $A_2 = 140.03$, $S_1 = 0.998006$, and $S_2 = 0.914232$. These parameter values were obtained by Rapp (1979b) by fitting the formula to the empirical variances of his 180, 180 model and other data. In summary:

For $2 \leq n \leq NM$, the error degree variances ϵ_{nm}^2 of Rapp's model;

for $NM < n \leq 100$, the degree variances of Rapp's model;

for $100 < n \leq 2000$, the σ_n^2 according to (3.4). The harmonic content of the geopotential, according to that formula, is negligible for $n > 2000$.

The error in geoid undulation due to the errors in the coefficients up to degree n has been calculated with the formula

$$\sigma^2 \epsilon N_n = a^2 \sum_{k=2}^n \sigma^2 \epsilon_k \quad (3.5)$$

If no coefficients above n are estimated, the total error must be

$$\sigma^2 \epsilon N_T = \sigma^2 \epsilon N_n + a^2 \sum_{k=n+1}^{2000} \sigma^2_k \quad (3.6)$$

(Compare to (2.76)).

Expression (3.6) depends on the "tail" of the spectrum containing the high frequency terms. The higher n , the least that is known about σ_n^2 , so this "tail" is the least reliable part of the spectrum model, and the total error calculated with (3.6) is the least credible among the results. Originally, when the least squares collocation results were obtained, the total error was not computed, though its calculation was added in the main program afterwards, when other results were found. For completeness' sake, the punched output of that first run was read by an auxiliary program, which then produced the printout shown in Table 3.2, including the total error in the last column, and also the full listing of Table C.2 in Appendix C. A minor mistake in the auxiliary program resulted in values of the total error that are incorrect. To obtain the "true" values e_n , the listed values e'_n should be corrected according to the formulas

$$e_n = (e'^2_n + 0.1074)^{\frac{1}{2}} \quad (3.7)$$

3.2 Results According to Least Squares Adjustment

Table 3.1 shows the accuracies of potential coefficients and geoidal undulations estimated from SST data collected during a mission whose parameters were:

Circular, polar orbit,
 satellite height: 160 km, a.c.,
 intersatellite separation: 300 km,
 accuracy of the data: $\sqrt{2} \times 10^{-6} \text{ m s}^{-1}$,
 averaging interval: 4 s,
 sampling interval: 4 s,
 length of the mission: 179 days,
 maximum degree and order in reference model: 20.

The error analysis was carried out according to least squares adjustment theory, as put forward in paragraph 2.8. The first column shows the relative percentage error, which is the ratio defined by expression (3.2) multiplied by 100. Notice that above $n = 270$ the error exceeds 100% consistently. The size of the errors become so large that the total undulation error, which decreases steadily up to $n = 270$, according to the last column, begins to increase quite perceptibly once more. The last but one column shows the error up to n , according to expression (3.5). The second column contains the values of $\frac{GM^2}{R^2} \left(\frac{a}{R}\right)^2 n \sigma^2 \epsilon_n$, the variance per degree of the error in the scaled coefficients (see expression (2.70) in par. 2.11). Notice the very low percentage errors for $n < 100$, which are much the same as those shown in the next paragraph for least squares collocation.

As explained in the last part of paragraph 2.10, the error in the recovered coefficients may show local peaks at those degrees satisfying the condition

$$n\psi = 2\pi k \quad (k = 1, 2, \dots)$$

Since $\psi = 2\sin^{-1}\left(\frac{a}{R}\right)$, for a separation of 300 km the maxima should occur within the band $0 \leq n \leq 331$ at degrees $n = 136$ and $n = 273$, approximately, the next peak above the band being at $n = 410$. The listing in table 3.1 is too coarsely spaced in n to show these peaks, which are rather narrow features, each atop a broader rise that surrounds it, but they are quite clear in the detailed listing of Table C.1 in Appendix C.

The values that appear both in Tables 3.1 and in Table C.1 can be modified according to expression (2.79) in paragraph 2.13, to obtain the results corresponding to missions with different parameters. Values corresponding to undulation errors (last two columns) are in meters.

N	PERCENTAGE ERROR	ERROR VARIANCE(POT.)	BAND ERROR (UNDUL.) (M)	TOTAL UNDUL. ERROR (M)
2	34837D-01	44945D-23	13507D-04	2.4620
10	62618D-02	21568D-23	39397D-04	2.4306
20	62555D-02	26011D-23	50898D-04	2.3888
30	31427D-02	30568D-23	62315D-04	1.9152
40	53409D-02	51921D-23	75516D-04	1.6198
50	73134D-02	79167D-23	91745D-04	1.4171
60	11369D-01	12498D-22	11239D-03	1.2560
70	19457D-01	20388D-22	13932D-03	1.1362
80	27223D-01	34489D-22	17520D-03	1.0444
90	43714D-01	61148D-22	22432D-03	.96483
100	68586D-01	11636D-21	29424D-03	.90239
110	10372	25104D-21	40090D-03	.84270
120	19283	71472D-21	58953D-03	.79056
130	59562	66954D-20	11204D-02	.7451
140	2.8004	10641D-18	72716D-02	.70351
150	2.8876	96610D-19	95061D-02	.66660
160	3.4877	12142D-18	11663D-01	.63330
170	4.3906	16709D-18	13958D-01	.60310
180	5.6244	23973D-18	16669D-01	.57544
190	7.2608	35197D-18	19969D-01	.55007
200	9.4254	52398D-18	24037D-01	.52674
210	12.249	70685D-18	29083D-01	.50525
220	16.920	11083D-17	35353D-01	.48546
230	20.715	18026D-17	43149D-01	.46731
240	26.962	27491D-17	52852D-01	.45079
250	35.325	42629D-17	65012D-01	.43604
260	48.103	71641D-17	80039D-01	.42344
270	143.98	58341D-16	11760	.41793
280	210.87	12199D-15	29200	.40503
290	224.30	11793D-15	36447	.52241
300	249.38	13374D-15	42921	.56145
310	278.35	15271D-15	49331	.60502
320	293.89	15662D-15	55621	.65062
330	211.29	74611D-16	60160	.60551

Table 3.1 Parameters: height 160 km, separation 300 km, $\sigma = \sqrt{2} \times 10^{-6} \text{ ms}^{-1}$
 Procedure : least squares adjustment

3.3 Results According to Least Squares Collocation

Table 3.2 shows the results corresponding to least squares collocation, the principle of which has been explained in paragraph 2.11. The mission parameters are the same as for Table 3.1. Comparing both tables one can see that the collocation accuracies are consistently better than those for least squares adjustment, particularly above degree $n = 210$. The results listed in the last column of this table, and also of Table C.2, Appendix C, have to be corrected according to expression (3.7), at the end of paragraph 3.1. When contrasting tables 3.1 and 3.2 one must bear in mind that the first corresponds purely to propagated noise, while the second contains hybrid variances: noise plus bias. The peaks in the error mentioned in the previous paragraph are much less noticeable, in fact the one at $n = 273$ has disappeared altogether (Table C.2), and only an "acceleration" in the increase of the error with n remains in the neighborhood of the missing peak. Nowhere the error exceeds 100%, also according to the theory.¹

Table 3.3 lists the accuracies corresponding to a mission with the same parameters as in the preceeding tables, except that the accuracy of the data is now four times worse, i.e., $\sqrt{2} \times 4 \times 10^{-6} \text{ms}^{-1}$.

Table 3.4 corresponds to the same parameters as in Table 3.1, but the height has been changed to 220 km above the Earth.

Table 3.5 is for the same parameters as Table 3.4, with the data noise increased to $\sqrt{2} \times 4 \times 10^{-6} \text{m s}^{-1}$. The results for Tables 3.3 through 3.5 are clearly worse than for Table 3.2, as can be expected, because the data is noisier, the signal weaker (higher altitude), or both, compared to the case of Table 3.2.

Table 3.6 corresponds to the accuracies that would be achieved if all the coefficients in a given degree could be estimated with the same accuracy as the zonal harmonic. The results were computed with a modified version of the main program of Appendix B that sets up and inverts only that part of the normal matrix corresponding to the zonals. In this way, an approximate analysis can be carried out at much less cost than the complete studies of tables 3.1 through 3.5. The mission parameters in 3.6 are the same as in Tables 3.1 and 3.2. In Table 3.7 the separation between satellites has been changed to 150 m, and in Table 3.8, to 600 km. The results in Table 3.7 are clearly much worse than for Table 3.6, showing a particular deterioration at low degrees due to the differential nature of the SST measurements that tends to eliminate the low frequency information, so the percentage of the error in the estimated coefficients increases as the satellites become closer. Table 3.8 shows the smallest band error and the best accuracies, but these are quite irregular because the error peaks in this case are spaced closer than in the other cases, and are much more prominent, so that they can be noticed even with the coarse spacing in n used in the table.

From the results given in this paragraph one can conclude that the orbits should be as low as possible, and the separation between satellites as wide as allowed by natural limitations, the main among which is the need to keep the radar beam from entering too deep into the upper layers of the atmosphere at the mid point. Data noise, of course, should be as low as technically feasible.

(1) The optimal estimator should not be worse than a null estimator (one that predicts only zeroes), whose error is always 100%.

N	PERCENTAGE ERROR	ERROR VARIANCE(POT.)	BAND ERROR (UNDUL.) (M)	TOTAL UNDUL. ERROR (M)
2				
10	.31895D-01	.37633D-23	.12859D-04	2.4409
20	.62495D-02	.21404D-23	.38899D-04	2.4004
30	.62514D-02	.25985D-23	.58582D-04	2.3662
40	.31419D-02	.35551D-23	.61987D-04	1.8870
50	.53401D-02	.61906D-23	.75243D-04	1.5863
60	.73125D-02	.79147D-23	.91518D-04	1.3707
70	.11368D-01	.12495D-22	.11221D-03	1.2126
80	.19434D-01	.26383D-22	.13916D-03	1.6800
90	.27219D-01	.34470D-22	.17507D-03	.99169
100	.43704D-01	.61120D-22	.22420D-03	.90751
110	.60558D-01	.11627D-21	.29412D-03	.84082
120	.10363	.25069D-21	.40074D-03	.77640
130	.19229	.71071D-21	.58963D-03	.71947
140	.58478	.54900D-20	.11213D-02	.66855
150	2.7821	.10502D-18	.69080D-02	.62256
160	2.8401	.93455D-19	.92654D-02	.58062
170	3.3757	.11375D-18	.11305D-01	.54205
180	4.1536	.14953D-18	.13472D-01	.50634
190	5.1600	.20177D-18	.15915D-01	.47304
200	6.4076	.27374D-18	.18724D-01	.44181
210	7.9146	.36947D-18	.21961D-01	.41234
220	9.7022	.49364D-18	.25671D-01	.38459
230	11.804	.65266D-18	.29896D-01	.35774
240	14.295	.85836D-18	.34685D-01	.33224
250	17.365	.11404D-17	.40145D-01	.30773
260	21.620	.15969D-17	.46571D-01	.28414
270	29.470	.26088D-17	.54997D-01	.26163
280	46.766	.61549D-17	.69239D-01	.24145
290	56.507	.81906D-17	.88813D-01	.22480
300	60.786	.86610D-17	.10640	.20990
310	65.941	.93360D-17	.12241	.19661
320	71.771	.10153D-16	.13770	.18524
330	77.665	.10937D-16	.15253	.17600
	82.269	.11312D-16	.16684	.16884

Table 3.2 Parameters: height 160 km, separation 300 km, $\sigma = \sqrt{2} \times 10^{-6}$ m s⁻¹
 Procedure: least squares collocation

N	PERCENTAGE ERROR	ERROR VARIANCE (POT.)	BAND ERROR (UNDUL.) (M)	TOTAL UNDUL. ERROR (M)
2				
10	.10858	.43616D-22	.2076D-04	2.4628
20	.24968D-01	.34291D-22	.15363D-03	2.4306
30	.3297D-01	.4155D-22	.2002D-03	2.3888
40	.12565D-01	.5686D-22	.24632D-03	1.9152
50	.21356D-01	.83016D-22	.29962D-03	1.6198
60	.29243D-01	.12657D-21	.36494D-03	1.4171
70	.45457D-01	.19980D-21	.44787D-03	1.2560
80	.77785D-01	.32586D-21	.53581D-03	1.1362
90	.10802	.55195D-21	.69954D-03	1.0444
100	.17468	.97638D-21	.96607D-03	.96484
110	.27388	.18556D-20	.11756D-02	.90239
120	.41348	.39899D-20	.16915D-02	.84270
130	.76434	.11229D-19	.23518D-02	.79056
140	2.2636	.82256D-19	.44394D-02	.74452
150	10.437	.14782D-17	.24124D-01	.70389
160	10.111	.11845D-17	.33025D-01	.66743
170	11.307	.12761D-17	.39847D-01	.63452
180	13.041	.14741D-17	.46345D-01	.60472
190	15.181	.17466D-17	.52965D-01	.57763
200	20.783	.20931D-17	.59913D-01	.55296
210	24.249	.25280D-17	.67334D-01	.53048
220	28.574	.30836D-17	.75370D-01	.51091
230	34.091	.38240D-17	.84215D-01	.49144
240	41.591	.48819D-17	.94183D-01	.47475
250	52.191	.65415D-17	.10504	.46002
260	65.333	.93055D-17	.12015	.44759
270	76.703	.13215D-16	.13810	.43799
280	84.246	.16550D-16	.15886	.43136
290	89.282	.18206D-16	.17993	.42704
300	92.782	.18685D-16	.19976	.42424
310	95.214	.18483D-16	.21706	.42245
320	96.843	.17869D-16	.23418	.42134
330	97.660	.17066D-16	.24880	.42066
		.15940D-16	.26188	.42023

Table 3.3 Parameters: height 160 km, separation 300 km, $\phi = \sqrt{2} \times 4 \times 10^{-6} \text{ m s}^{-1}$
Procedure: least squares collocation

N	PERCENTAGE ERROR	ERROR VARIANCE(POT.)	BAND ERROR (UNBUL.) (M)	TOTAL UNBUL. ERROR (M)
2	.20512D-01	.30072D-23	.11048D-04	2.4628
10	.69646D-02	.26682D-23	.4092D-04	2.4306
20	.10016D-01	.30825D-23	.55701D-04	2.3088
30	.42006D-02	.63787D-23	.72456D-04	1.9152
40	.70378D-02	.11101D-22	.94257D-04	1.6198
50	.11760D-01	.20469D-22	.12409D-03	1.4171
60	.20629D-01	.30790D-22	.16598D-03	1.2560
70	.37555D-01	.75958D-22	.22516D-03	1.1362
80	.57567D-01	.15422D-21	.31297D-03	1.0444
90	.10126	.32811D-21	.44268D-03	.96484
100	.17398	.74880D-21	.64305D-03	.90239
110	.28786	.19380D-20	.97371D-03	.84270
120	.58331	.65401D-20	.16016D-02	.79056
130	1.0973	.57791D-19	.34638D-02	.74452
140	9.5593	.12399D-17	.21658D-01	.70381
150	9.9570	.11487D-17	.30310D-01	.66731
160	11.905	.14148D-17	.38096D-01	.63442
170	14.503	.10438D-17	.46010D-01	.60469
180	17.932	.24369D-17	.54706D-01	.57779
190	22.025	.32343D-17	.64446D-01	.55347
200	27.057	.43178D-17	.75489D-01	.53150
210	33.372	.50404D-17	.83184D-01	.51206
220	41.529	.60779D-17	.10306	.49502
230	62.233	.11461D-16	.12091	.48077
240	65.497	.16223D-16	.14249	.46981
250	78.797	.21211D-16	.16745	.46254
260	88.562	.24284D-16	.19345	.45846
270	94.191	.24968D-16	.21793	.45644
280	97.096	.24183D-16	.23978	.45349
290	98.470	.22728D-16	.25803	.45303
300	99.103	.21087D-16	.27542	.45482
310	99.363	.19539D-16	.28995	.45471
320	99.766	.18047D-16	.30275	.45465
330	99.628	.16589D-16	.31410	.45461

Table 3.4 Parameters: height 220 km, separation 300 km, $\sigma = \sqrt{2} \times 10^{-6} \text{ m s}^{-1}$

Procedure: least squares collocation

N	PERCENTAGE ERROR	ERROR VARIANCE (POT.)	BAND ERROR (UNDUL.) (M)	TOTAL UNDUL. ERROR (M)
2				
10	.10510	.40658D-22	.40724D-04	2.4628
20	.27839D-01	.42631D-22	.16239D-03	2.4306
30	.46334D-01	.62090D-22	.22192D-03	2.3888
40	.16830D-01	.10201D-21	.28912D-03	1.9152
50	.31341D-01	.17679D-21	.3.645D-03	1.6198
60	.47018D-01	.32722D-21	.49586D-03	1.4171
70	.60076D-01	.62606D-21	.66343D-03	1.2569
80	.15013	.12138D-20	.90206D-03	1.1362
90	.23010	.24640D-20	.12511D-02	1.0444
100	.40468	.52404D-20	.17695D-02	.96484
110	.69510	.11952D-19	.25702D-02	.90240
120	1.1493	.30826D-19	.38909D-02	.84271
130	2.3236	.10378D-18	.63952D-02	.79050
140	7.3600	.86965D-18	.13693D-01	.74464
150	26.748	.97077D-17	.58429D-01	.70590
160	25.831	.77306D-17	.82246D-01	.67166
170	28.902	.83380D-17	.10006	.64113
180	33.715	.98525D-17	.11713	.61421
190	40.090	.12180D-16	.13498	.59082
200	48.164	.15466D-16	.15452	.57101
210	58.011	.19849D-16	.17638	.55497
220	69.164	.25086D-16	.24084	.54293
230	80.124	.30069D-16	.22733	.53409
240	88.820	.33138D-16	.25429	.53026
250	94.363	.33673D-16	.27986	.52796
260	97.346	.32373D-16	.30208	.52691
270	98.663	.30139D-16	.32310	.52646
280	99.319	.27761D-16	.34074	.52635
290	99.705	.25500D-16	.35617	.52616
300	99.833	.23362D-16	.36975	.52611
310	99.837	.21400D-16	.38178	.52600
320	99.944	.19688D-16	.39250	.52607
330	99.975	.18123D-16	.40210	.52606
340	99.985	.16681D-16	.41075	.52605

Table 3.5 Parameters: height 220 km, separation 300 km, $\sigma = \sqrt{2} \times 4 \times 10^{-6} \text{ m s}^{-1}$
Procedure: least squares collocation

N	PERCENTAGE ERROR	ERROR VARIANCE (POT.)	BAND ERROR (UNDUL.) (M)	TOTAL UNDUL. ERROR (M)
2				
10	.54171D-01	.10855D-22	.20911D-04	2.4620
20	.64022D-02	.22547D-23	.37100D-04	2.4306
30	.74292D-02	.21065D-23	.47124D-04	2.3880
40	.27053D-02	.26355D-23	.56300D-04	1.9152
50	.43779D-02	.30145D-23	.66059D-04	1.6190
60	.64363D-02	.61310D-23	.00361D-04	1.4171
70	.10564D-01	.10790D-22	.99090D-04	1.2560
80	.19621D-01	.20735D-22	.12650D-03	1.1362
90	.30675D-01	.43709D-22	.16065D-03	1.0444
100	.56042D-01	.10339D-21	.23695D-03	.96483
110	.10694	.20290D-21	.35343D-03	.90239
120	.20396	.97070D-21	.58402D-03	.84270
130	.51907	.51780D-20	.11265D-02	.79056
140	2.7408	.12060D-18	.36277D-02	.74452
150	2.9581	.11073D-18	.36479D-01	.70442
160	1.3367	.20104D-19	.36701D-01	.66762
170	1.1748	.19760D-19	.36709D-01	.63434
180	1.2541	.13631D-19	.36063D-01	.60406
190	1.4831	.16669D-19	.36943D-01	.57638
200	1.8796	.23555D-19	.37055D-01	.55096
210	2.5173	.37375D-19	.37221D-01	.52751
220	3.5442	.65073D-19	.37500D-01	.50580
230	5.2505	.12912D-18	.38010D-01	.48567
240	8.2395	.20517D-18	.39005D-01	.46695
250	13.900	.73070D-18	.41349D-01	.44961
260	25.079	.22880D-17	.47978D-01	.43383
270	53.941	.90005D-17	.66372D-01	.42092
280	93.490	.24598D-16	.10766	.41525
290	86.313	.19110D-16	.14537	.41366
300	73.100	.12520D-16	.16482	.40895
310	70.181	.10575D-16	.17813	.40341
320	72.265	.10276D-16	.18953	.39826
330	76.619	.10664D-16	.20042	.39397
	79.094	.10668D-16	.21113	.39063

Table 3.6 Parameters: height 160 km, separation 300 km, $\sigma = \sqrt{2} \times 10^{-6} \text{ m s}^{-1}$
 Procedure: least squares collocation
 (Based on zonals only)

N	PERCENTAGE ERROR	ERROR VARIANCE(POT.)	BAND ERROR (UNDUL.) (M)	TOTAL UNDUL. ERROR (M)
2	50.911	.95881D-17	.19728D-01	2.4629
10	12.197	.61828D-17	.58531D-01	2.4313
20	14.001	.74818D-17	.80666D-01	2.3901
30	4.9094	.06798D-17	.98988D-01	1.9178
40	7.7272	.10868D-16	.11735	1.6241
50	9.8631	.14399D-16	.13753	1.4237
60	14.335	.19649D-16	.16879	1.2663
70	22.340	.26879D-16	.18008	1.1517
80	28.336	.37365D-16	.22018	1.0674
90	39.298	.49417D-16	.25769	.99863
100	50.572	.63265D-16	.29932	.95074
110	58.704	.80422D-16	.34581	.91089
120	69.095	.91766D-16	.39360	.88312
130	77.970	.97599D-16	.44008	.86485
140	84.098	.97801D-16	.48322	.85345
150	89.952	.93749D-16	.52192	.84662
160	93.472	.87213D-16	.55592	.84267
170	95.848	.79627D-16	.68547	.84042
180	97.413	.71912D-16	.61104	.83918
190	98.417	.64578D-16	.63317	.83850
200	99.048	.57864D-16	.65237	.83813
210	99.434	.51849D-16	.66911	.83794
220	99.667	.46526D-16	.68377	.83784
230	99.806	.41843D-16	.69668	.83778
240	99.887	.37731D-16	.70810	.83775
250	99.935	.34118D-16	.71827	.83774
260	99.962	.30938D-16	.72734	.83773
270	99.978	.28130D-16	.73549	.83773
280	99.987	.25645D-16	.74283	.83773
290	99.993	.23437D-16	.74947	.83773
300	99.996	.21469D-16	.75556	.83773
310	99.998	.19709D-16	.76098	.83772
320	99.999	.18132D-16	.76598	.83772
330	99.999	.16713D-16	.77057	.83772

Table 3.7 Parameters: height 160 km, separation 150 meters $\sigma = \sqrt{2} \times 10^{-6} \text{ m s}^{-1}$
 Procedure: least squares collocation
 (Based on zonals only)

N	PERCENTAGE ERROR	ERROR VARIANCE (POT.)	BAND ERROR (UNDUL.) (M)	TOTAL UNDUL. ERROR (M)
2	.30368D-01	.34114D-23	.11767D-04	2.4620
10	.33459D-02	.61581D-24	.19914D-04	2.4306
20	.42366D-02	.68501D-24	.25397D-04	2.3088
30	.18197D-02	.11925D-23	.31853D-04	1.9152
40	.40211D-02	.29430D-23	.42568D-04	1.6198
50	.80181D-02	.11509D-22	.66534D-04	1.4171
60	.37230D-01	.13462D-21	.15760D-03	1.2560
70	.14423	.11204D-20	.15647D-02	1.1362
80	.49007D-01	.11545D-21	.15976D-02	1.0444
90	.53511D-01	.91628D-22	.16095D-02	.96404
100	.73030D-01	.13484D-21	.16230D-02	.90239
110	.11669	.31774D-21	.16402D-02	.84270
120	.26668	.13670D-20	.17202D-02	.79056
130	1.3372	.20708D-19	.24448D-02	.74451
140	1.4756	.29546D-19	.17653D-01	.70369
150	.70764	.58019D-20	.17723D-01	.66685
160	.69968	.40868D-20	.17029D-01	.63352
170	.91017	.71002D-20	.17095D-01	.60320
180	1.4794	.16586D-19	.10021D-01	.57540
190	3.2642	.71040D-19	.18433D-01	.55002
200	19.503	.22434D-17	.23663D-01	.52672
210	12.322	.79620D-18	.67046D-01	.50095
220	7.1526	.23962D-18	.60937D-01	.48906
230	7.2425	.22034D-18	.69573D-01	.47049
240	9.4383	.33607D-18	.70359D-01	.45318
250	15.256	.79516D-18	.71092D-01	.43712
260	32.677	.33060D-17	.76786D-01	.42268
270	86.509	.21062D-16	.10196	.41301
280	67.191	.11501D-16	.13517	.41019
290	52.194	.63856D-17	.14657	.40194
300	58.044	.62248D-17	.15478	.39365
310	63.954	.40618D-17	.16381	.38669
320	79.075	.11338D-16	.17553	.38192
330	91.945	.14129D-16	.19000	.37962

Table 3.8 Parameters: height 160 km, separation 600 km, $\sigma = \sqrt{2} \times 10^{-6} \text{ m s}^{-1}$

Procedure: least squares collocation

(Based on zonals only)

Finally, the results listed in Table 3.9 below show the sensitivity of the relative accuracies of the estimated coefficients to the choice of power spectrum model. The degree variances ε_n^2 of subroutine NVAR, described in paragraph 3.1 and in appendix B, have been replaced by those obtained according to a two-term model of the form described by expression (3.4), but with the following parameters' values:

$$A = 100, \quad B = 20, \quad A1 = 18.3906, \quad A2 = 658.6132, \quad S1 = 0.9943667, \\ S2 = 0.908949.$$

These values correspond to a model obtained by Jekeli ("2L" model, Report No. 275, Dept. of Geodetic Science, The Ohio State University, Columbus, Ohio, 1978). The values in the first column are the same as in Table 3.6; those in the second column correspond to the "2L" spectrum. As in the case of Tables 3.6 to 3.8, these values correspond to the zonals only.

Table 3.9

Relative Accuracies with Two Different Spectral Models

n	As in Table 3.6 (%)	Jekeli's "2L" (%)
2	$.54171 \times 10^{-1}$	$.55870 \times 10^{-1}$
20	$.74292 \times 10^{-2}$	$.74343 \times 10^{-2}$
40	.45779 "	.36486 "
60	$.10564 \times 10^{-1}$.87091 "
80	.30675 "	$.20738 \times 10^{-1}$
100	.10694	.72841 "
120	.51907	.382197
140	2.9581	2.1529
160	1.1748	.86360
180	1.4831	1.1068
200	2.5173	1.9143
220	5.2505	4.0815
240	13.900	11.106
260	53.941	46.794
280	86.313	82.380
300	70.181	65.245
320	76.689	73.190
330	76.327	79.894

The ε_n^2 up to $n = NM = 20$ are the same for both columns (subroutine MODEL in appendix B). Clearly, while the change in spectrum does make a difference, the changes have little influence on the calculated accuracies.

3.4 Accuracies of Different Harmonics of the Same Degree

Having come across the argument that SST data collected in a polar orbit should be most sensitive to the zonals, as all their variation occurs in the N-S direction, and least sensitive to the sectorials, with the tesserals falling somewhere in between, and the difference from zonals to sectorials being quite large, the author included in the main program statements to list the accuracies for the cosine terms ($\alpha = 0$) of all potential coefficients of degree $2 \leq n \leq 40$. The accuracies for $n = 30$ are listed below. The mission parameters are those for Table 3.1, and the principle used is that of least squares adjustment. The accuracies correspond to dimensionless, scaled coefficients (par. 2.3).

Table 3.10

Accuracies of potential coefficients of degree $n = 30$

m	$\sigma \hat{C}_{nm}$
0	2.08×10^{-13}
1	1.46 "
2	1.50 "
3	1.51 "
4	1.53 "
5	1.58 "
6	1.61 "
7	1.68 "
8	1.71 "
9	1.78 "
10	1.83 "
11	1.90 "
12	1.97 "
13	2.03 "
14	2.11 "
15	2.17 "
16	2.27 "
17	2.33 "
18	2.44 "
19	2.49 "
20	2.62 "
21	2.67 "
22	2.72 "
23	2.87 "
24	3.05 "
25	3.09 "
26	3.31 "
27	3.35 "
28	3.60 "
29	3.68 "
30	2.82 "

The values above are typical of those listed for other degrees in the interval $2 \leq n \leq 40$. While there are fluctuations, the sensitivity of the adjustment to the various harmonic terms of degree $n = 30$ does not change very much.

4. Validity of the Results

The numerical results of the previous section have been obtained under the simplifying assumptions of paragraph 2.1. Among those assumptions, numbers (1) to (4) define an orbital geometry more regular than what can be found in reality, and assumption (11) disregards all sources of error other than SST data errors. Of the remaining ones, (9) and (10) have been explained already in the first section of this report, while (5) to (8) merely describe what an ideally successful mission would produce in terms of data. Assumption (3) defines an idealized Earth rotation, where there are no fluctuations in the angular velocity Ω due to such causes as tidal friction, redistribution of atmospheric masses, lack of rigidity of the Earth, etc., and no changes in the inertial orientation of the spin axis due to precession-nutation and polar wandering. Changes in Ω are of two kinds: short term, due to solid Earth-atmosphere interaction, etc., altogether probably too small to matter, and secular, due to tidal effects caused by the Sun and the Moon, also very small and quite predictable from long records of observations. Polar motion is also well modelled from very long series of observations. The main effect of changes in Earth rotation is in the calculation of the satellites' orbits, as orbital errors affect also the accuracy of the results. Because of the existence of good models, this effect is probably negligible in the present context. So this section is going to consider only the consequences of assumptions (1), (2), (4), and (11) on the credibility of the results of the error analysis. The basic argument is that the actual data set, with its complex three-dimensional distribution, can be reduced or transformed into another with the geometry implied by the assumptions and with the same information content as the original. The analysis of this transformed data set can be done, then, in the manner explained in section 2, the accuracy of the estimated coefficients being much the same as that shown in the previous section.

4.1 The Geometry of the Real Orbit

The departure of the gravitational field from that of a central point mass causes the orbit to take a shape that is not exactly circular, however carefully the satellites are manouvered into it. Most of the departure from circularity is due to the part of the anomalous field that is already known from the study of terrestrial and spacecraft data, and the major portion of this known departure is caused by the second zonal, which is almost three orders of magnitude larger than any other harmonic. This zonal represents most of the effect of the Earth's equatorial bulge on the geopotential. The result is a wavy motion of the satellites, which alternatively run above and below the meansphere of radius R (average orbital radius), gain or lose ground in the along-track direction with respect to a perfectly uniform circular motion, and also move with respect to each other because of their different positions along the (more or less) common orbit, so the orientation of the line of sight is not always perpendicular to the radial direction, but fluctuates about, and there are also variations in the intersatellite distance. The non-zonal terms of the harmonic expansion introduce further irregularities, particularly in the across-track direction, so the orbit does not lie in any given plane except approximately. The effect of the non-zonals is, however, of the order of meters, while that of the second zonal amounts to several

kilometers. The discussion that follows suggests that errors of a few meters have negligible consequence, so only the departures due to oblateness need to be considered. If all measurements had been taken on a sphere of radius R , the line of sight being always perpendicular to the radial direction, and the separation between satellites constant, but the actual positions of the spacecrafts had been displaced in latitude and longitude from the ideal, periodical, regularly spaced pattern implied by the assumptions, one could transform this "semi-perfect" set of observations into a "perfect" set by interpolating horizontally the data from their actual positions to their ideal ones. As far as the signal content is concerned, this interpolation can be exact, because the information is band-limited, in the sense of paragraph 1.2, and the sampling is very dense. That such interpolation, to be exact, would probably require the use of all data values to create each interpolated value is of no consequence here, as this discussion is concerned only with the existence of valid transformation procedures, regardless of whether they are practical or not. The practical aspects of the matter are left for section 5. The only problem would be that the interpolated noise would not be exactly uncorrelated and of constant variance, its departure from those ideal qualities depending on how much the true groundtrack departs from the ideal one. Here one can only assume that, if this departure is not too large, neither would be the change in the nature of the noise too large. At this stage of the argument it will be assumed that the actual positions of the satellites can be known with negligible errors from orbital calculations, the effect of orbital error being treated later on in paragraph 4.3, where assumption (11) is discussed. As explained there, the model adopted for the line of sight velocity implies that such errors can have a very small effect on the estimated coefficients as long as they do not exceed a few meters, an accuracy achievable with existing orbit determination techniques.

The transformation of the actual set of observations into a set of pseudo-observations lying on the mean sphere along the ideal orbit can be carried out in two steps:

- (a) a vertical reduction of the original observations to the mean sphere, where an intermediate set consisting of pseudo-obs. with the following characteristics is created: the "midpoint" between "satellites" lies directly below the true midpoint, the "line of sight" is oriented North-South and perpendicular to the radial direction, the "satellites" are at the same distance from each other in all the pseudo obs; in other words: the intermediate pseudo obs. are identical to ideal observations in everything except their arrangement on the sphere;
- (b) a horizontal interpolation using the intermediate data set to form the final set of pseudo-obs. at regularly spaced points along the ideal orbit.

As already explained, the horizontal interpolation can be carried out, in principle, exactly, because of the band-limited nature of the gravitational signal. The main problem, therefore, is the vertical reduction or step (a). This step involves a downward or upward continuation of

the signal, depending on where the satellites happen to be with respect to the sphere, and a correction for the change in their relative position, which results in a variable intersatellite distance and line of sight direction. Both the continuation and this correction can be considered together, as an overall operation.

4.2 Vertical Reduction to the Mean Sphere

The discussion can be simplified by considering observations of line of sight relative acceleration, \hat{a}_{12} , rather than line of sight velocity, v_{12} . The signal being band-limited, it is possible to differentiate the velocity exactly by computing the Fourier coefficients of the data over the whole mission (assuming the orbit to be nearly periodic), and using these coefficients to calculate the acceleration, since the acceleration coefficients are related to the velocity ones by the simple relationship

$$\begin{Bmatrix} a_n \\ b_n \\ (\text{accel.}) \end{Bmatrix} = n\omega \begin{Bmatrix} a_n \\ b_n \\ (\text{veloc.}) \end{Bmatrix}$$

The N_p - vector of acceleration values $\underline{\alpha}$ can be obtained, formally, by multiplying the N_p - vector of velocity values by a $N_p \times N_p$ "differentiator" matrix S :

$$\underline{\alpha} = S \bar{v}_{12} \quad (4.1)$$

The model for the accelerations is, therefore,

$$\underline{\alpha} = S A \underline{c} \quad (4.2)$$

and the "observed" accelerations, which consist of differentiated signal and noise, are

$$\underline{\alpha}(\text{obs}) = S \bar{v}_{12}(\text{obs}) = S A \underline{c} + S \underline{n} \quad (4.3)$$

The least squares adjustment estimator is, therefore (paragraph (2.8))

$$\hat{\underline{c}} = (A^T S^T (D')^{-1} S A)^{-1} A^T S^T (D')^{-1} S \bar{v}_{12}(\text{obs}) \quad (4.4)$$

where D' is the variance-covariance matrix of the "differentiated" noise

$$\begin{aligned} D' &= E \{ (S \underline{n})(S \underline{n})^T \} = S E \{ \underline{n} \underline{n}^T \} S^T \\ &= S D S^T \end{aligned} \quad (4.5)$$

Replacing (4.5) in (4.4)

$$\begin{aligned}\hat{c} &= (A^T S^T (S^t)^T D^{-1} S^t S A)^{-1} A S^T (S^t)^T D^{-1} S^t \bar{v}_{12}(\text{obs}) \\ &= (A^T D^{-1} A)^{-1} A D^{-1} \bar{v}_{12}(\text{obs})\end{aligned}\quad (4.6)$$

where " S^t " indicates "The pseudo inverse of S " ($S^t S A = A$), so the least squares adjustment estimates of the coefficients based on the differentiated data are identical to those obtained from the data directly. The errors in the estimates being the same, any conclusions derived for accelerations are identical to the corresponding conclusions for velocities. The same principle applies to least squares collocation, as it can be seen by replacing $(A^T S^T (D')^{-1} S A)$ with $(A^T S^T (D')^{-1} S A + C^{-1})$ in the reasoning.

Figure 4.1 below shows the true position of the satellites, S_1 and S_2 , and their "pseudo-positions" on the mean sphere S'_1 and S'_2 (the "prima" symbols indicate the counterparts of real elements on the mean sphere). The relative positions shown have been chosen for pure convenience of representation: the satellites can be both above, both below, or on either side of the surface of the sphere.

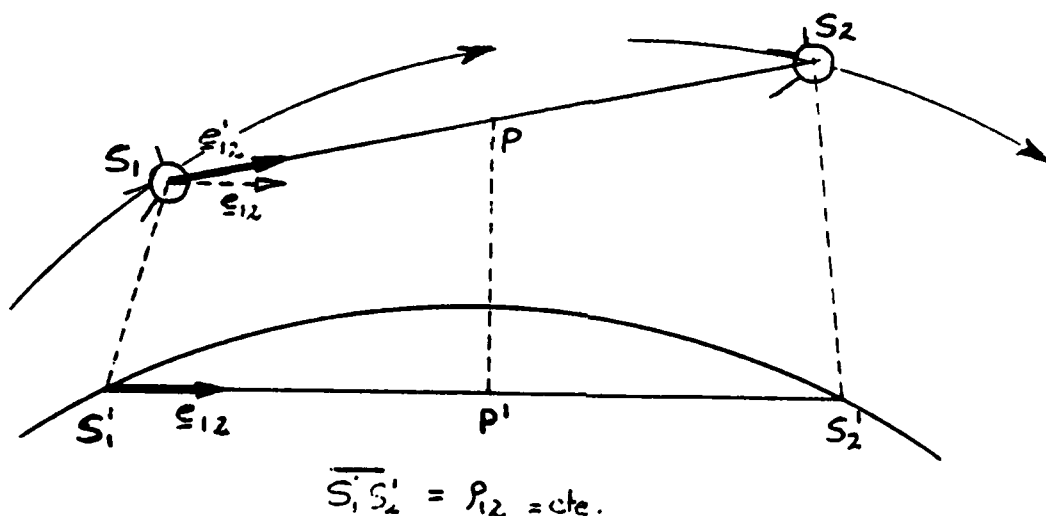


Figure 4.1: True Positions in Orbit and Pseudo-Positions on the Mean Sphere

Let

$$\delta \hat{a}(Q', Q) = \hat{a}(Q') - \hat{a}(Q) = \begin{Bmatrix} r'_0 \hat{a}_r(r', \phi', \lambda') - r_0 \hat{a}_r(r, \phi, \lambda) \\ \phi'_0 \hat{a}_\phi(r', \phi', \lambda') - \phi_0 \hat{a}_\phi(r, \phi, \lambda) \\ \lambda'_0 \hat{a}_\lambda(r', \phi', \lambda') - \lambda_0 \hat{a}_\lambda(r, \phi, \lambda) \end{Bmatrix} \quad (4.7)$$

be the variation in inertial acceleration between points Q and Q' where the r and ϕ components have been modified by the removal of a contribution from the zonals (paragraph 1.3). As it happens, this contribution comes only into a_r and a_ϕ , a_λ is free from this zero frequency problem. Let

$$\underline{\epsilon} = \underline{e}'_{12} - \underline{e}_{12}$$

be the difference between the unit vector in the direction of the actual line of sight, \underline{e}_{12} , and the unit vector \underline{e}'_{12} for the South-North perpendicular to the radial direction at the "pseudo-midpoint" P' . The difference between the true line of sight value and the corresponding "pseudo-observation" on the sphere is then

$$\begin{aligned} \delta \hat{a}_{12} &= \hat{a}'_{12} - \hat{a}_{12} \\ &= \underline{e}'_{12}^T (\hat{a}(S'_1) - \hat{a}(S'_2)) - \underline{e}_{12}^T (\hat{a}(S_1) - \hat{a}(S_2)) \\ &= \underline{e}'_{12}^T \delta \hat{a}(S'_1, S'_2) - (\underline{e}_{12} - \underline{\epsilon})^T \delta \hat{a}(S_1, S_2) \\ &= \underline{e}'_{12}^T (\delta \hat{a}(S'_1, S'_2) - \delta \hat{a}(S_1, S_2)) + \underline{\epsilon}^T \delta \hat{a}(S_1, S_2) \end{aligned} \quad (4.8)$$

Let d_{\max} be the maximum possible distance between a satellite and the corresponding "pseudo-satellite" position on the sphere. The value of d_{\max} will depend on the radial and horizontal components of the separation vector, but one could well argue that a purely radial separation should have much the same effect as the total displacement if both have the same size, because the lateral fluctuations are nearly one order of magnitude smaller than the radial one (appendix A). Consider the first term of (4.8). The contribution of the n th harmonic to this term is

$$\underline{e}'_{12}^T (\delta \hat{a}_n(S'_1, S'_2) - \delta \hat{a}_n(S_1, S_2))$$

where

$$\delta \hat{a}_n(S_1, S_2) = \begin{Bmatrix} \hat{a}_{rn}(S_1) r_0^{(1)} - \hat{a}_{rn}(S_2) r_0^{(2)} \\ \hat{a}_{\phi n}(S_1) \phi_0^{(1)} - \hat{a}_{\phi n}(S_2) \phi_0^{(2)} \\ \hat{a}_{\lambda n}(S_1) \lambda_0^{(1)} - \hat{a}_{\lambda n}(S_2) \lambda_0^{(2)} \end{Bmatrix} = \begin{Bmatrix} \delta \hat{a}_{rn}(S_1, S_2) \\ \delta \hat{a}_{\phi n}(S_1, S_2) \\ \delta \hat{a}_{\lambda n}(S_1, S_2) \end{Bmatrix} \quad (4.9)$$

\hat{a}_{rn} , $\hat{a}_{\phi n}$, $\hat{a}_{\lambda n}$ being the sum of all terms of degree n in the expansions of \hat{a}_r , \hat{a}_ϕ , \hat{a}_λ (expressions (1.8, a-c)). The variation of \hat{a}_{rn} with radial distance is

$$\hat{a}_{rn}(R, \phi, \lambda) - \hat{a}_{rn}(R + h, \phi, \lambda) \approx (1 - (\frac{R}{R+h})^{n+2}) \hat{a}_{rn}(R, \phi, \lambda) \quad (4.10)$$

and similarly for $\hat{a}_{\phi n}$, and $\hat{a}_{\lambda n}$. As both satellites follow the same orbit with a separation that is small compared to the wavelength of the second zonal and its disturbances, one can regard them, in a first approximation, as moving up and down simultaneously, so their heights are the same. In such case

$$\delta \hat{a}_{rn}(S'_1, S'_2) - \delta \hat{a}_{rn}(S_1, S_2) \approx (1 - (\frac{R}{R+h})^{n+2}) \delta \hat{a}_{rn}(S'_1, S'_2)$$

and similarly for the other components of \hat{a}_n , so

$$\delta \hat{a}_n(S'_1, S'_2) - \delta \hat{a}_n(S_1, S_2) \approx (1 - (\frac{R}{R+h})^{n+2}) \delta \hat{a}_n(S'_1, S'_2) \quad (4.11)$$

The magnitude of the first term of (4.8) is, therefore,

$$e_{12}^T (\delta \hat{a}_n(S'_1, S'_2) - \delta \hat{a}_n(S_1, S_2)) \leq ||e_{12}|| (1 - (\frac{R}{R+h})^{n+2}) ||\delta \hat{a}_n(S'_1, S'_2)||$$

As $||e_{12}|| = 1$ and $||\delta \hat{a}_n(S'_1, S'_2)|| \leq ||\delta \hat{a}_n||_{\max}$ (where $||\delta \hat{a}_n||_{\max}$ is the maximum size of the magnitude of \hat{a}_n on the mean sphere), and the segment $S'_1 S'_2$ has constant length, it follows that

$$e_{12}^T (\delta \hat{a}_n(S'_1, S'_2) - \delta \hat{a}_n(S_1, S_2)) \leq (1 - (\frac{R}{R+h})^{n+2}) ||\delta \hat{a}_n(S'_1, S'_2)||_{\max} \quad (4.12)$$

The difference between $\delta \hat{a}(S_1, S_2)$ and $\delta \hat{a}(S'_1, S'_2)$ is not very large, so the second term in (4.8) is, approximately,

$$\varepsilon^T \delta \hat{a}(S_1, S_2) \approx \varepsilon^T \delta \hat{a}(S'_1, S'_2)$$

The maximum value is

$$\varepsilon^T \delta \hat{a}(S'_1, S'_2) \leq ||\varepsilon||_{\max} ||\delta \hat{a}||_{\max}$$

The magnitude of $||\varepsilon||_{\max}$ is, to a first approximation (disregarding the curvature of the Earth), function of the relative displacement of the satellites:

$$||\varepsilon||_{\max} \approx \frac{\sqrt{\Delta r_{12}^2 + \Delta \rho_{12}^2 + \Delta \tau_{12}^2}}{\rho_{12}} \quad (4.13)$$

where Δr_{12} is radial, $\Delta \rho_{12}$ along the line of sight, and $\Delta \tau_{12}$ across-track. According to Appendix A, the largest displacements due to the anomalous field are: $\Delta \rho_{12\max} = 0.7$ km, $\Delta r_{12\max} = 0.7$ km, $\Delta \tau_{12\max} = 0.4$ km. $\Delta r_{\max} = 3.9$ km (vertical displacement of each satellite). Adding 1 km to $\Delta \rho_{12\max}$, $\Delta r_{12\max}$ and $\Delta \tau_{12\max}$, to introduce an extra error margin, the value of $||\varepsilon||_{\max}$ according to (4.13) is

$$||\varepsilon||_{\max} \approx 0.009$$

The contribution of the n th harmonic to the second term of (4.8), therefore, is

$$\varepsilon^T \delta \hat{a}_n(S'_1, S'_2) \leq 0.009 ||\delta \hat{a}_n||_{\max} \quad (4.14)$$

From (4.8), (4.12), and (4.14) one gets, finally,

$$\delta \hat{a}_{12} \leq [(1 - (\frac{R}{R+h})^{n+2}) + 0.009] ||\delta \hat{a}_n||_{\max} \quad (4.15)$$

as an upper bound for $\delta \hat{a}_{12}$. The maximum value of h is d_{\max} , as explained earlier. This maximum absolute displacement of any of the two satellites is

$$d_{\max} = \sqrt{(\Delta r_{\max} + \Delta r_{12\max})^2 + \Delta \rho_{12}^2 + \Delta \tau_{12\max}^2} \quad (4.16)$$

Replacing $(\Delta r_{\max} + \Delta r_{12\max})$, $\Delta \rho_{12\max}$, $\Delta \tau_{12\max}$ (1 km added to each) in (4.16) with their values according to appendix A :

$$d_{\max} \approx 4.7 \text{ km}$$

and the upper bound for $\delta \hat{a}_{12}$ becomes

$$\begin{aligned} \delta \hat{a}_{12n} &\leq [1.009 - (0.99928087)^{n+2}] ||\delta \hat{a}_n||_{\max} \\ &= p_n ||\delta \hat{a}_n||_{\max} \end{aligned} \quad (4.17)$$

This expression limits the difference between the actual line of sight acceleration along the non-circular orbit, and the corresponding pseudo-observation on the sphere. This is the largest possible value (if the argument behind (4.17) can be accepted) of the correction that has to be introduced in order to transform the original data set into the corresponding set of "accelerations" on the mean sphere. The factor p_n is

$$p_n = [1.009 + (0.99928087)^{n+2}] \quad (4.18)$$

If no correction is applied to the accelerations, and they are analyzed as if they were already on the mean sphere and on the ideal orbit, the error in the estimated coefficients will have two components: (1) that due to the data error, which has been listed in the previous section; (2) the error due to the fact that the uncorrected accelerations are not on the ideal orbit. As both errors have quite independent sources, the total rms error per degree is

$$\sigma \epsilon_n = [\sigma \epsilon_{n(1)}^2 + \sigma \epsilon_{n(2)}^2]^{\frac{1}{2}} \quad (4.19)$$

where $\sigma \epsilon_{n(1)}$ corresponds to the first, and $\sigma \epsilon_{n(2)}$ to the second source of error. The relative error per coefficient is, then

$$\rho_n(T) = \frac{\sigma \epsilon_n(2n+1)^{-1}}{\sigma_n(2n+1)^{-1}} = ((\frac{\sigma \epsilon_{n(1)}}{\sigma_n})^2 + (\frac{\sigma \epsilon_{n(2)}}{\sigma_n})^2)^{\frac{1}{2}} = (\rho_{n(1)}^2 + \rho_{n(2)}^2)^{\frac{1}{2}} \quad (4.20)$$

where $\rho_{n(1)}$ is the propagated noise listed in Tables 3.1 or 3.2 of section 3. If the only difference between the real and the ideal orbits were an increase in radial distance, or expansion, so $R - R' = d_{\max}$ were constant, then it would follow from (4.8), (4.10), and (4.17) that

$$\delta \hat{a}_{12n} = p_n \hat{a}_{12n} \quad (4.21)$$

as $\bar{e}_{12} = \bar{e}'_{12}$ and $\delta \hat{a}_{12n}(S_1, S_2) = \left(\frac{R}{R+d_{\max}}\right)^{n+2} \delta \hat{a}_{12n}(S'_1, S'_2)$ at all points along the orbit, so

$$\rho_n(2) = \frac{\sigma_{\epsilon n(2)}}{\sigma_n} = |\delta \hat{a}_{12n}|_{\max} \|\delta \hat{a}_{-n}\|_{\max}^{-1} = p_n \quad (4.22)$$

In reality $\delta \hat{a}_{12n}$ becomes modulated by the changes in distance between true and ideal orbit, as this distance cannot be constant. Consequently expression (4.21) is no longer true, but merely an approximation to a very complicated relationship. The error should be less than with a constant radial increase d_{\max} at almost every point, so perhaps the use of the right hand side of (4.22) as an upper bound for $\rho_n(2)$ is a realistic choice: $\rho_n(2) \leq p_n$.

Let the coefficients estimated from the original set of accelerations $\hat{a}_{12}(0)$ be called $\hat{C}_{nm}^{\alpha}(0)$, and let $\hat{a}_{12}(1) = \hat{a}_{12}(0) + \delta \hat{a}_{12}(0)$ be the original accelerations corrected with values $\delta \hat{a}_{12}(0)$ of $\delta \hat{a}_{12}$ computed using the $\hat{C}_{nm}^{\alpha}(0)$. Let $\hat{C}_{nm}^{\alpha}(1)$ be the coefficients obtained from the analysis of the $\hat{a}_{12}(1)$, and let $\delta \hat{a}_{12}(1)$ be a new estimate of $\delta \hat{a}_{12}$ based on the $\hat{C}_{nm}^{\alpha}(1)$. Correcting the original $\hat{a}_{12}(0)$ with the $\delta \hat{a}_{12}(1)$ and then analyzing again, one obtains $\hat{C}_{nm}^{\alpha}(2)$. If $\hat{a}_{12}(2) = \hat{a}_{12}(0) + \delta \hat{a}_{12}(1)$ is closer to the transformed set of pseudo-obs $\hat{a}_{12}(0) + \delta \hat{a}_{12}$ (that is the subject of this paragraph) than the $\hat{a}_{12}(1)$, then $\hat{C}_{nm}^{\alpha}(2)$ should be an improvement on $\hat{C}_{nm}^{\alpha}(1)$, $\delta \hat{a}_{12}(2)$ on $\delta \hat{a}_{12}(1)$, so $\rho_n(2) < \rho_n(1)$. Let $\hat{C}_{nm}^{\alpha}(M)$, $\delta \hat{a}_{12}(M)$, $\rho_n(M)$, etc. be the outcome of $M+1$ iterations of this analysis-correction-analysis procedure. As $M \rightarrow \infty$ $\hat{C}_{nm}^{\alpha}(M)$ may converge to some limit $\hat{C}_{nm}^{\alpha(\infty)}$ and $\rho_n(2)(M)$ to $\rho_n^{\infty}(2)$, where $\rho_n^{\infty}(2) < \rho_n(2)(M)$ because $\hat{C}_{nm}^{\alpha(\infty)}$ is better than $\hat{C}_{nm}^{\alpha}(M)$. As p_n is the ratio of $\delta \hat{a}_{12n}$ to $\hat{a}_{12n}(0)$, if the relative error in the $\hat{C}_{nm}^{\alpha}(M-1)$, and thus in the $\delta \hat{a}_{12}(M-1)$, is $\rho_n(T)(M-1)$, the error ratio for the corrected $\hat{a}_{12}(M) = \hat{a}_{12}(0) + \delta \hat{a}_{12}(M-1)$ and thus for the $\hat{C}_{nm}^{\alpha}(M)$ must be (1)

$$\rho_n^{(M)} \leq (\rho_n^2(1) + p_n^2 \rho_n^2(T))^{(M-1)\frac{1}{2}}$$

or

$$\rho_n^{2(M)} \leq \rho_n^2(1) + p_n^2 (\rho_n^2 \rho_n^2(T))^{(M-2)} + \rho_n^2(1) \quad (4.23)$$

so

$$\rho_n^{2(M)} \leq q_n^2 \rho_n^2(T)^{(M-2)} + q_n \rho_n^2(1) \leq q_n^3 \rho_n^2(T)^{(M-3)} + q_n^2 \rho_n^2(1) + q_n \rho_n^2(1) + \rho_n^2(1)$$

where $q_n = p_n^2$. Repeating this reasoning backwards $M-1$ times:

$$\begin{aligned} \rho_n^{2(M)} &\leq q_n^{(M-1)} (\rho_n^2(1) + q_n) + q_n^{(M-2)} \rho_n^2(1) + \dots + q_n \rho_n^2(1) + \rho_n^2(1) \\ &= q_n^M + \rho_n^2(1) [q_n^{(M-1)} + q_n^{(M-2)} + \dots + q_n + 1] \\ &= q_n^M + \rho_n^2(1) \frac{1 - q_n^M}{(1 - q_n)} \end{aligned} \quad (4.24)$$

(1) The noise S_n in the corrected accelerations $\hat{a}_{12}^{(M)} = \hat{a}_{12}^{(0)} + \delta \hat{a}_{12}^{(M-1)}$ is always the same, so $\rho_n(1)$ is independent of M .

so

$$\rho_n^\infty(T) = \lim_{M \rightarrow \infty} \rho_n^{(M)}(T) \leq \frac{\rho_n^{(1)}}{(1 - \rho_n^2)^{\frac{1}{2}}} = \frac{\rho_n^{(1)}}{(1 - \rho_n^2)^{\frac{1}{2}}} \quad \text{if } \rho_n < 1$$

Examining (4.18) one can see that for $n = 331$ (top of the band), is

$$\rho_n \approx 0.22$$

As both ρ_n and $\rho_n^{(1)}$ fall with decreasing n , for all n in the band is

$$\rho_n^{(M)}(T) < \rho_{331}^{(M)}(T) \quad \text{and} \quad \rho_n < \rho_{331} < 1$$

Therefore it is true that

$$\rho_n^\infty(T) \leq \frac{\rho_n^{(1)}}{(1 - \rho_n^2)^{\frac{1}{2}}} \quad (4.25)$$

The values of $\rho_n^\infty(T)$ and of $\rho_n^{(4)}(T)$ have been listed below, together with the corresponding values of the error $\rho_n^{(1)}$ given in Table 3.2 and derived under the simplifying assumptions. The closeness between the "true" and the "ideal" relative errors is clear. Moreover, the iterative procedure appears to converge very quickly, as $\rho_n^\infty(T)$ and $\rho_n^{(4)}(T)$ agree to three decimal places.

n	$\rho_n^{(1)} \times 100$	$\rho_n^\infty(T) \times 100$	$\rho_n^{(4)}(T) \times 100$
10	0.0063	0.0063	0.0063
100	0.0686	0.0688	0.0689
150	2.8401	2.8582	2.8583
200	7.9146	7.9982	7.9987
250	21.620	21.9581	21.9583
300	65.941	67.3613	67.3614
331	82.269	84.3747	84.3748

It must be remembered that, on the one hand, the reasoning leading to (4.25) is by no means rigorous, while, on the other hand, the assumptions made in it have been mostly on the conservative side. It appears that a series of iterations as described here should transform the original set of observations into a set of "accelerations" on the ideal orbit, in such way that the coefficients estimated from these transformed set would have much the same accuracies as those listed in section 3 and derived under the simplifying assumptions of paragraph 2.1. In this sense, the results of section 3 are supported by those above; they may very well indicate the maximum amount of information on the geopotential that can be extracted by linear estimation techniques from a real set of SST data.

4.3 The Effect of Errors in the Calculated Orbits

To apply the corrections $\delta a_{12}^{(M)}$ to the $\hat{a}_{12}^{(0)}$ one must know the position of the two satellites, S_1 and S_2 . In the previous paragraph it was assumed that this knowledge was exact. In reality, however, the gravity field model used to compute the orbits, the coordinates assigned to the tracking stations, and the tracking data used to calculate the orbits, all contain errors, so there is a discrepancy between computed and true orbits. With present tracking, coordinates, and models, the errors in the calculated orbits are not likely to exceed a few meters. The direct effect of these errors is an additional error in the corrections $\delta \hat{a}_{12}^{(M)}$, as the accelerations $a_{12}^{(0)} + \delta \hat{a}_{12}^{(M)}$ are "dropped" from their true positions to the calculated ones. The change in $\delta \hat{a}_{12}^{(M)}$ for a displacement of Δs meters is likely to have a size comparable to the effect of a purely vertical displacement of the same magnitude. From (4.11) follows that such change is

$$\Delta \delta a_{12n}^{(M)} = (1 - (\frac{R}{R + \Delta s})^{n+2}) \delta \hat{a}_{12n}^{(M)} \quad (4.26)$$

or, to a very good first approximation

$$\begin{aligned} \Delta a_{12n}^{(M)} &= -(n+2) \frac{\Delta s}{R} \delta \hat{a}_{12n}^{(M)} \\ &= \beta_n(\Delta s) \delta \hat{a}_{12n}^{(M)} \end{aligned} \quad (4.27)$$

Even for $n = 331$, at the very top of the band, the relative error β_n caused by an orbital error of 10 m is insignificant: $\beta_{331}^{(10)} = 5 \times 10^{-5}$. This error decreases with n , as indicated by (4.27), so it is smallest at $n = 0$. However, the size of the zero harmonic is so large that its net change over 10 m amounts to some 3 mgal. If no correction term for this and the other even zonals is introduced in the definition of the derivative of the line of sight velocity, as suggested in section 1, then the effect of a vertical displacement is

$$\beta_0(\Delta s) \delta \hat{a}_{120}^{(M)} = -2 \sin \frac{\psi}{2} \frac{\partial}{\partial r} \frac{GM}{r^2} \Delta s \quad (4.28)$$

or 0.138 mgal every 10 m. Because the orbital error is not constant, this change in the zero harmonic contribution is modulated by the complex shape of the error, so the power of the zero harmonic change spills over the whole spectrum corrupting all the estimated coefficients. As the power associated with $n > 100$, in mgal, is well below 0.138 mgal at satellite altitude, this can have serious consequences. In the model adopted here for a_{12} the zero harmonic has been excluded, so only the errors due to the other terms in the expansion, all of them quite negligible, are present.

5. Data Processing

The objective of this section is to include some thoughts on how to process the masses of information collected from a SST experiment into a global geopotential model of very fine resolution. This problem goes beyond the scope of this study, but some further elaboration of concepts introduced in previous sections may help clarify this difficult subject, and perhaps point out directions for future research.

5.1 An Iterative Approach

The argument used in the previous section to substantiate the numerical results of section 3 suggests that a model may be obtained through successive approximations. To be able to use the sort of "analysis-correction-analysis" approach hinted at in that argument, it is necessary to have certain regularities in the data that, though physically possible, may not occur in practice. On practical grounds one can question two assumptions made implicitly in last section: that the departures from perfectly circular orbits were due to the anomalous gravity field alone, and that the data were sampled uninterruptedly at constant intervals during the whole mission, all measurement errors having the same standard deviation.

Even when the compensating mechanism could eliminate all non-gravitational forces, and when gravitational fields (other than the Earth's) and the effect of the body-tide could be calculated exactly from existing models and thus discounted, the relative positions of the satellites are not going to vary as predicted from the action of the anomalous field alone. The reason for this is that it is impossible to determine and control exactly the state of each satellite at "injection" time, to make sure that both move along the same orbit, and that such orbit is as close to circular as the field would allow. As a consequence, besides the relative motion caused by the field there will be a "drift" due to incorrect initial conditions. This drift will follow a more or less arbitrary direction, resulting in the spacecrafts moving towards or away from each other until their separation and the direction of the line of sight change so much that observations taken at different times cannot be described sufficiently well by equations that assume a fixed distance and angle. Since the total relative motion can be calculated from the reference orbits with an accuracy of a few meters, the change in relative configuration with time should soon become apparent. This change should have a more or less periodic component due to the irregular gravitational field, and a trend due to previous orbital manouvers' errors. While these errors cannot be determined accurately, the drift itself increases with time until it becomes easy to estimate. The fact that the satellites are tracking each other continuously, in addition to being tracked from terrestrial stations, should help to obtain a good estimate of the drift and the drift-rate. When the drift reaches a maximum allowed value, the controlling rockets of either spacecraft can be fired briefly to reverse the drifting motion, so the drift begins to decrease (the reversal need not be exact). This scheme is a "dead zone" control policy where correcting action is applied only when a certain limit is about to be exceeded. As the purpose is to reverse the drift rate rather than to eliminate the drift altogether, the correction need not be particularly drastic. Even so, the use of such a scheme must increase the amount of fuel required

during the mission, and thus the overall cost. Of course, some correcting maneuvers of the sort described here will have to take place from time to time, to stop the two spacecraft from separating too much (so the radar beam does not cut too deeply inside the atmosphere, or is intercepted by the curvature of the Earth itself, at a separation of about 2700 km) or from becoming too close, as the shorter their distance, the weaker the signal and the less accurate the results, as shown in section 3, Tables 3.6, 3.7, and 3.8. The question is how often such maneuvers will take place, not whether they shall be needed at all. Compensatory changes in the design of the mission could allow the use of "dead zone" control to maintain relative orientation without raising the cost too much. It may be possible to choose a higher orbit, where less fuel for drag compensation is needed (the decrease in fuel requirement with height should be quite fast) so the balance can be used for maneuvering. The length of the mission could be increased, the accuracy of the data improved, or both, to compensate for the weaker signal at greater height. All of these factors, some contradictory, and others, as well, can only be balanced properly in a thorough mission design study incorporating the demands of data processing among the main questions to be considered. Given the magnitude of such demands, some regard for them appears natural.

Another assumption made in section 4 that may not be fulfilled in practice is the existence of uninterrupted series of measurements lasting the whole mission. Breaks will occur in the data, some much too large to be ignored or "patched up" by interpolation from surrounding data. There may be fluctuations, as well, in the quality of those measurements due to problems in the satellites themselves, or in the surrounding medium, as in the case of severe ionospheric perturbations. So the stream of data will not be perfectly uniform in quality (variations in the standard deviation of the errors) or unbroken. These departures from the assumptions, if severe enough, would make a close application of the ideas presented in earlier sections quite impossible. One could begin, as an alternative, by differentiating numerically the data to obtain line of sight accelerations. Supposing that the model of section 1 is correct, these accelerations on a sphere have the form

$$a_{12}(R, \phi', \lambda) = \sum_{\alpha=0}^1 \sum_{n=0}^N \sum_{m=0}^n \tilde{C}_{nm}^{\alpha} g_{nm}(\phi') \begin{Bmatrix} \cos \\ \sin \end{Bmatrix} m\lambda \quad (5.1)$$

where, according to expression (2.9) and (2.15,a-b)

$$g_{nm}(\phi') = (n+1) \left[L_{nm}(\phi' - \frac{\psi}{2}) + L_{nm}(\phi' + \frac{\psi}{2}) \right] \sin \frac{\psi}{2} + \\ + \frac{d}{d\phi} \left[L_{nm}(\phi' - \frac{\psi}{2}) - L_{nm}(\phi' + \frac{\psi}{2}) \right] \cos \frac{\psi}{2}$$

and

$$\tilde{C}_{nm}^{\alpha} = \frac{GM}{R^2} \left(\frac{a}{r} \right)^n C_{nm}^{\alpha}$$

Functions that can be expanded in series of the type of (5.1), which includes the ordinary spherical harmonic expansion, can be analyzed to obtain the values of the C_{nm}^{α} by very efficient methods resembling numerical quadratures. The derivation and implementation of optimal methods that minimize the estimation error in the presence of unhomogeneous and correlated noise have been discussed by Colombo (1981, paragraphs 2.9

and 2.12). While the procedures presented by this author in that work have been derived for the case

$$g_{nm}(\phi') = \bar{p}_{nm}(\phi')$$

(i.e., spherical harmonics) the extension to the more general case of (5.1) is quite direct. The only requirement is that the data occupy the nodes of a regular grid where the separation between meridians is constant. This can be done by interpolating the differentiated velocities on those nodes from surrounding data points, while also determining the correlations and standard deviations of the interpolated values from those of the observations, as these are needed to set up the optimal estimator. If no reliable interpolation is possible on some node, because of large data breaks in the vicinity, a value of zero with a "standard deviation" equal to the rms of the line of sight acceleration could be used instead.

By setting up an appropriate control mechanism to maintain the relative configuration of the satellites within sufficiently close limits, and by using the interpolated accelerations as pointed out above, the iterative scheme could proceed basically along the lines of section 4, except that the data would be analyzed as in Colombo (1981), rather than as in section 2. If such a control scheme proves to be feasible, the next important question is how to calculate the corrections δa_{12} of expression (4.8) from the \hat{C}_{nm} estimated in the previous iteration, to refine the pseudo-observations on the mean sphere. Because of the irregular shape of the orbit, calculation of these corrections using exact relationships is too laborious to be practical, even with very powerful computers. The main reason is the number of operations needed to obtain every $\hat{\delta a}_{12}$, which is proportional to the number of coefficients (some 11×10^4 if $N = 331$). This matter needs thorough investigation, but the answer should involve some sort of approximation, to reduce the computer burden. One possibility that may be worth exploring is as follows: consider a spherical shell extending 5 km above and 5 km below the mean orbital sphere. The whole orbit, according to Appendix A, should lie within this shell. Imagine the shell subdivided according to a regular grid, equal angular for instance, where the blocks are $y^0 \times y^0$ in size, so the shell is partitioned into cells each $y^0 \times y^0 \times 10$ km in volume (the size of y^0 should be decided by detailed study). The vertices of the cells are arranged in equal angular fashion, so one can compute the three inertial acceleration components at every vertex according to expressions (1.8, a-c) very efficiently using, for example, algorithms like those described by Colombo (1981). To calculate the correction δa_{12} one must know the value of a_{12} in the actual orbit and in the ideal orbit, and for that the three accelerations at points S_1 and S_2 , S_1' and S_2' (in Fig. 4.1) are needed. These accelerations can be computed from their values at the vertices of the cell containing those points by some interpolatory procedure, which should be a great deal easier than an exact calculation.

The type of approximate calculation of the acceleration components just described may be used, as well, to obtain the forcing function due to gravitation needed to integrate numerically satellite orbits with a very high degree and order field model, like the one whose determination is being discussed here. Such calculations may be necessary, for example, to reduce the orbital errors at each step of the iterative modelling procedure.

5.2 Other Methods

Instead of converting the data into pseudoobservations on the mean sphere by successive iterations, this could be done directly by estimating the pseudoobs. in one step from neighbouring data points. This means carrying out a series of local reductions that finally covers the whole sphere with a regular grid of estimated values. These values should correspond to a variable that can be described by an expansion of the type of (5.1), and which does not have to be the line of sight acceleration of equation (2.24). These local reductions can be done in many different ways. One possibility is to use least squares collocation in a local manner. A problem with local solutions by collocation is that the signal in SST measurements tends to be too strongly correlated over considerable distances, and this causes the variance-covariance matrix to be too ill-conditioned to be inverted in a dependable way. According to R. Rummel (private communication) a minimum separation of about 100 km between data points is necessary for stable inversion. As the actual points are likely to be spaced some 30 km apart along-track (with a sampling interval of 4 s) and by less than that across-track, (because the separation between adjacent passes should be of only a few kilometers by the end of a six-month's mission) some kind of paring, or decimation, of the data will be needed to achieve the larger spacing. This could be done in the first of two steps: beginning with decimated data, a set of pseudoobservations could be obtained without stability problems, and a first estimate of the harmonic coefficients could be made from this set. In the second step, all the data could be used after subtracting from them their nominal values according to the model produced in step one, which could have high degree terms already. Such residuals are going to be less correlated than the original measurements, because much of their low frequency content would have been removed, so the inversion of their variance-covariance matrix may be stable in spite of the close spacing of the data points.

If no control of the relative alignment of the satellites takes place and they are allowed to drift freely with respect to each other, the corresponding observation equations would lack the regular structure assumed in section 2. In such a case the ideas for analysing the data discussed in the previous paragraph are not applicable, and only non-iterative methods like the one just outlined seem to offer any real hope.

Any method that first creates a regularly spaced set of pseudoobservations on the mean sphere and then analyses it efficiently to obtain the potential coefficients requires two main things:

(a) a model for the data that is both practical and accurate. An example of this may be the model adopted in sections 1 and 2, but this idea needs further validation, as pointed out at the end of paragraph 1.3;

(b) an efficient and accurate way of reducing the measurements in the actual orbit to pseudoobservations on the mean sphere.

Both problems require more research to clarify them, and this clarification may be absolutely necessary before developing an effective technique for processing SST data.

5.3 The Use of Local Solutions

As mentioned in the introduction, there have been studies of the SST problem that have concentrated on purely local solutions that use data taken from inside a relatively small neighborhood of the points at the Earth's surface where certain quantities associated with the gravitational field are estimated. The advantage of the global approach is that every value that is estimated is obtained from the processing of all the data available, so it can be more accurate than a local solution based only on part of the data. . . . Global solutions may be free from the numerical instabilities that tend to be associated with local solutions. Global solutions have also some important limitations. A spherical harmonics model, for instance, must be truncated at some finite degree for practical reasons and this limits the size of the finest detail that the model can represent. Even if the number of coefficients is not a problem, some very fine but also quite strong features that may be sensed by the satellite pair, such as anomalies along ocean ridges and trenches, mountain ranges, etc., are likely to be smoothed out by an optimal global estimation procedure because, on a global scale, they are similar to measurement noise. Such small but marked features may be recovered by using local estimation methods, applied in the knowledge that sharp field variations may occur in certain areas. These methods may use residual SST data, with respect to the global solution, to ensure numerical stability and the removal of trends of non-local nature.

Local modelling should be regarded, therefore, as complementary to global analysis, because its careful application in selected areas may push the level of resolution to the very limits allowed by the information contained in SST data. Local solutions may permit also the combination of SST data with terrestrial measurements of gravity, with satellite altimetry over the oceans, and with knowledge of the geological structures that may be responsible for some of the high frequency content of the signal, all of which may be difficult to incorporate into a global solution.

6. Conclusions

According to the theory given in sections 1 and 2, assuming that the power spectrum of the geopotential is as described in paragraph 3.1, and that the reasoning of section 4 is valid, the results presented in section 3 can be summarized as follows: with two satellites in nearly the same circular, polar orbit, at a height of 160 km, 300 km apart, with a tracking accuracy of $\sqrt{2} \times 10^{-6} \text{ m s}^{-1}$, a sampling period of 4 s, an averaging period of 4 s, and a mission length of six months, the coefficients of the spherical harmonic expansion of the potential up to degree $n = 331$, may be estimated to the following extent:

(1) the relative accuracy of the potential coefficients could be better than 1% for $n \leq 130$, than 10% for $n \leq 210$, and than 50% for $n \leq 270$, using least squares collocation. With least squares adjustment, the results may be the same up to $n = 200$, and for higher degrees collocation may work better.

(2) the accuracy of the geoid undulation implied by the coefficients could be better than 0.05 mm rms for wavelengths of between 3000 km and 40030 km, and better than 10 cm rms in the band between 140 km and 3000 km.

The method of analysis of section 2 can be used for studying missions where the orbital plane is oblique to the equator. This would require some changes in the programs listed in Appendix B, subroutine ONEREV in particular, because those are written for the case of polar orbits only. As they are, they can be used to carry out an analysis of the magnitude reported here in any modern computer with some 1.5 megabytes of core. If the highest degree studied is $N = 331$, the central processor unit time required is of the order of one hour. The effect on the results of changes in some of the mission parameters can be studied, in the case of least squares adjustment, using the results of section 3 and the simple formulas of paragraph 2.13. Only potential coefficients and geoid undulations' accuracies have been calculated; the accuracies of other quantities, gravity anomalies, for example, can be obtained in a simple way from the coefficients' accuracies, a complete listing of which, degree by degree, appears in Appendix C.

The method of section 3 allows for a spherical, rotating Earth, and for data consisting of velocity averages. A number of simplifying assumptions listed in paragraph 2.1 are substantiated in sections 1 and 4, in an attempt to show that the results listed in section 3 represent the limit of accuracy for a global model obtainable from real SST data if the mission could be carried out without a single fault.

The accuracies listed being global, the undulation errors are likely to be worse in some areas, perhaps where the field is strongly anomalous, such as mid-ocean ridges, ocean trenches, mountain ranges, etc., and necessarily better than average over the remainder of the planet. In those areas where the model may perform poorly, local solutions (using the model as a reference field to calculate the residuals of satellite and terrestrial data, and these residuals, in turn, as the observed values) may provide the finer detail that a global technique alone cannot reveal.

As argued in section 5, an iterative solution based on the ideas of sections 2 and 4 may be used for the actual analysis of SST data. Alternatively, non-iterative methods could be developed for that purpose. All such methods should have in common the fact that they rely on some convenient approximation, as rigorous solutions such as those based on the "numerical" or the "analytical" (i.e., celestial mechanics) approaches are virtually impossible to implement, given the enormous number of harmonic coefficients to be adjusted and of observations. Two essential tasks to be accomplished through further research before a satisfactory technique can be found are, in all likelihood, the following:

(a) validation of the model of the line of sight relative acceleration used in sections 1 and 2, or its replacement by another that provides a better approximation and is just as tractable mathematically;

(b) development of a satisfactory procedure for reducing the SST measurements to a set of pseudoobservations regularly distributed over the mean orbital sphere, whose analysis can then be carried out with efficient algorithms.

Further work on how to model the SST signal should also help to clarify the question of the influence of orbital errors on the estimated quantities, influence that, according to the model adopted here, may be small.

References

- Bibby, J., and H. Toutenberg, Prediction and Improved Estimation in Linear Models, John Wiley and Sons, New York, 1977.
- Breakwell, J., Satellite Determination of Short Wavelength Gravity Variations, The Journal of Astronautical Sciences, Vol. XXVII, No. 4, Sept.-December, 1979.
- Colombo, O.L., Numerical Methods for Harmonic Analysis on the Sphere, Department of Geodetic Science Report No. 310, The Ohio State University, Columbus, Ohio, 1981.
- Douglas, B.C., C.C. Goad and F.F. Morrison, Determination of the Geopotential from Satellite-to-Satellite Tracking Data, NOAA Technical Memorandum NOS NGS 24, National Geodetic Survey, January 1980.
- Gravsat Users Working Group, The Requirements and Feasibility of the Gravsat Mission, NASA Headquarters, Geodynamics Branch, Washington, D.C., 1979.
- Hajela, D.P., Direct Recovery of Mean Gravity Anomalies from Satellite-to-Satellite Tracking, Dept. of Geodetic Science Report No. 218, The Ohio State University, Columbus, Ohio, 1974.
- Hajela, D.P., Improved Procedures for the Recovery of 5° Mean Gravity Anomalies from ATS-6/GEOS-3 Satellite-to-Satellite Range-Rate Observations, Dept. of Geodetic Science Report No. 276, The Ohio State University, Columbus, Ohio, 1978.
- Hobson, E.W., The Theory of Spherical and Ellipsoidal Harmonics, Chelsea Publishing Company, Reprint of the 1931 original edition, New York, 1965.
- Jekeli, C., and R.H. Rapp, Accuracy of the Determination of Mean Anomalies and Mean Geoid Undulations from a Satellite Gravity Field Mapping Mission, Dept. of Geodetic Science Report No. 307, The Ohio State University, Columbus, Ohio 1980.
- Kahn, W.D., J.W. Siry, W.T. Wells, Gravity Model Improvement, Manuscript, first two authors were with the Goddard Space Flight Center, Greenbelt, Maryland, 1978.
- Kahn, W.D. and W.T. Wells, Determination of Gravity Anomalies Using a Combination of Satellite-to-Satellite Tracking and Altimetry Data, Paper presented at the Spring Meeting of the A.G.U., Washington, D.C., June 1979.
- Kaula, W.M., Theory of Satellite Geodesy, Blaisdell Publishing Company, Waltham, Massachusetts, 1966.
- Keldych, M., and M. Lavrentieff, Sur les Suites Convergentes de Polynomes Harmoniques, Travaux de L'Institut Mathématique de Tbilissi, T.I., 1937.

- Krarup, T., A Contribution to the Mathematical Foundation of Physical Geodesy, Report of the Geodetic Institute, Copenhagen, 1969.
- Krynski, J., Possibilities of Low-Low Satellite Tracking for Local Geoid Improvement, Report of the Geodetic Institute of the Technical University at Graz No. 37, Graz, 1978.
- Lerch, F.J., S.M. Klosko, R.E. Laubscher, and C.A. Wagner, Gravity Model Improvement Using GEOS-3 (GEM 9 & 10), Goddard Space Flight Center Document X-921-77-246, Greenbelt, Maryland, 1977.
- Marsh, J.G., and B.D. Marsh, Gravity Anomalies Near the East Pacific Rise with Wavelengths Shorter than 3300 km Recovered from GEOS-3/ATS-6 Satellite-to-Satellite Doppler Tracking Data, NASA Technical Memorandum 79533, December, 1977.
- Martin, T.V., GEODYN Systems Operation Description, Wolf Research and Development Group Final Report on Contract NAS 5-11736-149, Maryland, 1972.
- Moritz, H., Statistical Methods in Physical Geodesy, in "Physical Geodesy" by Heiskanen and Moritz, W.H. Freeman and Company, 1967.
- Moritz, H., Advanced Physical Geodesy, Abacus Press, Kent, 1980.
- Muller, P.M., and W.L. Sjogren, Mascons: Lunar Mass Concentrations, Science, 161, pp. 680-684, 1968.
- National Academy of Science (USA), Applications of a Dedicated Gravitational Satellite Mission, Report of the Workshop on a Dedicated Gravitational Satellite Mission, Washington, D.C., 1979.
- Paik, H.J., Superconducting Tensor Gravity Gradiometer for Satellite Geodesy and Inertial Navigation, Journal of Astronautical Sciences, 1981.
- Pisacane, V.L., and S.M. Yionoulis, Recovery of Gravity Variations from Satellite-to-Satellite Tracking, Report SDO 5583, Applied Physics Laboratory, The Johns Hopkins University, Laurel, Maryland, 1980.
- Rapp, R.H., and D.P. Hajela, Accuracy Estimates of $1^\circ \times 1^\circ$ Mean Anomaly Determination from a High-Low Satellite-to-Satellite Tracking Mission, Dept. of Geodetic Science Report No. 295, The Ohio State University, Columbus, Ohio, 1979.
- Rapp, R.H., A Global $1^\circ \times 1^\circ$ Anomaly Field Combining Satellite, GEOS-3 Altimeter and Terrestrial Anomaly Data, Dept. of Geodetic Science Report No. 278, The Ohio State University, Columbus, Ohio, 1978.
- Rapp, R.H., Global Anomaly and Undulation Recovery Using GEOS-3 Altimeter Data, Dept. of Geodetic Science Report No. 285, The Ohio State University, Columbus, Ohio, 1979a.
- Rapp, R.H., Potential Coefficient and Anomaly Degree Variance Revisited, Dept. of Geodetic Science Report No. 293, The Ohio State University, Columbus, Ohio, 1979b.

- Rummel, R., K.P. Schwarz and M. Gerstl, Least Squares Collocation and Regularization, Bull. Geod., 53, pp. 343-361, 1979.
- Rummel, R., Geoid Heights, Geoid Height Differences, and Mean Gravity Anomalies from "Low-Low" Satellite-to-Satellite Tracking; an Error Analysis, Dept. of Geodetic Science Report No. 306, The Ohio State University, Columbus, Ohio, 1980.
- Schwarz, C., Gravity Field Refinement by Satellite-to-Satellite Doppler Tracking, Dept. of Geodetic Science Report No. 147, The Ohio State University, Columbus, Ohio, 1970.
- Wagner, C.A., and O.L. Colombo, Gravitational Spectra from Direct Measurements, Journal of Geophysical Research, Vol. 84, No. B9, August 10, 1979.
- Wagner, C.A., Gravitational Spectra from the Tracking of Planetary Orbiters, Journal of Geophysical Research, Vol. 84, No. B12, November 1979.
- Walsh, J.L., The Approximation of Harmonic Functions by Harmonic Polynomials and by Harmonic Rational Functions, Bull. American Mathematical Society. 35, pp. 499-544, July-August 1929.
- Wolff, M., Direct Measurements of the Earth's Gravity Potential Using a Satellite Pair, Journal of Geophysical Research, Vol. 14, pp. 5295-5300, 1969.

Appendix A: Orbital Perturbations

A spacecraft orbiting a planet cannot follow a perfectly circular orbit, as assumed in section 2, but must move in a more irregular course, because of anomalies, or fluctuations, in the actual gravity field compared to that of a central point mass. In the case of the Earth, most of this effect is due to the attraction of the equatorial bulge. In the spherical harmonic expansion of the anomalous field, the influence of this bulge is represented mostly by the second zonal. This term is much larger than all the others in the expansion, so most of the orbital perturbation is due to this term alone. The following calculations will take into account the second zonal in detail, and for the rest a displacement of 200 m in every direction will probably account well enough, provided no strong resonances occur, as assumed in paragraphs 2.1 and 2.6. For relative displacements between satellites, 400 m will be added to those caused by the second zonal alone. Another assumption made here is that the force corresponding to the second zonal is the same along the true orbit as along the ideal, mean circular orbit. As the total displacement of such craft is mostly vertical and of less than 5 km, it is easy to determine that the force of the second zonal cannot change by more than 0.3%, so it may be acceptable to regard it as having the same value along either orbit. As the rotation of the Earth has no effect on the force of a purely zonal field, it will be ignored. The motion in the orbital plane which is perpendicular to the equator, is supposed to be periodical, which is mathematically possible with the right initial conditions.

Consider the system of inertial coordinates with axes \vec{x} and \vec{y} , where \vec{y} coincides with the polar figure axis of the Earth, and \vec{x} is in the equator (figure A.1). The polar coordinates r and ϕ' correspond to a point moving along the orbit with an approximately uniform circular motion represented by

$$\phi' = [\omega t] \text{MODULE } 2\pi$$

The relationships between the components of the inertial acceleration in the (x, y) and the (r, ϕ') systems are

$$a_x = a_r \cos\phi' - a_\phi \sin\phi' \quad (\text{A.1,a})$$

$$a_y = a_r \sin\phi' + a_\phi \cos\phi' \quad (\text{A.1,b})$$

$$\text{or} \quad a_x(t) = a_r(t) \cos\omega t - a_\phi(t) \sin\omega t \quad (\text{A.2,a})$$

$$a_y(t) = a_r(t) \sin\omega t + a_\phi(t) \cos\omega t \quad (\text{A.2,b})$$

From the definition of the unnormalized Legendre function introduced in paragraph 2.2, the polar components of the acceleration are

$$\begin{aligned} a_r(t) &= -3 \frac{GM}{r^2} \left(\frac{a}{r}\right)^2 J_2 L_{nm}(\omega t) \\ &= 3 \frac{GM}{r^4} a^2 J_2 \left(\frac{3}{4} \cos 2\omega t - \frac{1}{4}\right) \end{aligned} \quad (\text{A.3,a})$$

$$\begin{aligned}
 a_{\phi}(t) &= \frac{GM}{r^2} \left(\frac{a}{r}\right)^2 J_2 \frac{dL_{nm}(\omega t)}{d(\omega t)} \\
 &= \frac{3}{2} \frac{GM}{r^4} a^2 J_2 \sin 2\omega t
 \end{aligned}
 \tag{A.3,b}$$

where $J_2 = C_{20}$ (unnormalized)

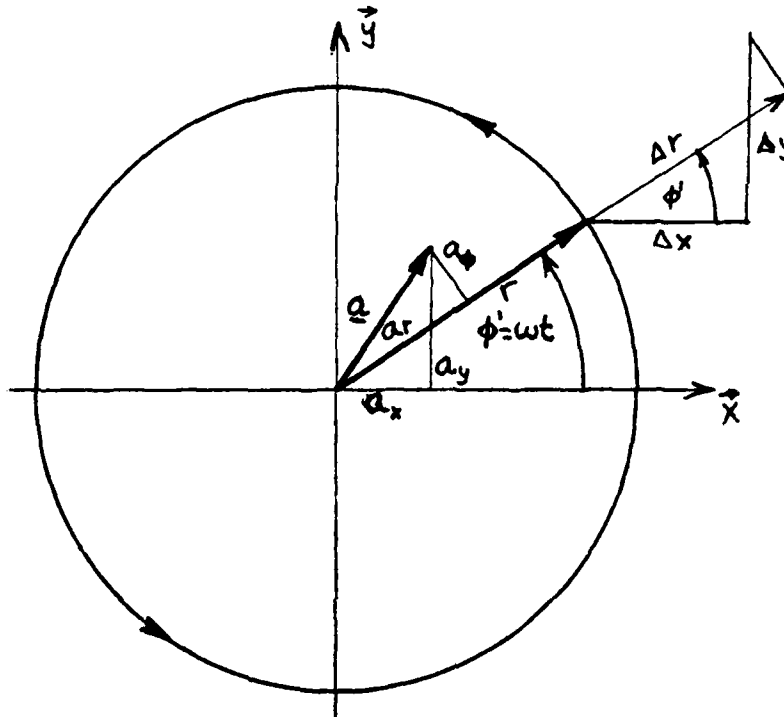


Figure A.1: Acceleration and Position in the (x,y) and $(r, \phi = \omega t)$ Coordinate Systems.

The radial perturbation in the position of the satellite is

$$\begin{aligned}
 \Delta r(t) &= \Delta x(t) \cos \omega t + \Delta y(t) \sin \omega t \\
 &= \left[\int_0^t dt' \int_0^{t'} a_x(t'') dt'' + \dot{\Delta x}_0 t + \Delta x_0 \right] \cos \omega t \\
 &\quad + \left[\int_0^t dt' \int_0^{t'} a_y(t'') dt'' + \dot{\Delta y}_0 t + \Delta y_0 \right] \sin \omega t
 \end{aligned}
 \tag{A.4}$$

where $\dot{\Delta x}, \Delta x_0$ etc., are initial conditions. As $\Delta r(t)$ is supposed to be periodical with the right $\Delta x_0, \dot{\Delta x}_0, \Delta y_0, \dot{\Delta y}_0$, and ignoring a constant term that merely changes the size of the orbit by a few kilometers, the radial displacement is

$$\Delta r(t) = \frac{-39}{72} \frac{GM}{r^4} \frac{a^2}{\omega^2} J_2 \cos 2\omega t
 \tag{A.5}$$

according to (A.2,a-b), (A.3,a-b), and (A.4). Furthermore $\omega = \sqrt{\frac{GM}{r^3}}$, so

$$\Delta r(t) = \frac{-39}{72} \frac{a^2}{r} J_2 \cos 2\omega t \quad (\text{A.6})$$

and using the values

$$a = 6371 \text{ km}$$

$$r = 6531 \text{ km}$$

$$J_2 = 1.1 \times 10^{-3}$$

(A.6) becomes

$$\Delta r(t) = -3.7 \cos 2\omega t \text{ [km]} \quad (\text{A.7})$$

So the amplitude of the oscillation due to J_2 alone is

$$\Delta r_{\text{MAX}} = 3.7 \text{ km} \quad (\text{A.8})$$

The relative radial displacement between two satellites, assuming that the change in their distance, and thus in ψ , can be ignored, is

$$\begin{aligned} \Delta r_{12}(t) &= -3.7 (\cos 2\omega t - \cos 2(\omega t + \psi)) \\ &= -3.7 \times 2 \sin \psi \sin(2\omega t + \psi) \\ &= 0.33 \sin(2\omega t + \psi) \end{aligned} \quad (\text{A.9})$$

for an intersatellite distance $\rho = 300 \text{ km}$, so

$$\Delta r_{12\text{MAX}} = 0.33 \text{ km} \quad (\text{A.10})$$

The relative motion along the line of sight can be estimated by integrating the relative velocity v_{12} . As this velocity is nearly a sinewave in time, of frequency 2ω , the expression for the variation in ρ is

$$\Delta \rho_{12}(t) = \sqrt{2} \frac{v_{12}(\text{rms})}{2\omega} \cos(2\omega t + \beta) \quad (\text{A.11})$$

where β is some phase angle of no consequence here. Replacing $v_{12}(\text{rms})$ with its total value according to Table 1.1, and adopting $\omega = 1.2 \times 10^{-3} \text{ rad s}^{-1}$ (as $r \approx 6531 \text{ km}$),

$$\Delta \rho_{12\text{MAX}} = 0.3 \text{ km} \quad (\text{A.12})$$

Because of the force is due to a zonal, the across-track displacement is

$$\Delta \tau_{12}(t) = 0 \text{ for all } t. \quad (\text{A.13})$$

The absolute along-track displacement of each satellite can be obtained from an expression similar to (A.7), but it is not needed in section 4. Finally, adding 200 m or 400 m, as the case may be, to account for the rest of the anomalous field, the perturbations amount, approximately, to

$$\Delta r_{MAX} = 3.7 + 0.2 = 3.9 \text{ km}$$

$$\Delta r_{12MAX} = 0.3 + (2 \times 0.2) = 0.7 \text{ km}$$

$$\Delta \rho_{12MAX} = 0.3 + (2 \times 0.2) = 0.7 \text{ km}$$

$$\Delta \tau_{12MAX} = 0.0 + (2 \times 0.2) = 0.4 \text{ km}$$

Appendix B: Computer Programs

This Appendix contains descriptions and listings of the main programs and subroutines used for the error analysis whose theory is contained in sections 1 and 2 and the results of which appear in section 3.

B.1 Main Program

Two main program versions were developed: the first one creates the non-zero diagonal blocks of $(A^T D^{-1} A)$, stores them in unit 10 (a tape file), creates the normal matrix's blocks by adding C^{-1} or not, depending on whether least squares collocation or least squares adjustment is required, inverts the blocks, and uses the diagonal elements of the inverses to calculate the error degree variances, the relative error per degree, and the corresponding accuracy of the geoid undulation; the second version of the main program does not create the normals but reads them from tape (unit 10, once more) and then proceeds as before. The reason for having two versions is that, with the first, one creates the normals and then carries out the error analysis using, say, least squares adjustment theory; as the normals are stored without C^{-1} , one can then use the second program to add C^{-1} to the stored matrix and then carry out the analysis according to collocation without having to recompute unnecessarily $(A^T D^{-1} A)$, which is the most time-consuming part of the analysis.

(a) Full Version

This program both creates and inverts the diagonal blocks of the normal required by the analysis. It calls subroutines ONEREV, MATV, MODEL, NVAR, and WRIT, which are listed in this Appendix; it also calls the system-provided subroutines ERRSET, SCLOK1, and RCLOK1, and the subroutines GGNOR (from the single precision library produced by the International Mathematical and Statistical Libraries Inc. (IMSL) company), and DSINV from the double precision library of the IBM System/360 Scientific Subroutine Package.

The program contains a device against a possible underestimation of the total execution time requested in the JOB card. The running time is checked inside the loop where the diagonal blocks are created, so that if this time is a few seconds below the assigned running time before a new block is to be calculated, the run terminates in an orderly way. The blocks created so far are left safely in unit 10, and the remaining ones can be created in a later run where the minimum order of the blocks is set to $MMIN = (\text{order of last (even, odd) pair of blocks completed previously} + 1)$. The time for eventual premature exit is the value of parameter YLIM in seconds, and should be smaller than the time declared in the JOB card by at least 10 seconds + compile time. Blocks created in additional runs should be stored in new tapes, which can be combined with the initial one by means of a simple FORTRAN program to produce a tape with all blocks in the required sequence (increasing order). The running time is checked with the help of SCLOK1 (which sets the time counter to zero before the main do loop) and RCLOK1 that "reads" the time counter at every turn in the loop.

All calculations are carried out in double precision, with the exception of those related to subroutine GGNOR, that take place in single precision. For this reason all variables are declared REAL 8, except array TP which is REAL 4.

The only COMMON statement is "P", through which the value of the total geoid undulation power POWNMX is communicated to the program from subroutine NVAR, which defines the values of the degree variances according to the model explained in section 3.

The various arrays are somewhat overdimensioned for the needs of the actual analysis, when $N = 331$. The maximum degree N is defined by the parameter NMAX which must be an odd number, for reasons given in the description of subroutine ONEREV (if the value declared happens to be even, by mistake, the program adds 1 to make it odd). The small arrays (dimensioned 500) should be at least of dimension NMAXP = NMAX + 1. As for the large arrays, their minimum dimensions should be

GNMS : $(NMAX - MMIN + 2) \times (NMAXP/2 + 1)$

AE : $\frac{1}{8} \times (NMAX + 2)^2$

AO : "

GNMS contains the Fourier coefficients of the columns of the A matrix, calculated by subroutine ONEREV, and AE, AO contain the elements of the normal matrix corresponding to a given order m and $(n-m)$ even and odd, respectively. Storage is in "upper-diagonal form" as required by the inversion subroutine DSINV.

Subroutine ERRSET is used to suppress unwanted error messages due to underflows in the calculations carried out by ONEREV.

The run parameters, including most of the mission parameters, are assigned values between statements 15 and 31. Two other parameters, the acceleration of gravity at ground level and the mean Earth radius, are assigned values in statements 50 and 51. The meanings of the symbolic names given to the parameters are explained in the comments of this section of the program. Parameter IAC, for example, tells the program whether a least squares adjustment or a least squares collocation error analysis is requested. The main parameter values are listed by the program (statements 36 and 37 if plotter output, as well as printer output, is desired) at the beginning of the run and, together with some other important values, saved at the start of the file created in unit 10, where the diagonal blocks are also stored. The length of day is supposed to be 24×3600 seconds exactly.

Certain loaders initialize all array areas to zero before execution, as in the case of the loader used to run this program. Others set arrays and registers not declared in the program to "indeterminate", or else the values left in core by a previous job remain unchanged. In such cases the program does not work unless additional DATA statements are written to give all array elements an initial value of zero.

AD-A111 872 OHIO STATE UNIV COLUMBUS DEPT OF GEODETIC SCIENCE A--ETC F/6 B/5
GLOBAL GEOPOTENTIAL MODELLING FROM SATELLITE-TO-SATELLITE TRACK--ETC(U)
OCT 81 O L COLOMBO F19628-79-C-0027

UNCLASSIFIED 317

AFGL-TR-81-0319

NL

2 of 2

ALP 8
11/8/82

END

DATE

FILED

04-82

DTIC

The run begins with the computation of $\sin(\frac{\psi}{2})$, $\cos(\frac{\psi}{2})$, and other quantities to be explained later, as well as the quantities $p \sin p \frac{\psi}{2}$, $\cos p \frac{\psi}{2}$ and $\csc p \frac{\psi}{2} \sin \frac{\psi}{2}$ stored in arrays SPC and CPS, respectively (statements 68 to 72). These numbers are used later to form the Fourier coefficients of the columns of A according to (2.13). Subroutines NVAR and MODEL are called to set up the array of degree variances of the geopotential, DVAR. The inverse of the variances of the scaled coefficients (equations (2.15,a-b)) are stored in array CM1. The variances produced by NVAR correspond to $n > NMOD$ and are in the form of gravity anomaly variances. They are converted to the inverse of geopotential variances in statement 81. All information relative to C^{-1} is stored in CM1 and in GMR.

The main loop begins at statement 91. Statements 92 through 95 check that the running time allocated in the JOB card is not exceeded. The elapsed time from the beginning of the main loop is printed at the beginning of a new pass through the loop (statement 93). Each pass creates the two diagonal blocks, one for n even, the other for n odd, corresponding to order $m = M$. There are four non-zero blocks for each m , but those corresponding to "sine" terms are identical to those for "cosine" terms (expression (2.51) is independent of α), so only one pair of blocks is needed. Statements 97 through 105 calculate the factors

$$FF(P) = \frac{Np}{4\sigma^2 \omega_0^2 \Delta a^2 (N+1)^2} [(1 - \cos((p\omega + m\Omega)\Delta a)(p\frac{\omega}{\omega_0} + m\frac{\Omega}{\omega_0})^{-4} + (1 - \cos((p\omega - m\Omega)\Delta a)(p\frac{\omega}{\omega_0} - \frac{\Omega}{\omega_0})^{-4}]$$

(see expression (2.51)) where ω_0 is the fundamental angular frequency for the whole mission (period $T_0 = Ndays \times 24 \times 3600$). The " a_p^{nm} " calculated with ONEREV are too large by a factor of $2(N+1)$, and this fact is accounted for in the denominator above.

After ONEREV has been called, it returns the "Fourier coefficients"

$$a_p^{nm} = \bar{h}_p^{nm} [p \sin p \frac{\psi}{2} \cos \frac{\psi}{2} + (n+1) \csc p \frac{\psi}{2} \sin \frac{\psi}{2}]$$

where the \bar{h}_p^{nm} correspond to all $[_{nm}(\phi')]$ with $m = M$, $n \geq M$, in array GPNMS. These coefficients are then multiplied by each other and scaled by the factor $FF(P)$ in statements 107 through 137, to form the element g_{nm}^{nm} in AIJ according to (2.51). If a collocation analysis is requested and AIJ corresponds to an element on the diagonal, the corresponding term in C^{-1} is added to AIJ in statement 136. Between 138 and 154 the calculated elements are stored in AE and AO, the arrays containing the blocks for $(n-m)$ even, and $(n-m)$ odd, respectively, in upper diagonal form. The vectors PIVE and PIVO are formed with the square roots of the diagonal elements. From 155 to 157 the two blocks and relevant information regarding their size are stored in unit 10, for further possible use. From 158 to 165 the two blocks are "pivoted" according to

$$G_{m,\alpha}^P \{ \text{even} \} = P^{-1} G_{m,\alpha} \{ \text{even} \} P^{-1} \quad (B.1)$$

where P is a matrix of "pivots", i.e., the square roots of the diagonal elements of $G_{m,\alpha,\{\text{even}\}}$. PIVE and PIVO are used for pivoting AE and AO, respectively. The "pivoted" blocks are inverted in statements 173 and 174 (there is no "AO" block for $M = N$). Notice that the program has been written in such a way that AE and AO correspond to even and to odd $n-m$, not n . As m is fixed during each pass of the main loop, the result depends on n , so AE sometimes contains "even", and sometimes "odd" elements, and the reciprocal is true of AO, depending on the value of m .

The accuracy of the inverse is tested by the inversion subroutine DSINV according to the tolerance limit defined in the main program (statement 172). If DSINV returns a value of zero in register IER1, the inversion can be regarded as successful (free of serious numerical instability). In addition to this test by DSINV, a further check has been written in the segment from statement 167 to 194. The idea is to calculate

$$\delta \underline{t} = \underline{t} - [(G_{m,\alpha,\{\text{even}\}}^P)^{-1} \quad G_{m,\alpha,\{\text{odd}\}}^P] \underline{t} = \underline{t} - \underline{t}'$$

(computed)

and then

$$\epsilon = [\delta \underline{t}^T \delta \underline{t} (\underline{t}^T \underline{t})^{-1}]^{\frac{1}{2}}$$

The exponent, in floating point notation, of ϵ is, approximately, the number of significant figures within which \underline{t} and \underline{t}' agree. Unfortunately, because 188 and 192 are not coded correctly, the values of ϵ printed at statement 193 are not useful. The elements of \underline{t} are random numbers created by the IMSL subroutine GGNOR.

From 196 to the end of the main loop the inverted normal blocks are obtained by "de-pivoting":

$$G_{m,\alpha,\{\text{odd}\}}^{-1} = P^{-1} (G_{m,\alpha,\{\text{even}\}}^P)^{-1} P^{-1} \quad (\text{B.2})$$

and the variance of the error per degree is totalized in array RMS as follows

$$\text{RMS}(n) = \text{RMS}(n) + \frac{G^2 M^2}{a^2} \left(\frac{a}{r}\right)^{2n} \sigma^2 \epsilon_{nmnm}^{00} \times \begin{cases} 1 & \text{if } m = 0 \\ 2 & \text{otherwise} \end{cases}$$

($\sigma^2 \epsilon_{nmnm}^{00} = \sigma^2 \epsilon_{nmnm}^{11}$) so, at the end of the main loop, $\text{RMS}(n) = \frac{G^2 M^2}{a^2} \left(\frac{a}{r}\right)^{2n} \sigma^2 \epsilon_n$, where $\sigma^2 \epsilon_n$ is the n degree variance of the errors, and the rest is the scaling factor squared (expressions (2.15,a-b)). From statement 219 to the end the error in the undulation up to degree n and this error plus the truncation error above n are both calculated and stored in arrays PPB and PPTR, respectively. Array PERC receives the formal percentage error per degree (expression (3.2) multiplied by 100). While "debugging" the program it was found useful to monitor the values of some of the coefficients' accuracies as they were being obtained. This feature was left in the program, where, for the reason given in paragraph 3.4, all the $\sigma^2 \epsilon_{nmnm}^{00}$ for $n \leq 40$ are still printed out (statement 210). If the inversion of AE or of AO fails, subroutine DSINV returns an explanatory

code in IER1 and IER2, which should be different from 0 and is also printed out. A failure to invert is most likely due to a set-up error; perhaps to an improperly dimensioned array; to a loader that does not preset all undefined values to 0 before execution; or to improperly punched cards. An example of all the messages printed during a normal run can be seen in paragraph B.4.

The program prints out all results in unit IU (a plotter, for instance) degree by degree (statement 238) in blocks of fifty lines, and at the end prints a summary in increments of 10 degrees. The results are also punched out (statements 219 and 220).

(b) Reduced Version

This version of the main program does not compute the normals, but reads them from unit 10 (disk or tape), where they have been stored during a previous run of the full version. It also reads the original mission parameters, with which the normals were created, as the first record in file 10 (stat. 22). Some of those parameters can be changed in value by re-scaling the normals (paragraph 2.13). The new parameters' values can be declared by inserting statements between lines 22 and 25 in the listing.

This version does not call subroutine ONEREV, and reads unit 10 from subroutine RED. Subroutine WRIT is not used. All the other subroutines called in the full version are also used here. The fact that there is no AO matrix block when $M = NMAX$ is taken into account (statements 94 and 98). Re-scaling according to (2.78) happens between 99 and 104. If no change in parameters is desired, FNSR is 1. Expression (2.84) for least squares collocation requires knowledge of the singular values and eigenvectors of the normal matrix, instead of the inverse. Lack of time and of familiarity with the decomposition subroutines available resulted in inversion being chosen for both least squares adjustment and for collocation. The fastest way to study the effect of parameter value changes on the results with collocation is, therefore, to run this reduced version with the new parameters. With $NMAX = 331$, this requires some 15 minutes. As no PIVE or PIVO arrays have been computed so far, this is done now in statements 122-125, and then pivoting is applied. From there on things are done much as in the full version, except that no test for numerical stability of the inversion is done in addition to that of DSINV. Results are printed and punched as in the full version.

B.2 Subroutine ONEREV

This subroutine computes the coefficients a_p^{nm} needed to find elements of the normal matrix according to expression (2.51). The a_p^{nm} are defined by expression (2.13)

$$a_p^{nm} = \bar{h}_p^{nm} \left[(n+1) \cos p \frac{\psi}{2} \sin \frac{\psi}{2} + p \sin p \frac{\psi}{2} \cos \frac{\psi}{2} \right]$$

as proportional to the Fourier coefficients \bar{h}_p^{nm} of the extended Legendre functions $[_{nm}(\phi)]$. The values of $(n+1) \cos p \frac{\psi}{2} \sin \frac{\psi}{2}$ and of $p \sin p \frac{\psi}{2} \cos \frac{\psi}{2}$ are passed on to the subroutine from the main program in arrays SPC

and CPS, respectively. The $L_{nm}(\phi')$ are sampled at equal intervals $\Delta\phi' = \frac{2\pi}{2(N+1)}$ (N is the highest degree in the band, so the highest frequency term in any L_{nm} is either $h_N^m \cos N\phi'$ or $h_N^m \sin N\phi'$), and then analysed with subroutine FFCSIN, which implements a mixed-radix Fast Fourier Transform (FFT) algorithm. FFCSIN belongs to the International Mathematical and Statistical Libraries (IMSL) Inc.'s double precision library. It returns $2(N+1)h_p^m$ instead of h_p^m , but this is taken into account in the main program. The $L_{nm}(\phi')$ are calculated taking advantage of the relationships (2.2,a-d), so only the values in the interval $0 \leq \phi' < \frac{\pi}{2}$ are absolutely necessary. These values are the same as those of the corresponding P_{nm} , which are obtained with subroutine LEGFDN. There are $(N+1)/2$ points⁽¹⁾ where the P_{nm} have to be calculated in $0 \leq \phi' < \frac{\pi}{2}$, so the space required by GPNMS is $(N - \text{MMIN} + 2) \times ((N + 1)/2)$. Here MMIN is the lowest order to be studied (a feature of the main program is that it allows the study of coefficients in the band $\text{MMIN} \leq m \leq N$; in the case of the results of section 3, $\text{MMIN} = 0$). The successive values of the P_{nm} are put first in array GPNMS. Then all values corresponding to the same P_{nm} are moved to REV, where L_{nm} is determined from (2.2,a-d), so the dimension of REV is $2(N+1)$. Then FFCSIN replaces the values of L_{nm} with those of the h_p^m , also in REV, and the latter are moved on to GPNMS, where they replace the original P_{nm} . IWK is an auxiliary array needed by FFCSIN (see IMSL Handbook). All a_p^{nm} (multiplied by $2(N+1)$) are returned to the main program. If the loader used does not preset all undefined registers to zero, a DO loop should be put at the beginning, between statements 5 and 6, setting to zero all arrays with dimensions different from 1. Alternatively, depending on the compiler, a DATA statement to the same effect could be used.

If an even function is added to an odd function, the Fourier coefficients of the sum are those of the even function in the cosine terms, and those of the odd function in the sine terms. This simple fact is exploited to reduce calculations by half, taking advantage of the even or odd nature of the L_{nm} with respect to ϕ' .

The a_p^{nm} with $p=0$ are handled separately from the rest, and are returned to the main program in array GMN (statement 78). Besides FFCSIN and LEGFDN, no other subroutines are called.

8.3 Subroutines LEGFDN, MODEL, and NVAR

Subroutine LEGFDN can calculate both the values of all normalized Legendre functions at colatitude THETA, for the same order $m = M$, up to degree $n = \text{NMAX}$, and also their derivatives. The functions are returned in array RLEG, the derivatives in DLEG; after exit, RLMN contains a redundant set of all sectorials up to degree $n = m$. All arrays, except DRTS and DIRT should have the dimension NMAX1 (statement 5). DRTS and DIRT should have twice that size. IR is a register that should be set to zero before the first call to this subroutine, in the main program. IFLAG tells the subroutine whether only the Legendre functions or these and their derivatives are required (only the P_{nm} were needed for the error analysis, so IFLAG was set to 1). The P_{nm} and their derivatives are calculated using recursive formulas given in Colombo ((1981), paragraphs (1.10) and (4.4)).

⁽¹⁾ $(N+1)/2$ must be integer, so $N = \text{NMAX}$ must be an odd number.

Subroutine MODEL sets the values of the first NMOD components of arrays DVAR and DVER to the values of the degree variances of the errors in the potential coefficients of the reference model with respect to which the residual line of sight velocities are determined. The values in the listing correspond to the first 30 degrees in a model obtained by R. H. Rapp at OSU from a global data set of $1^\circ \times 1^\circ$ mean anomalies by numerical quadratures. This model is, in fact, complete up to degree and order 180, though only the accuracies of the first 30 degrees are used here.

Subroutine NVAR initializes array DVAR so that its elements are the same as the degree variances for the gravity anomaly implied by R. Rapp's coefficients mentioned above, up to $n = 100$. Above $n = 100$, the variances are those obtained from a two-term model for the gravity anomaly spectrum, also the work of R. Rapp (1979b). The main program calls NVAR first and MODEL afterwards, so the first NMOD degree variances are, finally, those in MODEL (error variances), which correspond to dimensionless potential coefficients. The remainder comes from NVAR, so they must be converted to dimensionless potential from gravity anomaly variances, a step that occurs in statements 80 and 81 of the main program. In NVAR, statements 120 and 122 add all potential degree variances between $n = NMAX$ and $n = 2000$, and return this sum in POWNMX through COMMON/P/ to the main program.

The same caution regarding the initialization of undeclared arrays and variables to zero that was made for the main program and for ONEREV apply to LEGFDN and to MODEL (array DVAR) as well.

B.4 Sample Output

After the listings of the various routines described previously, the reader will find a sample of the printed output created by either version of the main program (they are the same). This listing should help whoever wants to use these programs to check that his own punched version works properly. The program should also punch out some cards with the results (statements 238 and 239). Because of a minor error in the program, now corrected, the standard deviation of the data is listed as 10^{-6} m s^{-1} , instead of as $\sqrt{2} \times 10^{-6} \text{ m s}^{-1}$, which is the actual value corresponding to the results printed in the sample. The parameters used, with the exception of σ , are as listed. To enter them into the main program, see comments at the beginning of either version.

The first page of the output contains a listing of the mission parameter values chosen. The "TIME BEFORE M" statements give the time in seconds at the beginning of a new pass through the main loop, and they are printed just before the time check in statement 95. the "ACCURACY OF INVERSION" lines should indicate the stability of the inversion of the blocks of order M, but they are useless because of the coding error mentioned in paragraph B.1. The other numbers are scaled variances $\frac{G^2 M^2 (a)^{2n}}{P^2}$ of the coefficients up to degree and order 40 ($\alpha=0$). If the numerical inversion of either block of order M fails the stability test in subroutine DSINV, a line is printed saying "AT ORDER m IER1 = x IER2 = y", where x and y are two integers whose value should be interpreted according to instructions in the Handbook of the SSP library. At the end of the run, the various accuracies are listed in unit IU, first degree by degree and then, in a final summary page, every 10 degrees.

REQUESTED OPTIONS: MAP, ID, OPT-2

OPTIONS IN EFFECT: NAME(MAIN) OPTIMIZE(2) LINECOUNT(60) SIZE(MAX) AUTOHSL(NONE) SOURCE EBCDIC POLIST NODECK OBJECT MAP NOFOUNAT CONSTNT NOXREF NOALC NOANSF ROTERN ISN FLAG(1)

PROGRAM FOR THE ERROR ANALYSIS OF THE GLOBAL MODELLING OF A GRAVITY FIELD FROM SATELLITE TO SATELLITE TRACKING DATA.

**** PROGRAMMED BY OSCAR L. COLOMBO, GEODETIC SCIENCE, THE OHIO STATE UNIVERSITY, SEPTEMBER 1969 *****

ISN 0002
ISN 0003
ISN 0004
ISN 0005
ISN 0006
ISN 0007
ISN 0008
ISN 0009
ISN 0010
ISN 0011
ISN 0012
ISN 0013
ISN 0014
ISN 0015

IMPLICIT REAL*8(A-H,O-Z)
REAL*4 EPS
REAL*4 V, Z
REAL*4 Y, X
REAL*4 YLIM
COMMON / F / FOUNTX
DIMENSION CMT(500), SPC(500), CFS(500), FF(500), DVAR(500),
2 RCM(500), IIS(500)
DIMENSION CPM(5000), AE(15000), AX(15000), CM(1500)
DIMENSION FIVE(500), FIVE(500), FIVE(500)
DIMENSION CMT(500), T(500), FE(500), FO(500), FE2(500), FO2(500)
DIMENSION FPE(500), FPTH(500), FENL(500)
DATA RNS/60000.00/
IX = 1
CALL ERSET(208.256, -1.2, IX, 0)

DEFINITION OF THE PROBLEM. EVERYTHING IS IN METERS AND IN SECONDS. ME AND NS MUST BE MUTUALLY PRIME, AND NS GT. 2*HMAX. THE SAMPLING INTERVAL DS MUST DIVIDE NS*24*3600 EXACTLY.

HMOD = MAXIMUM DEGREE AND ORDER IN REFERENCE MODEL.
HMAX = MAX DEGREE AND ORDER IN SIGNAL MODEL.
MMIN = MINIMUM ORDER CONSIDERED IN ANALYSIS.
ME = DURATION OF MISSION IN DAYS.
NS = NUMBER OF REVOLUTIONS OF SATELLITES PER DAY.
IS = HEIGHT OF SATELLITES ABOVE SPHERE OF EARTH.
D12 = SEPARATION BETWEEN THE TWO SATELLITES IN METERS.
SIGMA = STANDARD DEVIATION OF ERRORS IN DATA (RELATIVE VELOCITY) IN METERS PER SECOND.
DS = SAMPLING INTERVAL.
DA = AVERAGING INTERVAL.
YLIM = TIME IN SECONDS BEFORE EXITING FROM MAIN LOOP.
IU = UNIT NUMBER FOR PLOTTER.
IP = UNIT NUMBER FOR PUNCH.

ISN 0016
ISN 0017
ISN 0018
ISN 0019
ISN 0020
ISN 0021
ISN 0022

YLIM = 4740.
HMOD = 20
HMAX = 331
MMIN = 11
ME = 0
NS = 179
IS = 2930

FULL VERSION
OF MAIN PROGRAM

LEVEL 2.3.0 (JUNE 78)

MAIN

[illegible]


```

10R 0227 PTR = POW*RE*2+POW*RE*1.D-10
10R 0228 DO 110 N = 2, NMAX
10R 0229 PR = CHR(N)*RE*2*(2*N+1)/CHI(N)
10R 0230 PEAR = RMS(N)*RE*2
10R 0231 PTR = PTR-PR+PEAR
10R 0232 PB = PB+PEAR
10R 0233 PERC(N) = DSQRT(RMS(N)*CHI(N)/(CHR(N)*(2*N+1)))*100.DO
10R 0234 PPTR(N) = DSQRT(PB)
10R 0235 IF((N/60)*36.D0.N) WRITE(10,105)
10R 0236 WRITE(10,107) N,PERC(N),RMS(N),PPB(N),PPTR(N)
10R 0237 107 FORMAT(2X,16.4(7X,C13.5))
10R 0238 110 CONTINUE
10R 0239 WRITE(10,109)
10R 0240 DO 115 N = 2, NMAX
10R 0241 IF((N/10)*10.D0.N.OR.N.EQ.2) WRITE(10,107)N,PERC(N),RMS(N),
10R 0242 2 PPB(N),PPTR(N)
10R 0243 115 CONTINUE
10R 0244 STOP
10R 0245 END

```


REQUESTED OPTIONS: MAP, ID, OPT-2

OPTIONS IN EFFECT: NAME(MAIN) OPTIMIZE(2) LINECOUNT(60) SIZE(MAX) AUTOBBL(MORE)
SOURCE EBCDIC NOLIST NOCHECK OBJECT MAP NOFORNAT CONSTMT NOKEYF NOALC NOANSF NOTERN IBM FLAG(1)

SUBROUTINE WRITE(AE, AO, NEV, MOD, NNEV, MNOD)

THIS SUBROUTINE STORES IN 10 THE NORMALS IN LOWER
TRIANGULAR FORM.

IMPLICIT REAL*(A-H, O-Z)
DIMENSION AE(NNEV), AO(MNOD)
WRITE(10) NEV, MOD, NNEV, MNOD
WRITE(10) AE, AO
RETURN
END

IBM 0002
C
C
C
IBM 0003
IBM 0004
IBM 0005
IBM 0006
IBM 0007
IBM 0008

REQUESTED OPTIONS: MAP, ID, OPT-2

OPTIONS IN EFFECT: NAME(HAIR) OPTIMIZE(2) LINECOUNT(60) SIZE(MAX) AUTODBL(NONE)

SOURCE EXECUTIVE NOLIST MODECK OBJECT MAP MOSONMAT CONSTT MOKUEF NOALC NOANSF NUTENM IBM FLAG(1)

SUBROUTINE ONEREV(CPNS, M, SPC, CP8, NMAX, CRR)

THIS SUBROUTINE COMPUTES AND SAVES IN ARRAY CPNS THE
ONE REV. FOURIER COEFFICIENTS CPNM OF THE COLUMNS
OF THE MATRIX OF OBSERVATION EQUATIONS, FOR THE SPHERICAL
HARMONIC COEFFICIENTS OF ORDER M.

NMAX = THE HIGHEST DEGREE IN THE BAND. IT MUST BE
ALWAYS AN ODD NUMBER, AND LESS THAN 500 WITH THE ALWAYS
DIMENSIONED AS SHOWN BELOW.
THE DIMENSION OF CPNS SHOULD BE NO LESS THAN
(NMAX-MIN+2)*((NMAX+1)/2+1), WHERE NMAX IS ALWAYS ODD.

PROGRAMMED BY OSCAR L. COLOMBO, GEODETIC SCIENCE, OHIO STATE,
SEPTEMBER 1969

IMPLICIT REAL*8(A-H, O-Z)
DIMENSION NLEG(500), DLEG(1), RLNR(500), CPNS(1), SPC(1), CP8(1),
2 CRR(1), REV(2000), CP(500), SP(500), INK(4000)

NMAX1 = NMAX+1
PI = 4.00/DATAN(1.00)

NNIN = N
IF(M.LT.2) NNIR = 2

IR = 0
IFLAG = 1

NM2 = NMAX1/2+1
NMZ = NM2*(NMAX-MIN+2)

DO 5 L = 1, NMZ
5 CPNS(L) = 0.00

DPHI = PI/NMAX1
PHI = 0.00

DO 10 NR = 1, NM2
THETA = PI*0.500-PI

IF(NR.NE.NM2) GO TO 9
DO 7 I = 1, NMAX1

7 NLEG(I) = 0.00
9 CONTINUE

IF(NR.EQ.NM2.AND.M.NE.0) GO TO 6
CALL LEGFUN(M, THETA, NLEG, DLEG, NMAX, IR, RLNR, IFLAG)

6 PHI = PHI+DPHI
NM22 = NM2+2

10 CONTINUE
100 CONTINUE

100 CONTINUE
100 CONTINUE

100 CONTINUE
100 CONTINUE

100 CONTINUE
100 CONTINUE

100 CONTINUE
100 CONTINUE

100 CONTINUE
100 CONTINUE

100 CONTINUE
100 CONTINUE

100 CONTINUE
100 CONTINUE

100 CONTINUE
100 CONTINUE

100 CONTINUE
100 CONTINUE

100 CONTINUE
100 CONTINUE

100 CONTINUE
100 CONTINUE

100 CONTINUE
100 CONTINUE

100 CONTINUE
100 CONTINUE

100 CONTINUE
100 CONTINUE

100 CONTINUE
100 CONTINUE

100 CONTINUE
100 CONTINUE

100 CONTINUE
100 CONTINUE

100 CONTINUE
100 CONTINUE

100 CONTINUE
100 CONTINUE

100 CONTINUE
100 CONTINUE

LEGENDRE FUNCTIONS, TAKING ADVANTAGE OF THE FACT
THAT CONSECUTIVE FUNCTIONS ARE EITHER EVEN OR ODD ABOUT THE
EQUATOR.

```

100 0035      NMAX2 = NMAX+2
100 0036      NMAX3 = NMAX+3
100 0037      INK = 0
100 0038      IF((N/2)+2.NE.ND INK = 1
100 0039      NMI = NMAX1+2+1
100 0040      NML = NMAX1+2
100 0041      NMI = NMI+1
100 0042      ISHT = 0
100 0043      IND = 0
100 0044      IF((NMI/2)+2.NE.NMI) IND=1
100 0045      INDC = 1-IND
100 0046      INC = 0
100 0047      IF((NMI-ND/2)+2.NE.(NMI-ND)) INC = 1
100 0048      DO 50 M = NMI,NMAX,2
100 0049      18ET2 = 18ET+M2
100 0050      FORM THE SUM OF TWO CONSECUTIVE "EXTENDED" LEGENDRE FUNCTIONS
100 0051      IN ARRAY REV
100 0052
100 0053      DO 20 NR = 1,NM2
100 0054      NMR = NMAX2-NR
100 0055      NPPR = NMAX1+NR
100 0056      NMR = NMI-NR
100 0057      CP1 = CPMS(18ET+NR)
100 0058      CP2 = CPMS(18ET2+NR)
100 0059      REV(NR) = CP1+CP2
100 0060      IF(INK.EQ.1) GO TO 13
100 0061      REV(NR) = REV(NR)
100 0062      GO TO 15
100 0063      12 REV(NR) = -REV(NR)
100 0064      15 REV(NR) = CP1-CP2
100 0065      IF(IND.EQ.1) REV(NR) = -REV(NR)
100 0066      IF(INK.EQ.1) GO TO 16
100 0067      REV(NR) = REV(NR)
100 0068      GO TO 20
100 0069      16 REV(NR) = -REV(NR)
100 0070      20 CONTINUE
100 0071
100 0072      CALL PFCIN(REV,NM,CP,SP,INK)
100 0073
100 0074      COMPUTE THE FOURIER COEFFICIENTS OF TWO CONSECUTIVE "EXTENDED"
100 0075      LEGENDRE FUNCTIONS IN CP AND IN SP, RESPECTIVELY.
100 0076
100 0077      FORM THE CPN COEFFICIENTS, AND STORE THEM IN CPNRS
100 0078      IN PLACE OF THE VALUES OF THE CORRESPONDING LEGENDRE FUNCTIONS.
100 0079
100 0080      N1 = 0
100 0081      N2 = N+1
100 0082      IF(IND.EQ.0) CHN(N) = CP(1)+N1
100 0083      DO 30 NR = 1,N,2
100 0084      NT = NR+INDC
100 0085      NTP = NT+1
100 0086      N1 = NT+1
100 0087      IF(IND.EQ.1) GO TO 22

```

LEVEL 2.3.0 (JUNE 78) ONEEV 08/360 FORTRAN II EXTENDED

18N 0006 CPNBS(18RT+NT1) = CP(NTT)*S(BPC(NT)+NN1+CPS(NT))

18N 0007 CO TO 24

18N 0008 22 CPNBS(18RT+NT1) = SP(NTT)*S(BPC(NT)+NN1+CPS(NT))

18N 0009 24 NTA = NN+IND

18N 0010 NTAP = NTA+1

18N 0011 IF(ING.EQ.0) CO TO 26

18N 0012 CPNBS(18RT2+NT1) = CP(NTAP)*S(BPC(NTA)+NN2+CPS(NTA))

18N 0013 CO TO 28

18N 0014 26 CPNBS(18RT2+NT1) = SP(NTAP)*S(BPC(NTA)+NN2+CPS(NTA))

18N 0015 28 IF(IND.NE.0.OR.NN+1.NE.N) CO TO 30

18N 0016 NTE = NTA+2

18N 0017 CPNBS(18RT2+NT1+1) = SP(NTAP+2)*S(BPC(NTA)+NN2+CPS(NTA))

18N 0018 30 CONTINUE

18N 0019 18RT = 18RT+NT2

18N 0020 30 CONTINUE

18N 0021 RETURN

18N 0022 END

REQUESTED OPTIONS: MAP, ID, OPT-2

OPTIONS IN EFFECT: NAME(MAIN) OPTIMIZE(2) LINECOUNT(60) SIZE(MAX) AUTOBL(MORE)
SOURCE EXECUTIC NULIST MODECK OBJECT MAP NOFUUMAT COSTMT MUXREF NOALC NOANSF NOTERM IBM FLAG(1)

IBM 0002

SUBROUTINE LEGEND(M, THETA, RLEG, DLEG, MDX, IR, MLNN, IFLAG)

THIS SUBROUTINE COMPUTES ALL NORMALIZED LEGENDRE FUNCTIONS IN "RLEG" AND THEIR DERIVATIVES IN "DLEG". ORDER IS ALWAYS M, AND COLATITUDE IS ALWAYS THETA (RADIAN). MAXIMUM DEGREE IS MDX. ALL CALCULATIONS IN DOUBLE PRECISION. IR MUST BE SET TO ZERO BEFORE THE FIRST CALL TO THIS SUB. THE DIMENSIONS OF ARRAYS RLEG, DLEG, AND MLNN MUST BE AT LEAST EQUAL TO MDX+1. IF THIS SUBROUTINE IS TO BE USED TO COMPUTE FUNCTIONS AND THEIR DERIVATIVES FOR MORE THAN ONE ORDER M, THEN THE HIGHEST ORDER SHOULD BE COMPUTED IN THE FIRST CALL.

THIS PROGRAM DOES NOT COMPUTE DERIVATIVES AT THE POLES.

IF IFLAG = 1, ONLY THE LEGENDRE FUNCTIONS ARE COMPUTED.

PROGRAMMER: OSCAR L. COLOGNO, DEPT. OF GEODETIC SCIENCE,
THE OHIO STATE UNIVERSITY, AUGUST 1980. *****

```

      IMPLICIT REAL*8 (A-H,O-Z)
      DIMENSION RLEG(1), DLEG(1), MLNN(1)
      2. DRTS(1306), DIRT(1306)
      MDX1 = MDX+1
      MDX2P = 2*MDX+1
      M1 = M-1
      M2 = M-2
      M3 = M-3
      IF (IR.EQ.1) GO TO 10
      DO 5 N = 1, MDX2P
        DRTS(N) = DSQRT(M+1.D0)
        DIRT(N) = 1.D0/DRTS(N)
        5. COTHET = DCOS(THETA)
        10. SITHET = DSIN(THETA)
        IF (IFLAG.NE.1.AND.THETA.NE.0.D0)SITHET = 1.D0/SITHET
    
```

COMPUTE THE LEGENDRE FUNCTIONS

```

      MLNN(1) = 1.D0
      MLNN(2) = SITHET*DRTS(3)
      DO 15 N1 = 3, M1
        N2 = 2*N1
        15. MLNN(N1) = DRTS(N2+1)*DIRT(N2)*SITHET*MLNN(N1-1)
        IF (N1.GT.1) GO TO 20
        IF (N1.EQ.0) GO TO 16
        RLEG(2) = MLNN(2)
        RLEG(3) = DRTS(5)*COTHET*RLEG(2)
        GO TO 20
        16. RLEG(1) = 1.D0
           RLEG(2) = COTHET*DRTS(3)
    
```

DATE 80.273/21.48.21

OR/360 FORTRAN B EXTENDED

LEVEL 2.3.0 (JUNE 78)

LEGEND

```

18N 0035 20 CONTINUE
18N 0036   RLEG(N1) = RLNN(N1)
18N 0037   RLEG(N2) = DRTS(N1+2)*COTHET+RLEG(N1)
18N 0038   DO 30 N1 = N2,NMAX
18N 0039     N = N1-1
18N 0040     IF(M.EQ.0.AND.N.LT.2.OR.M.EQ.1.AND.N.LT.3) GO TO 30
18N 0041     N2 = 2*N
18N 0042     RLEG(N1) = DRTS(N2+1)*DIRT(N+M)+DIRT(N-M)*(DRTS(N2-1)*COTHET+
18N 0043     2 RLEG(N1-1)-DRTS(N+M-1)*DRTS(N-M-1)*DIRT(N2-3)*RLEG(N1-2))
18N 0044     GO TO 30
18N 0045 30 CONTINUE
18N 0046   IF(FLAG.EQ.1) RETURN
18N 0047   IF(SITHET.EQ.0.D0) WRITE(4,99)
18N 0048 99 FORMAT(' ',"LEGEND DOES NOT COMPUTE DERIVATIVES AT THE POLES
18N 0049 2 *****")
18N 0050   IF(SITHET.EQ.0.D0) RETURN
18N 0051   C C C
18N 0052   C C C
18N 0053   RLNN(1) = 0.D0
18N 0054   RLNN(2) = RLNN(2)
18N 0055   RLNN(2) = DRTS(3)*COTHET
18N 0056   DO 40 N1 = 3, N1
18N 0057     N = N1-1
18N 0058     N2 = 2*N
18N 0059     RLNN(N1) = DRTS(N2+1)*DIRT(N2)*(SITHET*RLNN(N)+COTHET*RLN)
18N 0060     RLNN(N1) = RLNN(N1)
18N 0061     RLNN(N1) = RLNN(N1)
18N 0062     DO 60 N1 = N2,NMAX
18N 0063       N = N1-1
18N 0064       N2 = N+2
18N 0065       DLEG(N1) = SITHET*(N *RLEG(N1)+COTHET-DRTS(N-M)*DRTS(N+M)*
18N 0066       2 DRTS(N2+1)*DIRT(N2-1)*RLEG(N1))
18N 0067     CONTINUE
18N 0068   RETURN
18N 0069   END
18N 0070

```

REQUESTED OPTIONS: MAP, IB, OPT-2

OPTIONS IN EFFECT: NAME(MAIN) OPTIMIZE(2) LINECOUNT(60) SIZE(MAX) AUTODBL(NONE)
SOURCE EXECDIC NOLIST NODECK OBJECT MAP NOPOUNAT CUSTMT NOXUEP NOALC NOANSF NOTERN IBM FLAG(1)

SUBROUTINE MODEL(DVER, NM0D)

IMPLICIT REAL*8(A-H, O-Z)

DIMENSION DVER(1), DVAR(30)

DVAR(1) = 0.0D0

DVAR(2) = 2729.D-12

DVAR(3) = 6394.D-12

DVAR(4) = 4364.D-12

DVAR(5) = 7237.D-12

DVAR(6) = 8783.D-12

DVAR(7) = 6783.D-12

DVAR(8) = 8485.D-12

DVAR(9) = 5727.D-12

DVAR(10) = 3118.D-12

DVAR(11) = 4998.D-12

DVAR(12) = 4413.D-12

DVAR(13) = 4838.D-12

DVAR(14) = 4438.D-12

DVAR(15) = 4198.D-12

DVAR(16) = 3864.D-12

DVAR(17) = 3633.D-12

DVAR(18) = 3416.D-12

DVAR(19) = 3229.D-12

DVAR(20) = 3051.D-12

DVAR(21) = 2894.D-12

DVAR(22) = 2761.D-12

DVAR(23) = 2635.D-12

DVAR(24) = 2522.D-12

DVAR(25) = 2417.D-12

DVAR(26) = 2321.D-12

DVAR(27) = 2232.D-12

DVAR(28) = 2149.D-12

DVAR(29) = 2072.D-12

DVAR(30) = 2001.D-12

DO 10 N=1, NM0D

DVER(N) = DVAR(N)

10 RETURN

END

ISN 0002

ISN 0003

ISN 0004

ISN 0005

ISN 0006

ISN 0007

ISN 0008

ISN 0009

ISN 0010

ISN 0011

ISN 0012

ISN 0013

ISN 0014

ISN 0015

ISN 0016

ISN 0017

ISN 0018

ISN 0019

ISN 0020

ISN 0021

ISN 0022

ISN 0023

ISN 0024

ISN 0025

ISN 0026

ISN 0027

ISN 0028

ISN 0029

ISN 0030

ISN 0031

ISN 0032

ISN 0033

ISN 0034

ISN 0035

ISN 0036

ISN 0037

ISN 0038

LEVEL 2.3.0 (JUNE 78) 05/360 FORTRAN H EXTENDED DATE 00.273/21.48.26 PAGE 1

REQUESTED OPTIONS: MAP, ID, OPT-2

OPTIONS IN EFFECT: NAME(HAIR) OPTIMIZE(2) LINECOUNT(40) SIZE(MAX) AUTODIAG(NONE)

SOURCE EXECUTIVE ROUTINE OBJECT MAP MAPUNIT COSTMT NUMBER MOALC MOANSF ROTERM IDH FLAG(1)

SUBROUTINE KVAR(DVAR, NMAX, DVAR0)

THIS SUBROUTINE COMPUTES ALL DEGREE VARIANCES UP TO
DEGREE "NMAX", USING SOME GIVEN MODEL.

IMPLICIT REAL*8 (A-H, O-Z)

COMMON / P / PUMNXX

DVAR0 = 0.00

DVAR(1) = 0

DVAR(2) = 7.6396518

DVAR(3) = 33.982865

DVAR(4) = 19.743429

DVAR(5) = 19.696163

DVAR(6) = 18.396314

DVAR(7) = 18.455112

DVAR(8) = 18.399362

DVAR(9) = 8.6398739

DVAR(10) = 9.1838627

DVAR(11) = 6.369710

DVAR(12) = 2.8993199

DVAR(13) = 6.7286266

DVAR(14) = 3.2833030

DVAR(15) = 3.8198187

DVAR(16) = 4.944726

DVAR(17) = 3.7168750

DVAR(18) = 4.1918269

DVAR(19) = 3.4360349

DVAR(20) = 2.2937336

DVAR(21) = 3.0853872

DVAR(22) = 3.5082969

DVAR(23) = 2.6197612

DVAR(24) = 2.6880871

DVAR(25) = 3.4761637

DVAR(26) = 2.2578367

DVAR(27) = 2.1490826

DVAR(28) = 2.5883294

DVAR(29) = 2.8568812

DVAR(30) = 2.9297785

DVAR(31) = 2.4778694

DVAR(32) = 2.4971826

DVAR(33) = 3.2048101

DVAR(34) = 3.9115437

DVAR(35) = 3.1078939

DVAR(36) = 2.9688243

DVAR(37) = 3.126138

DVAR(38) = 2.799143

DVAR(39) = 2.8229174

DVAR(40) = 2.1081861

DVAR(41) = 3.0844365

DVAR(42) = 3.8244301

DVAR(43) = 2.2443272

DVAR(44) = 3.0765796

00025400
00025500
00025600
00025700
00025800
00025900
00026000
00026100
00026200
00026300
00026400
00026500
00026600
00026700
00026800
00026900
00027000
00027100
00027200
00027300
00027400
00027500
00027600
00027700
00027800
00027900
00028000
00028100
00028200
00028300
00028400
00028500
00028600
00028700
00028800
00028900
00029000
00029100
00029200
00029300
00029400
00029500
00029600
00029700
00029800
00029900
00030000
00030100
00030200
00030300
00030400
00030500

DATE 80-273/21.48.26

08/360 PORTMAN H EXTENDED

RVAR

LEVEL 2.3.0 (JUNE 78)

ISN 0051	DVAR 48) =	2.919446	00036500
ISN 0052	DVAR 46) =	2.7205179	00030700
ISN 0053	DVAR 47) =	2.4344894	00036800
ISN 0054	DVAR 49) =	2.6109541	00036900
ISN 0055	DVAR 50) =	2.2844232	00031000
ISN 0056	DVAR 51) =	2.4322534	00031100
ISN 0057	DVAR 52) =	2.8176024	00031200
ISN 0058	DVAR 53) =	2.6879577	00031300
ISN 0059	DVAR 54) =	2.4527293	00031400
ISN 0060	DVAR 55) =	2.8557338	00031500
ISN 0061	DVAR 56) =	2.1636091	00031600
ISN 0062	DVAR 57) =	2.8039749	00031700
ISN 0063	DVAR 58) =	2.2159365	00031800
ISN 0064	DVAR 59) =	2.8578449	00031900
ISN 0065	DVAR 60) =	2.9285364	00032000
ISN 0066	DVAR 61) =	2.2489338	00032100
ISN 0067	DVAR 62) =	2.6909317	00032200
ISN 0068	DVAR 63) =	2.5195569	00032300
ISN 0069	DVAR 64) =	2.6975374	00032400
ISN 0070	DVAR 65) =	2.7474396	00032500
ISN 0071	DVAR 66) =	2.2045204	00032600
ISN 0072	DVAR 67) =	2.4193530	00032700
ISN 0073	DVAR 68) =	2.6966258	00032800
ISN 0074	DVAR 69) =	2.5628832	00032900
ISN 0075	DVAR 70) =	2.1792370	00033000
ISN 0076	DVAR 71) =	2.4727662	00033100
ISN 0077	DVAR 72) =	2.5711426	00033200
ISN 0078	DVAR 73) =	2.7585264	00033300
ISN 0079	DVAR 74) =	2.8786934	00033400
ISN 0080	DVAR 75) =	2.9366934	00033500
ISN 0081	DVAR 76) =	2.8071808	00033600
ISN 0082	DVAR 77) =	2.8442199	00033700
ISN 0083	DVAR 78) =	2.3198284	00033800
ISN 0084	DVAR 79) =	2.6385035	00033900
ISN 0085	DVAR 80) =	2.815119	00034000
ISN 0086	DVAR 81) =	2.8064117	00034100
ISN 0087	DVAR 82) =	2.1910590	00034200
ISN 0088	DVAR 83) =	2.7446152	00034300
ISN 0089	DVAR 84) =	2.8200313	00034400
ISN 0090	DVAR 85) =	2.3415316	00034500
ISN 0091	DVAR 86) =	2.6780626	00034600
ISN 0092	DVAR 87) =	2.6775625	00034700
ISN 0093	DVAR 88) =	2.5177941	00034800
ISN 0094	DVAR 89) =	2.4932026	00034900
ISN 0095	DVAR 90) =	2.4443577	00035000
ISN 0096	DVAR 91) =	2.7512543	00035100
ISN 0097	DVAR 92) =	2.2148969	00035200
ISN 0098	DVAR 93) =	2.8410976	00035300
ISN 0099	DVAR 94) =	2.5721650	00035400
ISN 0100	DVAR 95) =	2.2715440	00035500
ISN 0101	DVAR 96) =	2.8384263	00035600
ISN 0102	DVAR 97) =	2.3860799	00035700
ISN 0103	DVAR 98) =	2.6830127	00035800
ISN 0104	DVAR 99) =	2.2631829	00035900
ISN 0105	DVAR 100) =	2.3381125	00036000
ISN 0106	A = 1.00		00036100
ISN 0107	B = 2.00		00036200
ISN 0108			00036300
			00036400

DATE 08.273/21.48.26

08/360 FORTRAN B EXTENDED

FVAR

LEVEL 2.3.0 (JUNE 78)

00036500
00036600
00036700
00036800
00036900
00037000
00037100
00037200

A1 = 3.4650D0
A2 = 148.8370D0
B1 = 0.998005D0
S2 = 0.914252E6 CO TO 20
IF (MAX.I.E. 100) 101, NMAX
DO 10 N, 101, NMAX
DVAR(N) = (N-1)*(S1*(N-2)*A1/(N+A)+S2*(N+2)*A2/(N+B)*(N-2))

10 CONTINUE
20 CONTINUE
NMAX = NMAX+1
DO 30 N, NMAX, 2000
30 POWRDX = POWRDX+.2000027D11*((N-1)*(S1*(N+2)*A1/(N+A)+S2*(N+2)
2 *A2/(N+B)*(N-2)))/(N-1)*+2
RETURN
END

00037300
00037400

-112-

```

MISSION'//,' MAXIMUM DEGREE AND ORDER CONSIDERED = 2 MINIMUM ORDER ANALYZED = 16//
3. MINIMUM DEGREE AND ORDER IN REFERENCE MODEL = 15//
4. DURATION OF MISSION IN DAYS = 15//
5. NUMBER OF REVOLUTIONS DURING MISSION = 15//
6. HEIGHT OF THE SATELLITES ABOVE GROUND = 620.10 IN METERS//
7. SEPARATION BETWEEN SATELLITES = 620.10 IN METERS//
8. SAMPLING INTERVAL = .620.10 SECONDS//
9. ANALYTICAL INTERVAL = .620.10 SECONDS//
10. ACTUAL LENGTH OF DATA = .612.4 METERS PER SECOND////
IF(IAC.EQ.0) WRITE(6,3)
IF(IAC.EQ.0) WRITE(10,3)
IF(IAC.EQ.1) WRITE(10,4)
IF(IAC.EQ.1) WRITE(10,4)
3.FORMAT ANALYSIS IS BASED ON LEAST SQUARES ADJUSTMENT *****
4.FORMAT ANALYSIS IS BASED ON LEAST SQUARES COLLOCATION *****
ISEED = 20000
CANVA = 9.5302641DE
RE = 6371.D3
RS = RE*NS
CANS = CARNAS(RE/RS)**2
PSI122 = DARSIN(D12=.5DE/RS)
SINI22 = 2.D0*PSI122
COSI22 = COS(PSI122)
FI = 4.D0*DATAK(1,DG)
T0 = RE+24.D0*3600.D0
W0 = 2.D0*PI/T0
NSR = 2*MAXP
NH = T0/D0+.0000001D0
PN = NH / (SIGMA**2+W0**4*DAS**2+NSR**2)
WDA = PMS/PNSE
VDA = W0*DA
XDS = NS
XDE = RE
DO 5 KP = 1,NMAX
IDDI(KP) = ((KP-1)*KP)/2
5 CONTINUE

      FORM THE INVERSE OF THE DIAGONAL MATRIX C IN ARRAY CMI
CALL MVAR(DVAR,NMAX,DVAR0)
DO 8 N = 2,NMOD
  CH1(N) = 1.D0/DVAR(N)**2
  NMAXT = NMAX
  IF(NMOD).GT.NMAXO NMAXT = NMODI
  DO 9 N = NMODI,NMAXT
    CH1(N) = (2.D0*N+1.D0)*((N-1)*CANVA*1.D0)**2/DVAR(N)
    CH1(1) = 0.D0
    N = 2,NMAX
    CHR(N) = 1.D0/(CANS*(RE/RS)***)**2
    CH1(N) = CH1(N)*CHR(N)
  CONTINUE
  WRITE(6,17)
17 FORMAT('/// N M COEFFICIENTS VARIANCES (UP TO N,M = 10 )')//
CALL SCLOKI

```



```

18N 0132 EPS = 1.E-7
18N 0133 CALL DSINV(AE,NEV,EPS,IER1)
18N 0134 IF(N.NE.NMAX) CALL DSINV(AO,MOD,EPS,IER2)
18N 0135 IF(IER1.NE.0.OR.IER2.NE.0) WRITE(6,21) M,IER1,IER2
18N 0136 21 FORMAT('  ***** AT ORDER 15,1,1,1,1 ***** IER1 = ',I5,' IER2 = ',I5,'')
18N 0137 2 15, *****
18N 0138 IF(IER1.NE.0.OR.IER2.NE.0) GO TO 500
18N 0139 IF(M.EQ.NMAX) GO TO 334
18N 0140 DO 55 I = 1,NEV
18N 0141 55 CONTINUE
18N 0142 AE(1DD(I)+1) = AE(1DD(I)+1)*PIVE(I)**2
18N 0143 DO 65
18N 0144 65 CONTINUE
18N 0145 AO(1DD(I)+1) = AO(1DD(I)+1)*PIVO(I)**2
18N 0146 DO 60
18N 0147 60 CONTINUE
18N 0148 ITS = 0
18N 0149 IF((N-M)/2)*2.NE.N-M ITS = 1
18N 0150 I = (N-MIN)/2+1
18N 0151 IF(ITS.EQ.0) DIRV = AE(1DD(I)+1)*CHN(N)
18N 0152 IF(ITS.EQ.1) DIRV = AO(1DD(I)+1)*CHN(N)
18N 0153 IF(N.LE.40) WRITE(6,104) N,M,DIRV
18N 0154 104 FORMAT(215,G20.10)
18N 0155 DIRVO = DIRV**2.D0
18N 0156 IF(M.EQ.0) DIRVO = DIRV
18N 0157 RMS(N) = RMS(N)+DIRVO
18N 0158 80 CONTINUE
18N 0159 100 CONTINUE
18N 0160
18N 0161 END OF MAIN LOOP .
18N 0162 PRINT AND PUNCH ALL THE RESULTS .
18N 0163
18N 0164 500 WRITE(17,120) (N,RMS(N),R=2,NMAX)
18N 0165 120 FORMAT(413,G17.11)
18N 0166 WRITE(10,105)
18N 0167 105 FORMAT('1.20X, N PERCENTAGE ERROR TOTAL UNDOUL. ERROR (10)////')
18N 0168 20AND ERROR (UNDOUL.) (N)
18N 0169 POW = 0.D0
18N 0170 DO 106 N = 2,NMAX
18N 0171 POW = POW+CHN(N)*(2*N+1)/CHN(N)
18N 0172 PTR = POW*RE**2+POW*MOD=1.D-10
18N 0173 DO 106 N = 2,NMAX
18N 0174 PN = CHN(N)*RE**2*(2*N+1)/CHN(N)
18N 0175 PNR = PN*PTR-PN*PTR
18N 0176 PTR = PTR-PNR+PNR
18N 0177 PERC(N) = DSORT(RMS(N)*CHN(N)/(CHN(N)*(2*N+1)))*100.D0
18N 0178 PPR(N) = DSORT(PNR)
18N 0179 PPTR(N) = DSORT(PTR)
18N 0180 IF(N/50*20.EQ.N) WRITE(10,105)
18N 0181 105 FORMAT(10,107) N,PERC(N),RMS(N),PPR(N),PPTR(N)
18N 0182 107 FORMAT(20X,16.47X,G13.5)
18N 0183 110 CONTINUE
18N 0184 DO 115 N = 2,NMAX
18N 0185 115 CONTINUE
18N 0186 IF((R/10)*20.EQ.N.OR.N.EQ.2) WRITE(10,107) N,PERC(N),RMS(N),
18N 0187 2 PPR(N),PPTR(N)
18N 0188
18N 0189
18N 0190
18N 0191
18N 0192
18N 0193
18N 0194
18N 0195
18N 0196
18N 0197
18N 0198
18N 0199
18N 0200
18N 0201
18N 0202
18N 0203
18N 0204
18N 0205
18N 0206
18N 0207
18N 0208
18N 0209
18N 0210
18N 0211
18N 0212
18N 0213
18N 0214
18N 0215
18N 0216
18N 0217
18N 0218
18N 0219
18N 0220
18N 0221
18N 0222
18N 0223
18N 0224
18N 0225
18N 0226
18N 0227
18N 0228
18N 0229
18N 0230
18N 0231
18N 0232
18N 0233
18N 0234
18N 0235
18N 0236
18N 0237
18N 0238
18N 0239
18N 0240
18N 0241
18N 0242
18N 0243
18N 0244
18N 0245
18N 0246
18N 0247
18N 0248
18N 0249
18N 0250
18N 0251
18N 0252
18N 0253
18N 0254
18N 0255
18N 0256
18N 0257
18N 0258
18N 0259
18N 0260
18N 0261
18N 0262
18N 0263
18N 0264
18N 0265
18N 0266
18N 0267
18N 0268
18N 0269
18N 0270
18N 0271
18N 0272
18N 0273
18N 0274
18N 0275
18N 0276
18N 0277
18N 0278
18N 0279
18N 0280
18N 0281
18N 0282
18N 0283
18N 0284
18N 0285
18N 0286
18N 0287
18N 0288
18N 0289
18N 0290
18N 0291
18N 0292
18N 0293
18N 0294
18N 0295
18N 0296
18N 0297
18N 0298
18N 0299
18N 0300
18N 0301
18N 0302
18N 0303
18N 0304
18N 0305
18N 0306
18N 0307
18N 0308
18N 0309
18N 0310
18N 0311
18N 0312
18N 0313
18N 0314
18N 0315
18N 0316
18N 0317
18N 0318
18N 0319
18N 0320
18N 0321
18N 0322
18N 0323
18N 0324
18N 0325
18N 0326
18N 0327
18N 0328
18N 0329
18N 0330
18N 0331
18N 0332
18N 0333
18N 0334
18N 0335
18N 0336
18N 0337
18N 0338
18N 0339
18N 0340
18N 0341
18N 0342
18N 0343
18N 0344
18N 0345
18N 0346
18N 0347
18N 0348
18N 0349
18N 0350
18N 0351
18N 0352
18N 0353
18N 0354
18N 0355
18N 0356
18N 0357
18N 0358
18N 0359
18N 0360
18N 0361
18N 0362
18N 0363
18N 0364
18N 0365
18N 0366
18N 0367
18N 0368
18N 0369
18N 0370
18N 0371
18N 0372
18N 0373
18N 0374
18N 0375
18N 0376
18N 0377
18N 0378
18N 0379
18N 0380
18N 0381
18N 0382
18N 0383
18N 0384
18N 0385
18N 0386
18N 0387
18N 0388
18N 0389
18N 0390
18N 0391
18N 0392
18N 0393
18N 0394
18N 0395
18N 0396
18N 0397
18N 0398
18N 0399
18N 0400
18N 0401
18N 0402
18N 0403
18N 0404
18N 0405
18N 0406
18N 0407
18N 0408
18N 0409
18N 0410
18N 0411
18N 0412
18N 0413
18N 0414
18N 0415
18N 0416
18N 0417
18N 0418
18N 0419
18N 0420
18N 0421
18N 0422
18N 0423
18N 0424
18N 0425
18N 0426
18N 0427
18N 0428
18N 0429
18N 0430
18N 0431
18N 0432
18N 0433
18N 0434
18N 0435
18N 0436
18N 0437
18N 0438
18N 0439
18N 0440
18N 0441
18N 0442
18N 0443
18N 0444
18N 0445
18N 0446
18N 0447
18N 0448
18N 0449
18N 0450
18N 0451
18N 0452
18N 0453
18N 0454
18N 0455
18N 0456
18N 0457
18N 0458
18N 0459
18N 0460
18N 0461
18N 0462
18N 0463
18N 0464
18N 0465
18N 0466
18N 0467
18N 0468
18N 0469
18N 0470
18N 0471
18N 0472
18N 0473
18N 0474
18N 0475
18N 0476
18N 0477
18N 0478
18N 0479
18N 0480
18N 0481
18N 0482
18N 0483
18N 0484
18N 0485
18N 0486
18N 0487
18N 0488
18N 0489
18N 0490
18N 0491
18N 0492
18N 0493
18N 0494
18N 0495
18N 0496
18N 0497
18N 0498
18N 0499
18N 0500
18N 0501
18N 0502
18N 0503
18N 0504
18N 0505
18N 0506
18N 0507
18N 0508
18N 0509
18N 0510
18N 0511
18N 0512
18N 0513
18N 0514
18N 0515
18N 0516
18N 0517
18N 0518
18N 0519
18N 0520
18N 0521
18N 0522
18N 0523
18N 0524
18N 0525
18N 0526
18N 0527
18N 0528
18N 0529
18N 0530
18N 0531
18N 0532
18N 0533
18N 0534
18N 0535
18N 0536
18N 0537
18N 0538
18N 0539
18N 0540
18N 0541
18N 0542
18N 0543
18N 0544
18N 0545
18N 0546
18N 0547
18N 0548
18N 0549
18N 0550
18N 0551
18N 0552
18N 0553
18N 0554
18N 0555
18N 0556
18N 0557
18N 0558
18N 0559
18N 0560
18N 0561
18N 0562
18N 0563
18N 0564
18N 0565
18N 0566
18N 0567
18N 0568
18N 0569
18N 0570
18N 0571
18N 0572
18N 0573
18N 0574
18N 0575
18N 0576
18N 0577
18N 0578
18N 0579
18N 0580
18N 0581
18N 0582
18N 0583
18N 0584
18N 0585
18N 0586
18N 0587
18N 0588
18N 0589
18N 0590
18N 0591
18N 0592
18N 0593
18N 0594
18N 0595
18N 0596
18N 0597
18N 0598
18N 0599
18N 0600
18N 0601
18N 0602
18N 0603
18N 0604
18N 0605
18N 0606
18N 0607
18N 0608
18N 0609
18N 0610
18N 0611
18N 0612
18N 0613
18N 0614
18N 0615
18N 0616
18N 0617
18N 0618
18N 0619
18N 0620
18N 0621
18N 0622
18N 0623
18N 0624
18N 0625
18N 0626
18N 0627
18N 0628
18N 0629
18N 0630
18N 0631
18N 0632
18N 0633
18N 0634
18N 0635
18N 0636
18N 0637
18N 0638
18N 0639
18N 0640
18N 0641
18N 0642
18N 0643
18N 0644
18N 0645
18N 0646
18N 0647
18N 0648
18N 0649
18N 0650
18N 0651
18N 0652
18N 0653
18N 0654
18N 0655
18N 0656
18N 0657
18N 0658
18N 0659
18N 0660
18N 0661
18N 0662
18N 0663
18N 0664
18N 0665
18N 0666
18N 0667
18N 0668
18N 0669
18N 0670
18N 0671
18N 0672
18N 0673
18N 0674
18N 0675
18N 0676
18N 0677
18N 0678
18N 0679
18N 0680
18N 0681
18N 0682
18N 0683
18N 0684
18N 0685
18N 0686
18N 0687
18N 0688
18N 0689
18N 0690
18N 0691
18N 0692
18N 0693
18N 0694
18N 0695
18N 0696
18N 0697
18N 0698
18N 0699
18N 0700
18N 0701
18N 0702
18N 0703
18N 0704
18N 0705
18N 0706
18N 0707
18N 0708
18N 0709
18N 0710
18N 0711
18N 0712
18N 0713
18N 0714
18N 0715
18N 0716
18N 0717
18N 0718
18N 0719
18N 0720
18N 0721
18N 0722
18N 0723
18N 0724
18N 0725
18N 0726
18N 0727
18N 0728
18N 0729
18N 0730
18N 0731
18N 0732
18N 0733
18N 0734
18N 0735
18N 0736
18N 0737
18N 0738
18N 0739
18N 0740
18N 0741
18N 0742
18N 0743
18N 0744
18N 0745
18N 0746
18N 0747
18N 0748
18N 0749
18N 0750
18N 0751
18N 0752
18N 0753
18N 0754
18N 0755
18N 0756
18N 0757
18N 0758
18N 0759
18N 0760
18N 0761
18N 0762
18N 0763
18N 0764
18N 0765
18N 0766
18N 0767
18N 0768
18N 0769
18N 0770
18N 0771
18N 0772
18N 0773
18N 0774
18N 0775
18N 0776
18N 0777
18N 0778
18N 0779
18N 0780
18N 0781
18N 0782
18N 0783
18N 0784
18N 0785
18N 0786
18N 0787
18N 0788
18N 0789
18N 0790
18N 0791
18N 0792
18N 0793
18N 0794
18N 0795
18N 0796
18N 0797
18N 0798
18N 0799
18N 0800
18N 0801
18N 0802
18N 0803
18N 0804
18N 0805
18N 0806
18N 0807
18N 0808
18N 0809
18N 0810
18N 0811
18N 0812
18N 0813
18N 0814
18N 0815
18N 0816
18N 0817
18N 0818
18N 0819
18N 0820
18N 0821
18N 0822
18N 0823
18N 0824
18N 0825
18N 0826
18N 0827
18N 0828
18N 0829
18N 0830
18N 0831
18N 0832
18N 0833
18N 0834
18N 0835
18N 0836
18N 0837
18N 0838
18N 0839
18N 0840
18N 0841
18N 0842
18N 0843
18N 0844
18N 0845
18N 0846
18N 0847
18N 0848
18N 0849
18N 0850
18N 0851
18N 0852
18N 0853
18N 0854
18N 0855
18N 0856
18N 0857
18N 0858
18N 0859
18N 0860
18N 0861
18N 0862
18N 0863
18N 0864
18N 0865
18N 0866
18N 0867
18N 0868
18N 0869
18N 0870
18N 0871
18N 0872
18N 0873
18N 0874
18N 0875
18N 0876
18N 0877
18N 0878
18N 0879
18N 0880
18N 0881
18N 0882
18N 0883
18N 0884
18N 0885
18N 0886
18N 0887
18N 0888
18N 0889
18N 0890
18N 0891
18N 0892
18N 0893
18N 0894
18N 0895
18N 0896
18N 0897
18N 0898
18N 0899
18N 0900
18N 0901
18N 0902
18N 0903
18N 0904
18N 0905
18N 0906
18N 0907
18N 0908
18N 0909
18N 0910
18N 0911
18N 0912
18N 0913
18N 0914
18N 0915
18N 0916
18N 0917
18N 0918
18N 0919
18N 0920
18N 0921
18N 0922
18N 0923
18N 0924
18N 0925
18N 0926
18N 0927
18N 0928
18N 0929
18N 0930
18N 0931
18N 0932
18N 0933
18N 0934
18N 0935
18N 0936
18N 0937
18N 0938
18N 0939
18N 0940
18N 0941
18N 0942
18N 0943
18N 0944
18N 0945
18N 0946
18N 0947
18N 0948
18N 0949
18N 0950
18N 0951
18N 0952
18N 0953
18N 0954
18N 0955
18N 0956
18N 0957
18N 0958
18N 0959
18N 0960
18N 0961
18N 0962
18N 0963
18N 0964
18N 0965
18N 0966
18N 0967
18N 0968
18N 0969
18N 0970
18N 0971
18N 0972
18N 0973
18N 0974
18N 0975
18N 0976
18N 0977
18N 0978
18N 0979
18N 0980
18N 0981
18N 0982
18N 0983
18N 0984
18N 0985
18N 0986
18N 0987
18N 0988
18N 0989
18N 0990
18N 0991
18N 0992
18N 0993
18N 0994
18N 0995
18N 0996
18N 0997
18N 0998
18N 0999
18N 1000
18N 1001
18N 1002
18N 1003
18N 1004
18N 1005
18N 1006
18N 1007
18N 1008
18N 1009
18N 1010
18N 1011
18N 1012
18N 1013
18N 1014
18N 1015
18N 1016
18N 1017
18N 1018
18N 1019
18N 1020
18N 1021
18N 1022
18N 1023
18N 1024
18N 1025
18N 1026
18N 1027
18N 1028
18N 1029
18N 1030
18N 1031
18N 1032
18N 1033
18N 1034
18N 1035
18N 1036
18N 1037
18N 1038
18N 1039
18N 1040
18N 1041
18N 1042
18N 1043
18N 1044
18N 1045
18N 1046
18N 1047
18N 1048
18N 1049
18N 1050
18N 1051
18N 1052
18N 1053
18N 1054
18N 1055
18N 1056
18N 1057
18N 1058
18N 1059
18N 1060
18N 1061
18N 1062
18N 1063
18N 1064
18N 1065
18N 1066
18N 1067
18N 1068
18N 1069
18N 1070
18N 1071
18N 1072
18N 1073
18N 1074
18N 1075
18N 1076
18N 1077
18N 1078
18N 1079
18N 1080
18N 1081
18N 1082
18N 1083
18N 1084
18N 1085
18N 1086
18N 1087
18N 1088
18N 1089
18N 1090
18N 1091
18N 1092
18N 1093
18N 1094
18N 1095
18N 1096
18N 1097
18N 1098
18N 1099
18N 1100
18N 1101
18N 1102
18N 1103
18N 1104
18N 1105
18N 1106
18N 1107
18N 1108
18N 1109
18N 1110
18N 1111
18N 1112
18N 1113
18N 1114
18N 1115
18N 1116
18N 1117
18N 1118
18N 1119
18N 1120
18N 1121
18N 1122
18N 1123
18N 1124
18N 1125
18N 1126
18N 1127
18N 1128
18N 1129
18N 1130
18N 1131
18N 1132
18N 1133
18N 1134
18N 1135
18N 1136
18N 1137
18N 1138
18N 1139
18N 1140
18N 1141
18N 1142
18N 1143
18N 1144
18N 1145
18N 1146
18N 1147
18N 1148
18N 1149
18N 1150
18N 1151
18N 1152
18N 1153
18N 1154
18N 1155
18N 1156
18N 1157
18N 1158
18N 1159
18N 1160
18N 1161
18N 1162
18N 1163
18N 1164
18N 1165
18N 1166
18N 1167
18N 1168
18N 1169
18N 1170
18N 1171
18N 1172
18N 1173
18N 1174
18N 1175
18N 1176
18N 1177
18N 1178
18N 1179
18N 1180
18N 1181
18N 1182
18N 1183
18N 1184
18N 1185
18N 1186
18N 1187
18N 1188
18N 1189
18N 1190
18N 1191
18N 1192
18N 1193
18N 1194
18N 1195
18N 1196
18N 1197
18N 1198
18N 1199
18N 1200
18N 1201
18N 1202
18N 1203
18N 1204
18N 1205
18N 1206
18N 1207
18N 1208
18N 1209
18N 1210
18N 1211
18N 1212
18N 1213
18N 1214
18N 1215
18N 1216
18N 1217
18N 1218
18N 1219
18N 1220
18N 1221
18N 1222
18N 1223
18N 1224
18N 1225
18N 1226
18N 1227
18N 1228
18N 1229
18N 1230
18N 1231
18N 1232
18N 1233
18N 1234
18N 1235
18N 1236
18N 1237
18N 1238
18N 1239
18N 1240
18N 1241
18N 1242
18N 1243
18N 1244
18N 1245
18N 1246
18N 1247
18N 1248
18N 1249
18N 1250
18N 1251
18N 1252
18N 1253
18N 1254
18N 1255
18N 1256
18N 1257
18N 1258
18N 1259
18N 1260
18N 1261
18N 1262
18N 1263
18N 1264
18N 1265
18N 1266
18N 1267
18N 1268
18N 1269
18N 1270
18N 1271
18N 1272
18N 1273
18N 1274
18N 1275
18N 1276
18N 1277
18N 1278
18N 1279
18N 1280
18N 1281
18N 1282
18N 1283
18N 1284
18N 1285
18N 1286
18N 1287
18N 1288
18N 1289
18N 1290
18N 1291
18N 1292
18N 1293
18N 1294
18N 1295
18N 1296
18N 1297
18N 1298
18N 1299
18N 1300
18N 1301
18N 1302
18N 1303
18N 1304
18N 1305
18N 1306
18N 1307
18N 1308
18N 1309
18N 1310
18N 1311
18N 1312
18N 1313
18N 1314
18N 1315
18N 1316
18N 1317
18N 1318
18N 1319
18N 1320
18N 1321
18N 1322
18N 1323
18N 1324
18N 1325
18N 1326
18N 1327
18N 1328
18N 1329
18N 1330
18N 1331
18N 1332
18N 1333
18N 1334
18N 1335
18N 1336
18N 1337
18N 1338
18N 1339
18N 1340
18N 1341
18N 1342
18N 1343
18N 1344
18N 1345
18N 1346
18N 1347
18N 1348
18N 1349
18N 1350
18N 1351
18N 1352
18N 1353
18N 1354
18N 1355
18N 1356
18N 1357
18N 1358
18N 1359
18N 1360
18N 1361
18N 1362
18N 1363
18N 1364
18N 1365
18N 1366
18N 1367
18N 1368
18N 1369
18N 1370
18N 1371
18N 1372
18N 1373
18N 1374
18N 1375
18N 1376
18N 1377
18N 1378
18N 1379
18N 1380
18N 1381
18N 1382
18N 1383
18N 1384
18N 1385
18N 1386
18N 1387
18N 1388
18N 1389
18N 1390
18N 1391
18N 1392
18N 1393
18N 1394
```

PAGE 5

DATE 86.274/00.02.02

00029700
00029000

08/060 FORTNAH II EXTENDED

MAIN

LEVEL 2.3.0 (JUNE 78)

100 0103
100 0104
100 0105
110 CONTINUE
110 STOP
END

REQUESTED OPTIONS: MAP, ID, OPT-2

OPTIONS IN EFFECT: NAME(MAIN) OPTIMIZE(2) LINECOUNT(60) RIZZI(MAX) AUTO-DRL(NONE)
SOURCE ENCBIC POLIST NODECK OBJECT MAP NOFORMAT GO-TMT NOXDEF NOALC NOANSY ROTERN ISM FLAG(1)

SUBROUTINE RDM(AF, AO, REV, MOD, NREV, NMOD)

READS THE NORMALS FROM UNIT 10

IMPLICIT REAL*(A-H,O-Z)
DIMENSION AF(NREV), AO(NMOD)
READ(10) AF, AO
RETURN
END

ISN 0002
ISN 0003
ISN 0004
ISN 0005
ISN 0006
ISN 0007

ERROR ANALYSIS OF A SATELLITE TO SATELLITE TRACKING MISSION

MAXIMUM DEGREE AND ORDER CONSIDERED * 11
 MINIMUM DEGREE CONSIDERED * 2 MINIMUM ORDER ANALYZED * 0
 MAXIMUM DEGREE AND ORDER IN REFERENCE MODEL * 20
 DURATION OF MISSION IN DAYS * 179
 NUMBER OF REVOLUTIONS DURING MISSION * 2933
 HEIGHT OF THE SATELLITES ABOVE GROUND * 160000.0000 IN METERS
 SEPARATION BETWEEN SATELLITES * 300000.0000 IN METERS
 AVERAGING INTERVAL * 4.000000000 SECONDS
 SAMPLING INTERVAL * 4.000000000 SECONDS
 ACCURACY OF THE DATA * .1000D-05 METERS PER SECOND

ANALYSIS IS BASED ON LEAST SQUARES ADJUSTMENT

B N COEFFICIENTS VARIANCES (UP TO N,N = 10)

TIME BEFORE N	0.00 SECONDS		
ACCURACY OF INVERSION, N	0"		
2	.446727949D-24	.1186309042D-14	.1092473701D-14
3	.344444472D-24		
4	.317393454D-24		
5	.238724499D-24		
6	.191765346D-24		
7	.18789738D-24		
8	.1326842714D-24		
9	.1138915819D-24		
10	.6327279525D-28		
11	.7389421863D-23		
TIME BEFORE N	0.01 SECONDS		
ACCURACY OF INVERSION, N	1"		
2	.6048172089D-24	.1863041300D-14	.1104797430D-14
3	.6194742956D-23		
4	.1789635767D-24		
5	.1937257723D-23		
6	.1633747934D-24		
7	.9387707878D-24		
8	.6984804134D-23		
9	.5647601539D-24		
10	.4379491904D-25		
11	.2994807711D-24		
TIME BEFORE N	0.03 SECONDS		
ACCURACY OF INVERSION, N	2"		
2	.2685761113D-24	.4728952219D-14	.1048487996D-14
3	.2914233052D-24		
4	.1935174717D-24		
5	.1813781500D-24		
6	.1147107039D-24		
7	.9380313350D-23		
8	.7674747319D-25		

9	2	6589376468D-23		
10	2	5239386630D-25		
11	2	4640497613D-25		
TIME BEFORE INVERSION, M = 3"				
3	3	2781831375D-24		
4	3	2876589263D-24		
5	3	2816374929D-24		
6	3	1548998318D-24		
7	3	1195823648D-24		
8	3	9679008266D-25		
9	3	7993143278D-25		
10	3	6786386718D-25		
11	3	5776510686D-25		
TIME BEFORE INVERSION, M = 4"				
4	4	1789198476D-24		
5	4	2281324673D-24		
6	4	1548791110D-24		
7	4	1278338618D-24		
8	4	1889388478D-24		
9	4	8812541843D-25		
10	4	7849249363D-25		
11	4	6148146385D-25		
TIME BEFORE INVERSION, M = 5"				
5	5	1496128687D-24		
6	5	2247745936D-24		
7	5	1644859364D-24		
8	5	1378181370D-24		
9	5	1896787214D-24		
10	5	9201954166D-25		
11	5	7888656640D-25		
TIME BEFORE INVERSION, M = 6"				
6	6	1313771510D-24		
7	6	1732356965D-24		
8	6	1321311834D-24		
9	6	1894862496D-24		
10	6	9296781911D-25		
11	6	7834218947D-25		
TIME BEFORE INVERSION, M = 7"				
7	7	156658345D-24		
8	7	1873184298D-24		
9	7	148444787D-24		
10	7	1248218892D-24		
11	7	1021836742D-24		
TIME BEFORE INVERSION, M = 8"				
8	8	981855648D-25		
9	8	1378633284D-24		
10	8	1198384851D-24		
11	8	9349494144D-25		
TIME BEFORE INVERSION, M = 9"				
9	9	7869826271D-25		
10	9	1619917818D-24		
11	9	1243636679D-24		
TIME BEFORE INVERSION, M = 10"				
10	10	642421238D-25		
11	10	8879246834D-25		
TIME BEFORE INVERSION, M = 12 SECONDS				
11	11	2856732285D-25		
TIME BEFORE INVERSION, M = 15 SECONDS				
11	11	294326982D-15	.1867868398D-15	
TIME BEFORE INVERSION, M = 14 SECONDS				
11	11	2422228672D-14	.1311879440D-14	
TIME BEFORE INVERSION, M = 16 SECONDS				
11	11	4661984699D-16	.2366614983D-16	
TIME BEFORE INVERSION, M = 16 SECONDS				
11	11	9222981164D-16	.8278733415D-16	
TIME BEFORE INVERSION, M = 15 SECONDS				
11	11	3116885742D-15	.1148591316D-15	
TIME BEFORE INVERSION, M = 15 SECONDS				
11	11	1578892489D-15	.3928231147D-15	
TIME BEFORE INVERSION, M = 17 SECONDS				
11	11	7821666937D-15	.4336888690D-17	
TIME BEFORE INVERSION, M = 15 SECONDS				
11	11	228846849D-15	.222846849D-15	

ERROR ANALYSIS OF A SATELLITE TO SATELLITE TRACKING MISSION
 MAXIMUM DEGREE AND ORDER CONSIDERED - 11
 MINIMUM DEGREE CONSIDERED - 2 MINIMUM ORDER ANALYZED - 0
 MAXIMUM DEGREE AND ORDER IN REFERENCE MODEL - 20
 DURATION OF MISSION IN DAYS - 179
 NUMBER OF REVOLUTIONS DURING MISSION - 2933
 HEIGHT OF THE SATELLITES ABOVE GROUND - 160000.0000 IN METERS
 SEPARATION BETWEEN SATELLITES - 300000.0000 IN METERS
 AVERAGING INTERVAL - 4.000000000 SECONDS
 SAMPLING INTERVAL - 4.000000000 SECONDS
 ACCURACY OF THE DATA - .1000D-05 METERS PER SECOND

ANALYSIS IS BASED ON LEAST SQUARES ADJUSTMENT *****

N	PERCENTAGE ERROR	ERROR VARIANCE (POT.)	BAND ERROR (UNDUL.) (M)	TOTAL UNDUL. ERROR (M)
2	.23249D-01	.19988D-23	.90087D-05	3.9607
3	.19749D-01	.11898D-22	.23748D-04	3.9591
4	.16323D-01	.19978D-23	.25398D-04	3.9582
5	.98932D-02	.86348D-23	.24562D-04	3.9552
6	.68082D-02	.19598D-23	.30079D-04	3.9539
7	.73315D-02	.36269D-23	.33177D-04	3.9496
8	.59267D-02	.19299D-23	.34337D-04	3.9467
9	.67629D-02	.24502D-23	.35982D-04	3.9435
10	.58216D-02	.10643D-23	.37019D-04	3.9407
11	.61638D-02	.21758D-23	.38193D-04	3.9370

	PERCENTAGE ERROR	ERROR VARIANCE/POT.	BAND ERROR (UNDUL.) (NO	TOTAL UNDUL. ERROR (NO
2	.20249D-01	.19995D-23	.90057D-05	2.9607
10	.85216D-02	.10643D-23	.37019D-04	2.9607

Appendix C : Detailed Listings Degree by Degree

This Appendix contains the full listing of the formal accuracies of the potential coefficients from the error analysis of the SST mission using (a) least squares adjustment theory, and (b) least squares collocation theory. The rms of the total undulation error (last column) for least squares collocation should be corrected as indicated in paragraph 3.1. Notice the fluctuations in percentage error in the neighborhoods of $n = 136$ and $n = 273$.

N	PERCENTAGE ERROR	ERROR VARIANCE (POT.)	BAND ERROR (UNDOUL.) (M)	TOTAL UNDOUL. ERROR (M)
50	.79134D-02	.79167D-23	.91745D-04	1.4171
51	.58443D-02	.88323D-23	.93613D-04	1.4662
52	.98469D-02	.86226D-23	.94790D-04	1.3846
53	.63907D-02	.92230D-23	.95432D-04	1.3683
54	.91565D-02	.94551D-23	.96100D-04	1.3484
55	.98216D-02	.18190D-22	.19153D-03	1.3313
56	.18367D-01	.18371D-22	.19350D-03	1.3166
57	.18251D-01	.11700D-22	.19567D-03	1.3066
58	.11289D-01	.11370D-22	.19783D-03	1.2859
59	.14840D-01	.12261D-22	.19910D-03	1.2716
60	.15690D-01	.12490D-22	.14800D-03	1.2546
61	.13164D-01	.13471D-22	.14800D-03	1.2494
62	.12190D-01	.13746D-22	.11721D-03	1.2282
63	.13700D-01	.14823D-22	.11721D-03	1.2152
64	.14523D-01	.15139D-22	.12228D-03	1.2032
65	.17121D-01	.16360D-22	.12496D-03	1.1937
66	.14123D-01	.16696D-22	.12765D-03	1.1794
67	.17030D-01	.18017D-22	.13640D-03	1.1687
68	.17670D-01	.18437D-22	.13532D-03	1.1584
69	.16710D-01	.19997D-22	.13631D-03	1.1458
70	.19457D-01	.26300D-22	.13932D-03	1.1362
71	.20952D-01	.22827D-22	.14249D-03	1.1271
72	.20049D-01	.22578D-22	.14567D-03	1.1171
73	.20600D-01	.24411D-22	.14903D-03	1.1066
74	.20862D-01	.25040D-22	.15240D-03	1.0969
75	.23890D-01	.27969D-22	.15597D-03	1.0871
76	.24362D-01	.27813D-22	.15953D-03	1.0784
77	.26095D-01	.30128D-22	.16333D-03	1.0705
78	.25813D-01	.30945D-22	.16714D-03	1.0616
79	.27977D-01	.33552D-22	.17116D-03	1.0534
80	.27222D-01	.34499D-22	.17520D-03	1.0444
81	.28694D-01	.37436D-22	.17949D-03	1.0356
82	.27633D-01	.38590D-22	.18379D-03	1.0256
83	.31947D-01	.41837D-22	.18805D-03	1.0172
84	.30766D-01	.43083D-22	.19294D-03	1.0081
85	.30516D-01	.46393D-22	.19781D-03	1.0011
86	.37450D-01	.48363D-22	.20271D-03	.99332
87	.37450D-01	.52660D-22	.20791D-03	.98562
88	.39469D-01	.54599D-22	.21310D-03	.97749
89	.42139D-01	.57580D-22	.21820D-03	.96934
90	.43714D-01	.61140D-22	.22320D-03	.96103
91	.43866D-01	.64911D-22	.22820D-03	.95149
92	.48016D-01	.69070D-22	.23320D-03	.94129
93	.49327D-01	.73740D-22	.23820D-03	.93022
94	.50379D-01	.78270D-22	.24320D-03	.91782
95	.56049D-01	.86032D-22	.24818D-03	.90313
96	.55235D-01	.88981D-22	.25409D-03	.88726
97	.60522D-01	.98066D-22	.26083D-03	.86956
98	.58601D-01	.19154D-21	.27051D-03	.84993
99	.67774D-01	.11224D-21	.27842D-03	.81338
			.28610D-03	.90794

N	PERCENTAGE ERROR	ERROR VARIANCE(POT.)	BAND ERROR (UNBUL.) (M)	TOTAL UNBUL. ERROR (M)
100	68585D-01	11634D-21	29424D-03	96290
101	67653D-01	12984D-21	30751D-03	10660
102	69782D-01	13399D-21	31185D-03	88976
103	74331D-01	14913D-21	32141D-03	88358
104	76523D-01	15513D-21	33164D-03	87149
105	81863D-01	17337D-21	34152D-03	87539
106	84443D-01	18873D-21	35210D-03	84557
107	90432D-01	20291D-21	36361D-03	83973
108	93414D-01	21210D-21	37526D-03	83398
109	10026	23937D-21	38799D-03	84839
110	10372	25104D-21	40040D-03	84278
111	11162	28493D-21	41568D-03	83717
112	11570	30616D-21	42551D-03	83172
113	12492	34304D-21	44542D-03	82634
114	12982	36126D-21	46168D-03	82103
115	14068	41830D-21	47971D-03	81578
116	14669	44610D-21	49823D-03	81061
117	18668	51844D-21	51892D-03	80550
118	16723	63817D-21	54031D-03	80046
119	18294	63543D-21	56439D-03	79547
120	19263	71472D-21	58953D-03	79056
121	21222	84973D-21	61099D-03	78570
122	22869	94343D-21	64033D-03	78090
123	25023	11387D-20	68505D-03	77616
124	26959	12979D-20	72058D-03	77147
125	30170	15964D-20	76422D-03	76685
126	33162	18944D-20	81298D-03	76227
127	37378	23897D-20	87059D-03	75775
128	42698	30300D-20	93859D-03	75329
129	49297	39702D-20	10208D-02	74807
130	59562	56954D-20	11284D-02	74451
131	71323	80264D-20	12645D-02	74020
132	98982	10193D-19	14006D-02	73593
133	13528	27890D-19	18297D-02	73172
134	27136	11038D-18	27979D-02	72755
135	30583	13784D-18	36639D-02	72343
136	83080	40637D-18	54772D-02	71937
137	37068	19587D-18	61093D-02	71534
138	30320	12809D-18	65712D-02	71135
139	30987	13243D-18	69683D-02	70741
140	28004	10641D-18	72716D-02	70351
141	27930	10418D-18	75567D-02	69965
142	27258	97610D-19	78144D-02	69583
143	27360	96776D-19	80618D-02	69206
144	27194	94094D-19	82953D-02	68832
145	27438	94206D-19	85229D-02	68462
146	27517	93343D-19	87423D-02	68096
147	27867	94232D-19	89304D-02	67733
148	28098	94341D-19	91697D-02	67374
149	28535	95601D-19	93793D-02	67019

N	PERCENTAGE ERROR	ERROR VARIANCE (FOT.)	BAND ERROR (UNDUL.) (M)	TOTAL UNDUL. ERROR (M)
180	2.8876	.94610D-19	.95861D-02	.66668
181	2.9385	.98829D-19	.97925D-02	.66320
182	2.9814	.99699D-19	.99730D-02	.65973
183	3.0309	.10223D-18	.10263D-01	.65634
184	3.0893	.10467D-18	.10461D-01	.65297
185	3.1529	.10679D-18	.10614D-01	.64962
186	3.2101	.10879D-18	.10829D-01	.64631
187	3.2798	.11079D-18	.11029D-01	.64303
188	3.3436	.11279D-18	.11230D-01	.63973
189	3.4152	.11479D-18	.11430D-01	.63647
190	3.4877	.11679D-18	.11630D-01	.63318
191	3.5608	.11879D-18	.11830D-01	.62992
192	3.6342	.12079D-18	.12030D-01	.62668
193	3.7081	.12279D-18	.12230D-01	.62340
194	3.7825	.12479D-18	.12430D-01	.62009
195	3.8583	.12679D-18	.12630D-01	.61688
196	3.9358	.12879D-18	.12830D-01	.61369
197	4.0149	.13079D-18	.13030D-01	.61052
198	4.0954	.13279D-18	.13230D-01	.60738
199	4.1774	.13479D-18	.13430D-01	.60426
200	4.2609	.13679D-18	.13630D-01	.60116
201	4.3459	.13879D-18	.13830D-01	.59808
202	4.4324	.14079D-18	.14030D-01	.59502
203	4.5204	.14279D-18	.14230D-01	.59198
204	4.6099	.14479D-18	.14430D-01	.58896
205	4.7009	.14679D-18	.14630D-01	.58596
206	4.7934	.14879D-18	.14830D-01	.58298
207	4.8874	.15079D-18	.15030D-01	.58002
208	4.9829	.15279D-18	.15230D-01	.57708
209	5.0799	.15479D-18	.15430D-01	.57416
210	5.1784	.15679D-18	.15630D-01	.57126
211	5.2784	.15879D-18	.15830D-01	.56838
212	5.3799	.16079D-18	.16030D-01	.56552
213	5.4829	.16279D-18	.16230D-01	.56268
214	5.5874	.16479D-18	.16430D-01	.55986
215	5.6934	.16679D-18	.16630D-01	.55706
216	5.8009	.16879D-18	.16830D-01	.55428
217	5.9099	.17079D-18	.17030D-01	.55152
218	6.0204	.17279D-18	.17230D-01	.54878
219	6.1324	.17479D-18	.17430D-01	.54606
220	6.2459	.17679D-18	.17630D-01	.54336
221	6.3609	.17879D-18	.17830D-01	.54068
222	6.4784	.18079D-18	.18030D-01	.53802
223	6.5974	.18279D-18	.18230D-01	.53538
224	6.7179	.18479D-18	.18430D-01	.53276
225	6.8399	.18679D-18	.18630D-01	.53016
226	6.9634	.18879D-18	.18830D-01	.52758
227	7.0884	.19079D-18	.19030D-01	.52502
228	7.2149	.19279D-18	.19230D-01	.52248
229	7.3429	.19479D-18	.19430D-01	.51996
230	7.4724	.19679D-18	.19630D-01	.51746
231	7.6034	.19879D-18	.19830D-01	.51498
232	7.7359	.20079D-18	.20030D-01	.51252
233	7.8699	.20279D-18	.20230D-01	.51008
234	7.9999	.20479D-18	.20430D-01	.50766
235	8.1324	.20679D-18	.20630D-01	.50526
236	8.2674	.20879D-18	.20830D-01	.50288
237	8.4039	.21079D-18	.21030D-01	.50052
238	8.5419	.21279D-18	.21230D-01	.49818
239	8.6814	.21479D-18	.21430D-01	.49586
240	8.8224	.21679D-18	.21630D-01	.49356
241	8.9649	.21879D-18	.21830D-01	.49128
242	9.1089	.22079D-18	.22030D-01	.48902
243	9.2544	.22279D-18	.22230D-01	.48678
244	9.4014	.22479D-18	.22430D-01	.48456
245	9.5499	.22679D-18	.22630D-01	.48236
246	9.6999	.22879D-18	.22830D-01	.48018
247	9.8514	.23079D-18	.23030D-01	.47802
248	10.0044	.23279D-18	.23230D-01	.47588
249	10.1589	.23479D-18	.23430D-01	.47376
250	10.3149	.23679D-18	.23630D-01	.47166
251	10.4724	.23879D-18	.23830D-01	.46958
252	10.6314	.24079D-18	.24030D-01	.46752
253	10.7919	.24279D-18	.24230D-01	.46548
254	10.9539	.24479D-18	.24430D-01	.46346
255	11.1174	.24679D-18	.24630D-01	.46146
256	11.2824	.24879D-18	.24830D-01	.45948
257	11.4489	.25079D-18	.25030D-01	.45752
258	11.6169	.25279D-18	.25230D-01	.45558
259	11.7864	.25479D-18	.25430D-01	.45366
260	11.9574	.25679D-18	.25630D-01	.45176
261	12.1299	.25879D-18	.25830D-01	.44988
262	12.3039	.26079D-18	.26030D-01	.44802
263	12.4794	.26279D-18	.26230D-01	.44618
264	12.6564	.26479D-18	.26430D-01	.44436
265	12.8349	.26679D-18	.26630D-01	.44256
266	13.0149	.26879D-18	.26830D-01	.44078
267	13.1964	.27079D-18	.27030D-01	.43902
268	13.3794	.27279D-18	.27230D-01	.43728
269	13.5639	.27479D-18	.27430D-01	.43556
270	13.7499	.27679D-18	.27630D-01	.43386
271	13.9374	.27879D-18	.27830D-01	.43218
272	14.1264	.28079D-18	.28030D-01	.43052
273	14.3169	.28279D-18	.28230D-01	.42888
274	14.5089	.28479D-18	.28430D-01	.42726
275	14.7024	.28679D-18	.28630D-01	.42566
276	14.8974	.28879D-18	.28830D-01	.42408
277	15.0939	.29079D-18	.29030D-01	.42252
278	15.2919	.29279D-18	.29230D-01	.42098
279	15.4914	.29479D-18	.29430D-01	.41946
280	15.6924	.29679D-18	.29630D-01	.41796
281	15.8949	.29879D-18	.29830D-01	.41648
282	16.0989	.30079D-18	.30030D-01	.41502
283	16.3044	.30279D-18	.30230D-01	.41358
284	16.5114	.30479D-18	.30430D-01	.41216
285	16.7199	.30679D-18	.30630D-01	.41076
286	16.9299	.30879D-18	.30830D-01	.40938
287	17.1414	.31079D-18	.31030D-01	.40802
288	17.3544	.31279D-18	.31230D-01	.40668
289	17.5689	.31479D-18	.31430D-01	.40536
290	17.7849	.31679D-18	.31630D-01	.40406
291	17.9999	.31879D-18	.31830D-01	.40278
292	18.2169	.32079D-18	.32030D-01	.40152
293	18.4349	.32279D-18	.32230D-01	.40028
294	18.6539	.32479D-18	.32430D-01	.39906
295	18.8739	.32679D-18	.32630D-01	.39786
296	19.0949	.32879D-18	.32830D-01	.39668
297	19.3169	.33079D-18	.33030D-01	.39552
298	19.5399	.33279D-18	.33230D-01	.39438
299	19.7639	.33479D-18	.33430D-01	.39326

N	PERCENTAGE ERROR	ERROR VARIANCE(POT.)	BARD ERROR (UNDUL.) (M)	TOTAL UNDUL. ERROR (M)
200	9.4254	.8298D-18	.24037D-01	.52874
201	9.6003	.8470D-18	.24493D-01	.52451
202	9.9314	.8682D-18	.24961D-01	.52230
203	10.299	.89318D-18	.25430D-01	.52011
204	10.746	.91699D-18	.25926D-01	.51793
205	10.799	.94391D-18	.26423D-01	.51577
206	11.329	.96819D-18	.26923D-01	.51363
207	11.929	.99810D-18	.27430D-01	.51151
208	11.953	.72790D-18	.27930D-01	.50931
209	12.249	.78505D-18	.28430D-01	.50722
210	12.591	.82942D-18	.28930D-01	.50520
211	12.910	.85413D-18	.29430D-01	.50316
212	13.275	.89263D-18	.30023D-01	.50114
213	13.606	.92738D-18	.30623D-01	.49914
214	13.992	.96972D-18	.31230D-01	.49718
215	14.340	.10071D-17	.31840D-01	.49518
216	14.748	.10533D-17	.32460D-01	.49323
217	15.113	.10939D-17	.33080D-01	.49123
218	15.544	.11440D-17	.33664D-01	.48929
219	15.928	.11833D-17	.34230D-01	.48737
220	16.304	.12434D-17	.34664D-01	.48546
221	16.788	.12912D-17	.35333D-01	.48358
222	17.269	.13513D-17	.35779D-01	.48170
223	17.694	.14033D-17	.36779D-01	.47985
224	18.203	.14690D-17	.37518D-01	.47801
225	18.649	.15252D-17	.38269D-01	.47618
226	19.187	.15971D-17	.39025D-01	.47438
227	19.655	.16589D-17	.40631D-01	.47259
228	20.224	.17367D-17	.41451D-01	.47081
229	20.715	.18026D-17	.42293D-01	.46905
230	21.318	.18877D-17	.43149D-01	.46731
231	21.533	.19682D-17	.44020D-01	.46558
232	21.813	.20546D-17	.44923D-01	.46387
233	23.013	.21321D-17	.45842D-01	.46210
234	23.689	.22366D-17	.46776D-01	.46030
235	24.257	.23197D-17	.47736D-01	.45844
236	24.975	.24334D-17	.48712D-01	.45720
237	25.672	.25248D-17	.49716D-01	.45557
238	26.335	.26499D-17	.50746D-01	.45396
239	26.962	.27491D-17	.51785D-01	.45237
240	27.773	.28871D-17	.52852D-01	.45079
241	28.435	.29922D-17	.53949D-01	.44923
242	29.300	.31478D-17	.55064D-01	.44769
243	29.995	.32656D-17	.56212D-01	.44617
244	30.920	.34330D-17	.57379D-01	.44467
245	31.656	.35640D-17	.58552D-01	.44310
246	32.640	.37528D-17	.59830D-01	.44171
247	33.427	.38945D-17	.61064D-01	.44027
248	34.498	.41066D-17	.62345D-01	.43884
249			.63667D-01	.43743

N	PERCENTAGE ERROR	ERROR VARIANCE(POT.)	BAND ERROR (UNDEL.) (M)	TOTAL UNDEL. ERROR (M)
250	35.328	42629D-17	55012D-01	42604
251	36.488	45031D-17	66483D-01	43447
252	37.374	46777D-17	67810D-01	43332
253	38.648	49528D-17	69284D-01	43286
254	39.603	51498D-17	70763D-01	43070
255	41.021	54705D-17	72320D-01	42942
256	42.071	56979D-17	73989D-01	42817
257	43.673	60083D-17	75561D-01	42694
258	44.856	63517D-17	77240D-01	42574
259	46.728	68238D-17	79020D-01	42458
260	48.183	71641D-17	82769D-01	42344
261	50.362	77722D-17	84766D-01	42234
262	52.097	82422D-17	86918D-01	42128
263	55.012	91026D-17	89183D-01	42026
264	57.441	98294D-17	91696D-01	41930
265	61.608	11197D-16	94437D-01	41841
266	65.698	12615D-16	97682D-01	41761
267	72.732	15315D-16	10164	41694
268	82.291	19420D-16	10706	41649
269	99.043	27068D-16	11769	41646
270	143.98	50341D-16	13502	41793
271	197.22	10844D-15	16377	42183
272	276.78	21159D-15	19601	43059
273	323.18	28079D-15	21531	44200
274	268.62	19562D-15	24037	45026
275	325.01	28372D-15	25291	46169
276	237.43	13082D-15	26421	46709
277	213.63	14392D-15	27409	47217
278	223.98	13103D-15	28340	47665
279	222.25	12787D-15	29200	48098
280	218.07	12199D-15	30028	48503
281	217.96	12075D-15	30912	48900
282	216.00	11752D-15	31576	49281
283	216.94	11747D-15	32311	49661
284	216.20	11562D-15	33034	50031
285	217.89	11688D-15	33735	50402
286	217.90	11535D-15	34430	50768
287	220.18	11672D-15	35108	51137
288	220.69	11622D-15	35704	51502
289	223.44	11807D-15	36447	51873
290	228.30	11793D-15	37119	52241
291	227.45	12019D-15	37762	52616
292	228.54	12028D-15	38417	52990
293	232.84	12590D-15	39062	53372
294	233.29	12313D-15	39712	53753
295	237.11	12693D-15	40353	54143
296	238.43	12839D-15	41000	54532
297	242.56	12960D-15	41610	54911
298	243.09	13035D-15	42204	55299
299	248.30	13353D-15		55738

N	PERCENTAGE ERROR	ERROR VARIANCE(POT.)	BAND ERROR (UNDO.) (M)	TOTAL UNDO.. ERROR (M)
300	249.88	.13740D-15	.42921	.56145
301	254.24	.13760D-15	.43567	.56564
302	255.42	.13767D-15	.44283	.56981
303	256.35	.14182D-15	.44850	.57410
304	261.32	.14185D-15	.45406	.57835
305	266.80	.14697D-15	.46130	.58274
306	267.18	.14556D-15	.46769	.58708
307	272.60	.15024D-15	.47417	.59156
308	272.89	.14929D-15	.48031	.59598
309	278.54	.15423D-15	.48699	.60054
310	278.35	.15271D-15	.49331	.60502
311	284.21	.15710D-15	.49976	.60964
312	283.37	.15562D-15	.50604	.61416
313	289.44	.16100D-15	.51246	.61882
314	287.73	.15779D-15	.51867	.62336
315	293.99	.16355D-15	.52502	.62804
316	291.18	.15892D-15	.53113	.63256
317	297.60	.16463D-15	.53738	.63722
318	293.39	.16168D-15	.54334	.64168
319	299.95	.16499D-15	.54945	.64628
320	293.89	.16662D-15	.55521	.65072
321	300.55	.16283D-15	.56111	.65511
322	291.82	.15189D-15	.56638	.65923
323	298.83	.16700D-15	.57250	.66334
324	296.38	.14921D-15	.57758	.66748
325	293.48	.14983D-15	.58259	.67149
326	279.42	.12983D-15	.58699	.67477
327	279.94	.12419D-15	.59161	.67828
328	281.18	.10716D-15	.59528	.68198
329	287.49	.11717D-15	.59907	.68500
330	211.29	.74611D-16	.60169	.68851
331	217.07	.78121D-16	.60423	.69233

N	PERCENTAGE ERROR	ERROR VARIANCE(POT.)	BAND ERROR (UNBUL.) (M)	TOTAL UNBUL. ERROR (M)
2	.31095D-01	.37655D-23	.12359D-01	2.4109
3	.19965D-01	.12132D-22	.25400D-04	2.4304
4	.11134D-01	.57349D-23	.27201D-04	2.4369
5	.99531D-02	.57532D-23	.31200D-04	2.4321
6	.71400D-02	.21600D-23	.32375D-04	2.4203
7	.74792D-02	.37453D-23	.34040D-04	2.4229
8	.62366D-02	.21302D-23	.36067D-04	2.4183
9	.63223D-02	.30017D-23	.37761D-04	2.4130
10	.62495D-02	.21404D-23	.38899D-04	2.4004
11	.69913D-02	.27944D-23	.40333D-04	2.4036
12	.67133D-02	.21962D-23	.41423D-04	2.3995
13	.68339D-02	.26977D-23	.42721D-04	2.3941
14	.62720D-02	.22672D-23	.43703D-04	2.3812
15	.70929D-02	.26731D-23	.45047D-04	2.3847
16	.69100D-02	.23304D-23	.46030D-04	2.3843
17	.73733D-02	.27122D-23	.47230D-04	2.3766
18	.73733D-02	.34691D-23	.48207D-04	2.3720
19	.68691D-02	.27910D-23	.49447D-04	2.3696
20	.82314D-02	.25903D-23	.50302D-04	2.3662
21	.19306D-02	.29635D-23	.51636D-04	2.2904
22	.18249D-02	.27429D-23	.52724D-04	2.2244
23	.20249D-02	.30449D-23	.53003D-04	2.1723
24	.23229D-02	.35159D-23	.54970D-04	2.1229
25	.23753D-02	.31219D-23	.56193D-04	2.0621
26	.34792D-02	.11047D-23	.57235D-04	2.0249
27	.32137D-02	.33102D-23	.58499D-04	1.9913
28	.36467D-02	.36467D-23	.59379D-04	1.9030
29	.31419D-02	.36245D-23	.60012D-04	1.9253
30	.36000D-02	.30551D-23	.61070D-04	1.8976
31	.36029D-02	.30723D-23	.61353D-04	1.8364
32	.37644D-02	.30104D-23	.61550D-04	1.8263
33	.35762D-02	.41070D-23	.61750D-04	1.7099
34	.33221D-02	.41070D-23	.62007D-04	1.7472
35	.39999D-02	.44520D-23	.63440D-04	1.7143
36	.42013D-02	.44520D-23	.64400D-04	1.6853
37	.44640D-02	.40034D-23	.71074D-04	1.6352
38	.53000D-02	.47934D-23	.72010D-04	1.6340
39	.50770D-02	.51057D-23	.73020D-04	1.6044
40	.53401D-02	.51057D-23	.73243D-04	1.5843
41	.53671D-02	.56090D-23	.76742D-04	1.5842
42	.56047D-02	.56302D-23	.78216D-04	1.5304
43	.67007D-02	.60000D-23	.79770D-04	1.5208
44	.59600D-02	.61169D-23	.80120D-04	1.4977
45	.63020D-02	.66010D-23	.82511D-04	1.4764
46	.69020D-02	.66599D-23	.84630D-04	1.4571
47	.65110D-02	.71792D-23	.86260D-04	1.4393
48	.74046D-02	.72536D-23	.87959D-04	1.4146
49	.80790D-02	.70202D-23	.89745D-04	1.4003

Table C.2 Parameters as for table 3.2
Procedure: least squares collocation

N	PERCENTAGE ERROR	ERROR VARIANCE (POT.)	BAND ERROR (UNBUI.) (M)	TOTAL UNBUI. ERROR (M)
80	73123D-02	79147D-23	91810D-04	1.3787
81	83440D-02	85314D-23	93390D-04	1.3614
82	96350D-02	86487D-23	93231D-04	1.3435
83	83963D-02	93210D-23	97217D-04	1.3254
84	91634D-02	94634D-23	99173D-04	1.3080
85	95211D-02	10198D-22	10124D-03	1.2904
86	18386D-01	10368D-22	10338D-03	1.2732
87	19231D-01	11174D-22	10547D-03	1.2561
88	11280D-01	11373D-22	10763D-03	1.2414
89	11540D-01	12260D-22	10920D-03	1.2266
90	13680D-01	12493D-22	11221D-03	1.2128
91	13163D-01	13470D-22	11462D-03	1.1998
92	12109D-01	13743D-22	11762D-03	1.1837
93	13763D-01	14020D-22	11937D-03	1.1762
94	14521D-01	15136D-22	12211D-03	1.1577
95	17128D-01	16320D-22	12479D-03	1.1479
96	17122D-01	16692D-22	12740D-03	1.1390
97	17629D-01	18015D-22	13031D-03	1.1210
98	17643D-01	18432D-22	13315D-03	1.1111
99	16789D-01	19904D-22	13615D-03	1.0980
70	19434D-01	20303D-22	13916D-03	1.0840
71	20931D-01	22024D-22	14234D-03	1.0706
72	20647D-01	22572D-22	14332D-03	1.0679
73	20059D-01	24400D-22	14880D-03	1.0370
74	23040D-01	25033D-22	15226D-03	1.0439
75	24149D-01	27092D-22	15583D-03	1.0366
76	26093D-01	27103D-22	15941D-03	1.0274
77	23099D-01	30936D-22	16320D-03	1.0191
78	27973D-01	30936D-22	16700D-03	1.0098
79	27219D-01	33548D-22	17103D-03	1.0012
80	20692D-01	34470D-22	17307D-03	99169
81	27620D-01	37437D-22	17969D-03	98234
82	31445D-01	38966D-22	18366D-03	97187
83	30700D-01	41030D-22	18823D-03	96299
84	36913D-01	43060D-22	19202D-03	95336
85	38463D-01	46000D-22	19769D-03	94601
86	37431D-01	48214D-22	20299D-03	93773
87	39661D-01	52632D-22	20700D-03	92957
88	42133D-01	54237D-22	21303D-03	92261
89	43020D-01	59270D-22	21869D-03	91464
90	43704D-01	61120D-22	22420D-03	90731
91	48094D-01	66099D-22	23010D-03	89960
92	49323D-01	69041D-22	23619D-03	89383
93	50363D-01	73734D-22	24261D-03	88593
94	56094D-01	78224D-22	24907D-03	87804
95	53210D-01	86013D-22	25980D-03	87206
96	60116D-01	88923D-22	26244D-03	86583
97	50500D-01	90046D-22	27040D-03	85961
98	67766D-01	10147D-21	27910D-03	85260
99		11221D-21	28599D-03	84677

N	PERCENTAGE ERROR	ERROR VARIANCE(POT.)	BAND ERROR (UNDUL.) (M)	TOTAL UNDUL. ERROR (M)
100	65358D-01	11627D-21	29412D-03	84002
101	67457D-01	12901D-21	30209D-03	83399
102	69670D-01	13307D-21	31173D-03	82723
103	74321D-01	14909D-21	32129D-03	82058
104	76302D-01	15496D-21	33094D-03	81404
105	81031D-01	17332D-21	34140D-03	80755
106	84411D-01	18051D-21	35197D-03	80117
107	90416D-01	20204D-21	36340D-03	79486
108	93365D-01	21179D-21	37311D-03	78863
109	10024	23927D-21	38704D-03	78240
110	10363	25660D-21	40074D-03	77640
111	11160	28460D-21	41492D-03	77040
112	11530	29951D-21	42932D-03	76447
113	12409	34208D-21	44523D-03	75861
114	12964	36229D-21	46143D-03	75282
115	14063	41000D-21	47940D-03	74710
116	14644	44460D-21	49795D-03	74145
117	15950	51001D-21	51863D-03	73506
118	16607	55577D-21	53994D-03	73034
119	18203	65466D-21	56481D-03	72407
120	19229	71071D-21	58903D-03	71947
121	21295	84040D-21	61737D-03	71413
122	22404	93637D-21	64761D-03	70805
123	24996	11362D-20	68229D-03	70362
124	26019	12843D-20	71940D-03	69845
125	30122	15914D-20	76303D-03	69334
126	32913	18664D-20	81178D-03	68820
127	37405	23779D-20	86063D-03	68327
128	42216	29631D-20	93300D-03	67831
129	48050	38367D-20	10171D-02	67341
130	50070	49000D-20	11213D-02	66853
131	50070	62218D-19	12560D-02	66374
132	50757	84040D-19	14579D-02	65890
133	13178	94401D-19	17789D-02	65427
134	24973	13047D-18	20802D-02	64961
135	24973	18027D-18	25020D-02	64499
136	46093	31075D-18	30927D-02	64043
137	30633	19027D-18	37430D-02	63590
138	30633	12753D-18	45223D-02	63141
139	30633	13062D-18	55223D-02	62697
140	27021	10266D-18	69000D-02	62250
141	27730	96040D-19	72033D-02	61820
142	27030	95062D-19	74800D-02	61367
143	27117	92531D-19	77230D-02	60959
144	26927	92251D-19	79617D-02	60534
145	27152	92250D-19	81933D-02	60113
146	27191	91140D-19	84163D-02	59694
147	27507	91027D-19	86340D-02	59282
148	27704	91712D-19	88470D-02	58872
149	27070	92092D-19	90303D-02	58465

N	PERCENTAGE ERROR	ERROR VARIANCE (POT.)	BAND ERROR (UNDOUL.) (M)	TOTAL UNDOUL. ERROR (M)
189	2.8481	92405D-19	92454D-02	58962
191	2.8068	95039D-19	94712D-02	51862
192	2.9244	96115D-19	96758D-02	51262
193	2.9761	98046D-19	98705D-02	54672
194	3.0213	99344D-19	10011D-01	54402
195	3.0781	10179D-18	10284D-01	56095
196	3.1294	10365D-18	10486D-01	55711
197	3.1910	10628D-18	10690D-01	55399
198	3.2477	10846D-18	10894D-01	54952
199	3.313	11123D-18	11099D-01	54577
200	3.3757	11375D-18	11303D-01	54295
201	3.4465	11687D-18	11513D-01	53895
202	3.5131	11979D-18	11723D-01	53470
203	3.5803	12316D-18	11933D-01	53106
204	3.6397	12624D-18	12146D-01	52745
205	3.7393	12994D-18	12361D-01	52307
206	3.8153	13338D-18	12570D-01	52031
207	3.8993	13730D-18	12780D-01	51678
208	3.9799	14114D-18	13020D-01	51320
209	4.0684	14545D-18	13245D-01	50900
210	4.1536	14983D-18	13472D-01	50634
211	4.2463	15417D-18	13702D-01	50291
212	4.3363	15850D-18	13935D-01	49950
213	4.4330	16355D-18	14171D-01	49611
214	4.5202	16836D-18	14410D-01	49275
215	4.6064	17362D-18	14653D-01	48941
216	4.7294	17872D-18	14898D-01	48609
217	4.8362	18411D-18	15147D-01	48280
218	4.9399	18987D-18	15400D-01	47953
219	5.0315	19594D-18	15656D-01	47627
220	5.1600	20177D-18	15915D-01	47304
221	5.2764	20824D-18	16179D-01	46983
222	5.3897	21447D-18	16443D-01	46664
223	5.5111	22133D-18	16716D-01	46347
224	5.6291	22790D-18	16991D-01	46032
225	5.7556	23530D-18	17270D-01	45719
226	5.8793	24314D-18	17552D-01	45407
227	6.0101	25011D-18	17839D-01	45098
228	6.1300	25761D-18	18130D-01	44790
229	6.2747	26582D-18	18425D-01	44483
230	6.4076	27374D-18	18724D-01	44181
231	6.5497	28246D-18	19028D-01	43870
232	6.6877	29097D-18	19335D-01	43578
233	6.8352	30007D-18	19648D-01	43279
234	6.9702	30894D-18	19964D-01	42982
235	7.1312	31869D-18	20286D-01	42687
236	7.2793	32804D-18	20611D-01	42393
237	7.4301	33835D-18	20942D-01	42101
238	7.5915	34821D-18	21277D-01	41810
239	7.7559	35907D-18	21616D-01	41521

R	PERCENTAGE ERROR	ERROR VARIANCE (POT.)	BAND ERROR (UNDBL.) (H)	TOTAL UNDBL. ERROR (H)
200	7.9146	.36947D-18	.21961D-01	.41334
201	0.0040	.37094D-18	.22310D-01	.40948
202	0.2409	.39106D-18	.22663D-01	.40663
203	0.4251	.40395D-18	.23022D-01	.40300
204	0.5945	.41542D-18	.23306D-01	.40099
205	0.7769	.42017D-18	.23734D-01	.39819
206	0.9618	.44021D-18	.24120D-01	.39540
207	9.1400	.45363D-18	.24566D-01	.39263
208	9.3209	.46627D-18	.24009D-01	.38987
209	9.5161	.48049D-18	.25270D-01	.38712
210	9.7022	.49364D-18	.25671D-01	.38439
211	9.9042	.50853D-18	.26070D-01	.38167
212	10.096	.52539D-18	.26474D-01	.37896
213	10.305	.53087D-18	.26003D-01	.37627
214	10.503	.55259D-18	.27297D-01	.37358
215	10.719	.56911D-18	.27717D-01	.37091
216	10.922	.58431D-18	.28142D-01	.36826
217	11.147	.60173D-18	.28372D-01	.36561
218	11.356	.61763D-18	.29080D-01	.36298
219	11.500	.63601D-18	.29449D-01	.36036
220	11.689	.65266D-18	.29896D-01	.35774
221	12.045	.67200D-18	.30340D-01	.35515
222	12.260	.68950D-18	.30806D-01	.35256
223	12.510	.71065D-18	.31270D-01	.34998
224	12.747	.73012D-18	.31739D-01	.34741
225	13.000	.74923D-18	.32216D-01	.34486
226	13.244	.76923D-18	.32697D-01	.34231
227	13.518	.79231D-18	.33103D-01	.33979
228	13.715	.81231D-18	.33670D-01	.33726
229	14.042	.83623D-18	.34179D-01	.33474
230	14.291	.86061D-18	.34680D-01	.33224
231	14.591	.88161D-18	.35170D-01	.32974
232	14.832	.90710D-18	.35640D-01	.32726
233	15.164	.93550D-18	.36290D-01	.32478
234	15.435	.95911D-18	.37321D-01	.32232
235	15.763	.98911D-18	.37321D-01	.31986
236	16.095	.10149D-17	.37069D-01	.31742
237	16.607	.10404D-17	.36427D-01	.31498
238	17.030	.10750D-17	.30950D-01	.31254
239	17.630	.11100D-17	.30530D-01	.31013
240	17.763	.11404D-17	.40145D-01	.30773
241	17.763	.11010D-17	.40730D-01	.30533
242	10.607	.12190D-17	.41370D-01	.30293
243	10.517	.12472D-17	.41950D-01	.30053
244	10.060	.12911D-17	.42570D-01	.29818
245	19.329	.13423D-17	.43265D-01	.29582
246	19.697	.13790D-17	.43840D-01	.29346
247	20.212	.14103D-17	.44509D-01	.29112
248	20.610	.14053D-17	.45179D-01	.28870
249	21.182	.15483D-17	.45070D-01	.28645

N	PERCENTAGE ERROR	ERROR VARIANCE (POT.)	BAND ERROR (UNDUL.) (M)	TOTAL UNDUL. ERROR (M)
280	21.620	.18969D-17	.46571D-01	.28414
281	22.264	.16765D-17	.47396D-01	.28103
282	22.783	.17339D-17	.48834D-01	.27954
283	23.488	.18293D-17	.48891D-01	.27725
284	24.049	.16980D-17	.49584D-01	.27498
285	24.894	.20147D-17	.50402D-01	.27272
286	25.352	.21019D-17	.51241D-01	.27047
287	26.340	.22454D-17	.52123D-01	.26824
288	27.331	.23501D-17	.53033D-01	.26602
289	28.493	.25383D-17	.53997D-01	.26382
290	29.470	.26188D-17	.54997D-01	.26163
291	30.850	.29183D-17	.56064D-01	.25947
292	32.064	.31223D-17	.57183D-01	.25730
293	33.093	.34183D-17	.58382D-01	.25512
294	34.195	.36902D-17	.59651D-01	.25294
295	37.195	.40540D-17	.61013D-01	.25079
296	38.853	.44121D-17	.62466D-01	.24868
297	40.853	.47413D-17	.64019D-01	.24710
298	42.845	.50548D-17	.65667D-01	.24517
299	44.868	.53703D-17	.67411D-01	.24329
300	46.766	.56849D-17	.69253D-01	.24145
301	48.527	.60037D-17	.71130D-01	.23965
302	50.125	.63370D-17	.73071D-01	.23789
303	51.460	.66849D-17	.75071D-01	.23617
304	52.623	.70430D-17	.77130D-01	.23446
305	53.560	.74070D-17	.79250D-01	.23281
306	54.330	.77820D-17	.81430D-01	.23117
307	55.039	.79479D-17	.83694D-01	.22955
308	55.551	.80623D-17	.86022D-01	.22795
309	56.130	.81559D-17	.88422D-01	.22637
310	56.587	.82682D-17	.90813D-01	.22480
311	57.034	.83682D-17	.93190D-01	.22324
312	57.355	.85289D-17	.95190D-01	.22170
313	57.867	.86540D-17	.96119D-01	.22016
314	58.176	.88371D-17	.97045D-01	.21864
315	58.692	.89443D-17	.99624D-01	.21716
316	59.010	.90594D-17	.10135	.21566
317	59.341	.91552D-17	.10305	.21421
318	59.877	.92519D-17	.10473	.21276
319	60.427	.94344D-17	.10640	.21132
320	60.786	.96100D-17	.10805	.20990
321	61.355	.97459D-17	.10969	.20849
322	61.738	.98774D-17	.11132	.20710
323	62.327	.99670D-17	.11293	.20573
324	62.733	.99641D-17	.11454	.20437
325	63.341	.99979D-17	.11613	.20303
326	63.768	.90482D-17	.11771	.20171
327	64.392	.91370D-17	.11929	.20041
328	64.839	.91843D-17	.12086	.19912
329	65.470	.92834D-17		.19785

R	PERCENTAGE ERROR	ERROR VARIANCE(POT.)	BAND ERROR (UNDEL.) (M)	TOTAL UNDEL. ERROR (M)
300	65.941	.93360D-17	.12241	.19661
301	66.594	.94396D-17	.12397	.19830
302	67.072	.94933D-17	.12551	.19417
303	67.735	.95990D-17	.12706	.19390
304	68.224	.96530D-17	.12859	.19181
305	68.897	.97622D-17	.13012	.19067
306	69.395	.98198D-17	.13164	.18934
307	70.074	.99200D-17	.13316	.18843
308	70.579	.99863D-17	.13468	.18735
309	71.263	.10095D-16	.13619	.18628
310	71.771	.10153D-16	.13770	.18524
311	72.458	.10261D-16	.13920	.18422
312	72.966	.10319D-16	.14070	.18322
313	73.633	.10426D-16	.14219	.18224
314	74.159	.10481D-16	.14368	.18120
315	74.844	.10507D-16	.14517	.18035
316	75.344	.10640D-16	.14665	.17944
317	76.025	.10743D-16	.14813	.17858
318	76.514	.10792D-16	.14960	.17760
319	77.190	.10937D-16	.15107	.17683
320	77.665	.10937D-16	.15253	.17600
321	78.333	.11035D-16	.15399	.17520
322	78.706	.11071D-16	.15544	.17441
323	79.445	.11166D-16	.15690	.17365
324	79.866	.11192D-16	.15834	.17291
325	80.519	.11283D-16	.15978	.17219
326	80.803	.11294D-16	.16120	.17148
327	81.535	.11303D-16	.16263	.17080
328	81.705	.11361D-16	.16404	.17013
329	82.442	.11451D-16	.16545	.16949
330	82.269	.11312D-16	.16684	.16884
331	82.955	.11409D-16	.16822	.16822

ATE
LME